UNIVERSITÀ DEGLI STUDI DI MILANO

PhD Course in Environmental Sciences

XXIX Cycle

Development of an integrated system biology model for predicting mixtures of chemicals acting on the same pathway

PhD Thesis

Maria BATTISTONI

R10617

Scientific tutor: Prof.ssa Elena MENEGOLA

Scientific co-tutor: Prof.ssa Roberta PENNATI

Academic year: 2015-2016

SSD: BIO/06

Thesis performed at the Biosciences Department

“Look wide, and even when you think you are looking wide, look wider still."

Robert Baden-Powell

TABLE OF CONTENTS

ABSTRACT

Exposure of the embryo to environmental chemicals (pesticides, air and water pollutants) can result in congenital malformations or developmental defects such as oro-facial cleftings. Unfortunately, the human embryo is not usually exposed to a single substance, but to many substances simultaneously. Despite the efforts in elucidating mechanism of action (MoA) of substances that perturb the normal embryonic development, only a small part of involved pathways have been understood to date (Giavini and Menegola, 2004). This is why, evaluating the toxicity of mixtures of multiple chemicals is one of the major objectives of today's toxicology despite the effect of exposure to a mixture is still difficult to understand. To arrive in the future to the creation of a realistic overall picture of human exposure to mixtures, the development of integrated approaches between *in vitro* and *in silico* techniques and computational systems biology, able to predict the effects of mixtures starting from the concentrations of their individual components, will be essential. Recent studies suggest that the similarity of molecular initiating events (MIEs) is not an essential requirement to induce additive effects, because mixtures composed of chemicals with different MIE can exhibit mixture effects too, probably acting on the same biological pathway and contributing to the same adverse outcome (EFSA, 2013). This is in recognition of emerging evidence that biological effects can be similar, although the molecular details of toxicological mechanisms may profoundly differ in many respects (Kortenkamp, 2007). Considering the previously reported data, this could be the case of embryonic co-exposure to fluconazole (FLUCO) and ethanol (Eth). Both, in fact, lead to the same adverse outcome (AO), craniofacial malformations, both after *in utero* and *in vitro* exposure. The two molecules are able to induce cranio-facial defects (in embryos visible as cranio-facial abnormalities), probably acting on the same Adverse Outcome Pathway (AOP) altering, with different MIEs, the biological event cascade regulated by the morphogen retinoic acid (RA).

The specific aim of this PhD project was to investigate this hypothesis through the development of an *in silico* model, useful to simulate and predict the effects on embryo development after co-exposure to substances with independent MoAs but acting on the same biological pathway and potentially contributing to the same adverse outcome (cranio-facial malformations). The *in silico* model was based on experimental data and validated by *in vitro* experiments. For this purpose, the project was divided into three parts.

In the first part, we evaluated the effects of the molecules on post-implantation rat embryos cultures, using the *in vitro* technique WEC (Whole Embryo Culture). Embryos were cultured in presence of increasing concentration of RA (0.025-0.0375-0.05-0.125-0.25 µM), to increasing concentrations of Eth (17-42.5-85-127 mM), to increasing concentrations of FLUCO (62.5-125-250-500 µM). Specific and concentration related abnormalities at the level of the branchial arches (reductions or fusions) were observed after exposure to single Eth or FLUCO and were comparable to those elicited by RA. These results suggest a common AO for Eth, FLUCO and RA. Embryos were then co-exposed to binary mixtures of FLUCO and Eth. To better characterize the contribution of each component to the observed effects, the "fixed + moving" approach was applied: embryos were exposed to the no effect concentration (NOAEL) of one chemical ("fixed") and increasing concentrations of the other chemical ("moving"). A significant enhancement of teratogenic effects was observed after co-exposure to FLUCO and Eth in comparison to the single exposure. The mixture between the two NOAELs was effective too, inducing almost 40% of branchial arch abnormalities. These data suggest the presence of a cumulative effect in mixture, probably due to the capability of both molecules to perturb RA endogenous concentrations in specific tissues (the precursors of cranio-facial skeletal tissues, originated in the embryonic hindbrain). This theory could be explained considering the ability of Eth to induce alcohol-dehydrogenases (including ADH7, the embryonic enzyme involved in RA synthesis) and the inhibitory effects of FLUCO on cytochromes p450 (including CYP26, involved in embryonic RA degradation).

In the second part of the project, we evaluated these hypothetical mechanisms inducing the Eth-FLUCO mixture effects through the development of an *in silico* tool, able to simulate both the formation of the physiological RA gradient in the rat embryo hindbrain and its perturbation after exposure to FLUCO, Eth and to their binary mixtures. The obtained system biology model, developed using an integrated approach combining mathematical modelling, molecular docking and *in vitro* experiments, seems to be reasonably predictive for the mixture's effects, confirming the accuracy of the hypothesized pathogenic pathway. Experimental data and model predictions, in fact, showed a promising agreement. The model, in spite of its limitations, could have many potential mechanistic or predictive applications for the study of risk assessment. However, since the model is based on experimental data obtained in mammals, the last part of the project was aimed to evaluate alternative animal models.

In the third part of the project, the evaluation of the effects after co-exposure to FLUCO and Eth were performed using the ascidian *Ciona intestinalis* embryo model as a new alternative teratological screening test (AET, Ascidian Embryo Teratogenicity assay). An ascidian species was selected because Ascidiacea represent the sister group of Vertebrates. For this purpose, *C. intestinalis* embryos were exposed to Eth alone (1.7-8.5-17-42.5-85 mM) to FLUCO alone (7.8-15.75-31.5-250 µM), or co-exposed to binary mixtures of FLUCO and Eth until the larval stage, applying the fix + moving protocol. Specific and concentration related abnormalities at the level of the anterior structures were elicited by Eth or FLUCO, and were comparable to those described in literature after RA exposure. A significant enhancement of the general teratogenicity was observed after co-exposure to FLUCO and Eth in comparison to the single exposure, suggesting the presence of a mixture effect induced by FLUCO and Eth also in this model. These results, similar to those observed in the WEC model, encourage the use of AET as a complementary alternative method for embryotoxicity studies on mixtures. The possibility to translate data obtained in this model in our *in silico* model is still to evaluate.

In conclusion, our data suggest that: 1. the integrated use of data from *in vitro* and *in silico* approaches used in this study support the hypothesis that embryonic exposure to FLUCO and Eth can lead to the same AO (craniofacial abnormalities) acting with different MIEs but both converging on the same AOP by altering the RA production (Eth) and the RA catabolism (FLUCO); 2. the hypothesis that substances with different MoAs but acting on the same pathway could produce an additive effect also at concentrations considered not effective is supported; 3. the obtained results highlight the potential additive effect that could occur after exposure to azoles and ethanol, suggesting a precautionary position in alcohol consumption during azoles exposure in pregnancy. The overall view of the obtained results support the need of a cumulative risk assessment not only for chemicals grouped on the base of similarities in chemical structure or derived from mechanistic considerations but also for chemicals differently acting on the same biological pathway.

RIASSUNTO

L'esposizione embrionale a composti chimici ambientali (pesticidi, contaminanti acquatici o dell'aria), può provocare malformazioni congenite o anomalie dello sviluppo come le schisi oro-facciali. Purtroppo, la realtà dell'esposizione embrionale umana è caratterizzata dalla presenza contemporanea di più sostanze anziché di una singola sostanza per volta. Nonostante gli sforzi fatti finora per chiarire il meccanismo di azione (*mechanism of action*, MoA) delle sostanze che possono perturbare il normale sviluppo embrionale, ad oggi sono stati compresi solo una piccola parte dei pathway coinvolti (Giavini and Menegola, 2004). Per questo motivo, la valutazione della tossicità delle miscele di più sostanze chimiche è uno dei principali obiettivi della tossicologia moderna, nonostante gli effetti dati dall'esposizione a miscele siano ancora difficili da capire. Per giungere in futuro alla realizzazione di un quadro complessivo realistico dell'esposizione umana a queste sostanze, lo sviluppo di approcci integrati tra tecniche *in vitro* e *in silico* e tra modelli computazionali di *system biology* in grado di prevedere gli effetti delle miscele partendo dalla concentrazione dei loro singoli componenti si rivelerà essenziale. Studi recenti suggeriscono che la somiglianza tra eventi molecolari iniziali (*molecular initiating events*, MIEs) non è un requisito essenziale nell'induzione di effetti additivi, perché miscele di composti chimici con MIE diversi possono comunque presentare effetti miscela, probabilmente agendo sullo stesso pathway biologico e contribuendo allo stesso effetto avverso (EFSA, 2013). Esistono infatti prove emergenti che indicano che gli effetti biologici possono essere simili, nonostante i dettagli molecolari dei meccanismi tossicologici differiscano profondamente per molti aspetti (Kortenkamp, 2007). Considerando i dati precedentemente riportati, questo può essere il caso della co-esposizione embrionale a fluconazolo (FLUCO) ed etanolo (Eth). Entrambi, infatti, possono portare allo stesso effetto avverso (*adverse outcome*, AO), le malformazioni cranio-facciali, sia dopo esposizione *in utero* che *in vitro*. Le due molecole sono in grado di indurre malformazioni craniofacciali (visibili negli embrioni come anomalie cranio-facciali), agendo probabilmente sullo stesso *adverse outcome pathway* (AOP) alterando, con MIE diversi, la cascata di eventi biologici regolata dal morfogeno acido retinoico (RA).

L'obiettivo specifico di questo progetto di dottorato era verificare questa ipotesi tramite lo sviluppo di un modello *in silico* capace di simulare e predire gli effetti sullo sviluppo embrionale dati dalla co-esposizione a sostanze con MoA indipendenti ma che agiscono sullo stesso pathway biologico e che contribuiscono potenzialmente allo stesso effetto avverso (malformazioni cranio-

facciali). Lo sviluppo del modello *in silico* si è basato su dati sperimentali e validato da esperimenti *in vitro*. A questo scopo, il progetto è stato diviso in tre parti.

Nella prima parte, sono stati valutati gli effetti delle molecole su embrioni post-impianto di ratto utilizzando la tecnica *in vitro* WEC (*Whole Embryo Culture*). Gli embrioni sono stati coltivati in presenza di concentrazioni crescenti di RA (0.025-0.0375-0.05-0.125-0.25 µM), di concentrazioni crescenti di Eth (17-42.5-85-127 mM), di concentrazioni crescenti di FLUCO (62.5-125-250-500 µM). Sono state osservate anomalie specifiche e concentrazione-dipendente a livello degli archi branchiali (riduzioni o fusioni) dopo l'esposizione al singolo Eth o FLUCO, comparabili a quelle ottenute con RA. Questi risultati suggeriscono un AO comune per Eth, FLUCO e RA. Gli embrioni sono stati quindi co-esposti alle miscele binarie di FLUCO e Eth. Per meglio caratterizzare il contributo di ciascun componente agli effetti osservati, è stato applicato l'approccio "fixed + moving": gli embrioni sono stati esposti alla concentrazione non effetto di una sostanza ("fixed") e a concentrazioni crescenti dell'altra ("moving"). È stato osservato un aumento significativo degli effetti teratogeni dopo la co-esposizione a FLUCO e Eth rispetto all'esposizione singola. Anche la miscela delle due NOAELs è risultata con effetto, inducendo quasi il 40% delle anomalie agli archi branchiali. Questi dati suggeriscono la presenza di un effetto cumulativo in miscela, probabilmente dovuto alla capacità di entrambe le molecole di perturbare la concentrazione endogena di RA in tessuti specifici (i precursori dei tessuti scheletrici cranio-facciali, che si originano nel rombencefalo embrionale). Questa teoria può essere spiegata considerando l'abilità di Eth di indurre le alcol deidrogenasi (compresa ADH7, l'enzima embrionale coinvolto nella sintesi di RA) e gli effetti inibitori del FLUCO sul citocromo p450 (compreso CYP26, coinvolto nella degradazione dell'RA embrionale).

Nella seconda parte, sono stati valutati gli ipotetici meccanismi che inducono gli effetti miscela Eth-FLUCO tramite lo sviluppo di uno strumento *in silico*, in grado di simulare sia la formazione di un gradiente di RA nel rombencefalo di un embrione di ratto sia la sua perturbazione in seguito ad esposizione a fungicidi azolici, ad Eth e alle loro miscele binarie. Il modello di *system biology*, sviluppato utilizzando un approccio integrato che combina modelli matematici, docking molecolare ed esperimenti *in vitro*, sembra essere ragionevolmente predittivo per gli effetti miscela, confermando l'accuratezza del pathway ipotizzato. Infatti, i dati sperimentali e le predizioni del modello mostrano un accordo promettente. Il modello, nonostante i suoi limiti, potrebbe avere molte potenziali applicazioni meccanicistiche o predittive per lo studio della

valutazione del rischio. Tuttavia, dal momento che il modello si basa su dati sperimentali ottenuti nei mammiferi, l'ultima parte del progetto era finalizzato a valutare modelli animali alternativi.

Nella terza parte, la valutazione degli effetti dati dalla co-esposizione a FLUCO e Eth è stata effettuata utilizzando il modello di embrione di ascidia *Ciona intestinalis* come un nuovo test alternativo per lo screening teratologico (*ascidian embryo teratogenicity assay*, AET). È stata scelta una specie di ascidia in quanto gli Ascidiacea rappresentano il *sister group* dei Vertebrati. A questo scopo, embrioni di *C. intestinalis* allo stadio di neurula precoce (7 hpf) sono stati esposti per 15 h a concentrazioni crescenti di Eth (1.7-8.5-17-42.5-85 mM), concentrazioni crescenti di FLUCO (7.8-15.75-31.5-250 µM) o co-esposti alle miscele binarie di FLUCO e Eth, applicando il protocollo fix + moving, fino allo stadio di larva. Sono state osservate anomalie specifiche e concentrazione-dipendenti a livello dello strutture anteriori dopo l'esposizione singola a Eth o FLUCO, paragonabili a quelle descritte in letteratura dopo esposizione con RA. È stato osservato inoltre un aumento significativo della teratogenicità generale dopo la co-esposizione a FLUCO e Eth rispetto alle esposizioni singole, il che suggerisce la presenza di un effetto miscela indotto da FLUCO e Eth anche in questo modello. I risultati ottenuti, simili a quelli osservati nel modello WEC, incoraggiano l'uso dell'AET come un metodo alternativo complementare per gli studi di embriotossicità. La possibilità di traslare i dati ottenuti in questo modello nel nostro modello *in silico* è ancora valutare.

Concludendo, i nostri dati: 1. Suggeriscono che l'uso integrato di dati provenienti dagli approcci *in vitro* e *in silico* usati in questo studio supporta l'ipotesi che l'esposizione embrionale a FLUCO e Eth può portare allo stesso AO (anomalie cranio-facciali) agendo con MIE diversi ma entrambi convergenti sullo stesso pathway biologico, alterando la produzione di RA (Eth) e il suo catabolismo (FLUCO); 2. Avvalorano l'ipotesi per cui sostanze con MoA diversi che agiscono sullo stesso pathway possono produrre un effetto additivo anche a concentrazioni considerate non effetto; 3. Sottolineano il potenziale effetto additivo che potrebbe verificarsi dopo esposizione contemporanea ad azoli ed etanolo, suggerendo cautela nel consumo di alcol durante l'esposizione ad azoli durante la gravidanza. La visione d'insieme dei risultati ottenuti supportano la necessità di una valutazione del rischio cumulativo non solo per quelle sostanze raggruppate sulla base di somiglianze nella struttura chimica o derivati da considerazione meccanicistiche, ma anche per quelle sostanze che agiscono diversamente sullo stesso pathway biologico.

GENERAL INTRODUCTION

1. CRANIO-FACIAL DEFECTS

Congenital anomalies are a major cause of infant mortality and childhood morbidity, affecting 2-3% of newborns. Among congenital anomalies, oral cleft (cleft lip and/or palate alone or associated with other cranio-facial deformities) are one of the most frequent (1:700 live births), both as isolated anomalies and in syndromic conditions (Mossey et al., 2009). The most frequent defects associated with facial clefts are malformation of the limbs, followed by cardiovascular and other facial anomalies. Cranio-facial anomalies, other than cleft lip and palate, occur in 1 in every 1600 newborns in the United States of America (USA) and include jaw deformities, malformed or missing teeth, defects in the ossification of facial or cranial bones, and facial asymmetries. In Europe, higher prevalence rates of cleft lip/palate are reported from northern countries (Mossey and Little, 2002), even if such a geographical distribution is not the rule worldwide. Evidence suggests that oral clefts are multifactorial in origin, involving both genetic and environmental risk factors (Mossey et al., 2009). The specific causes inducing cranio-facial defects are unknown, even if some risk factors have been identified, such as maternal active and passive smoking (Hackshaw et al., 2011; Sabbagh et al., 2015), maternal diabetes (Spilson et al., 2001), use of medicaments, such as some antiepileptic drugs, during the first trimester of pregnancy (Nguyen et al., 2009; Alsaad et al., 2015). The human embryo is not usually exposed to a single substance, but to many substances simultaneously and the effect of exposure to a mixture of chemicals is still difficult to understand. The chemicals a pregnant woman may be exposed to are numerous and include several categories: medicines, recreational drugs (alcohol, smoking, cocaine, etc.), workplace chemicals, environmental chemicals (pesticides, air and water pollutants). Although experimental teratology data are considered sufficient for risk assessment, in the case of a possible, multiple aetiology of an adverse outcome (AO), the risk of a multiple exposure to different risk factors showing additive effects should be taken into account. An adverse outcome pathway (AOP) describes a framework of information about the progression of toxicity events starting from one molecular initiating events (MIE). Alterations along a sequence of more and more complex biological organizations are described as key events (KEs) and lead, at the end, to the AO. The possibility that different AOP could converge and induce the same AO is to take in account. Detailed mechanistic knowledge is necessary in order to develop alternative testing methods on chemicals potentially acting on the same AOP. The elucidation of the different potential chemical actors switching on the same or different MIEs/ KEs but contributing to the same AO (for our purposes cranio-facial defects) is fundamental in order to plan researches on the contribution of multiple exposures for facial cleftings.

2. CRANIOFACIAL DEVELOPMENT

2.1. Role of Neural Crest Cells

The oropharyngeal region is of considerable importance for both feeding and respiration, but it also generates important endocrine structures, such as the thyroid and parathyroid, as well as being the site of formation of the thymus (Graham, 2003). The development of this region of the embryo is extremely complex, involving interaction between a numbers of different embryonic cell types whose development must be well co-ordinated. The oropharyngeal apparatus has a segmented origin arising from series of bulges clearly visible on the lateral surface of the embryonic head: the branchial arches. In Mammals, there are six transient branchial arches, of which the first and the second are involved in craniofacial morphogenesis.

The neural crest cells (NCCs) play a pivotal role in the correct development of this region. The NCCs are a transient vertebrate cell type, characterized by its site of origin within the central nervous system (CNS), multipotency, and its ability to migrate and differentiate into numerous derivatives (Le Douarin and Kalcheim, 1999). Each branchial arch is characterized by a mesenchymal (the embryonic connective) core, externally constituted by migrated NCCs, which surrounds a central group of mesodermal cells (**Fig. 1**).

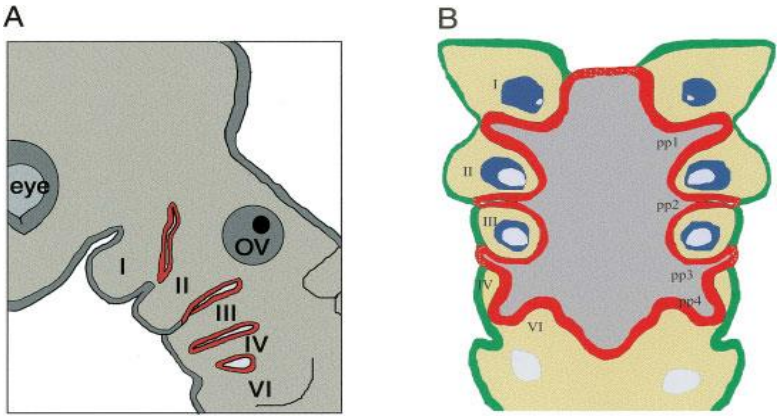

Fig. 1. The pharyngeal arches. **A**: A side view of the head region of an embryo. The pharyngeal arches are numbered from anterior to posterior I, II, III, IV and VI. The pharyngeal pouches (derived from the anterior gut) are labelled red, while the external epithelium is grey. The position of the eye vesicle as well as the otic vesicle (OV) are indicated. **B**: A longitudinal section through the pharyngeal arches. Again, the arches are labelled I through VI. The surface epithelium is green, the neural crest cells yellow, the mesoderm blue and the endoderm red. (Figure from Graham et al., 2003)

The NCCs migrated into the branchial apparatus will originate the connective and skeletal tissues of each arch, while the mesodermal mesenchyme will form the musculature and the endothelial cells of the arch arteries (Noden, 1983; Couly et al., 1993; Trainor and Tam, 1995). NCCs migrated into the branchial arches originate from the hindbrain (rhomboencephalon, segmented

in 7 metameric units, named rhombomeres) and from the caudal midbrain regions (Noden, 1983). Three distinct cell streams detach during the neural tube formation and reach the branchial apparatus (Lumsden et al., 1991): the NCCs that fill the first arch arise from the caudal midbrain and rhombomeres 1 and 2 of the hindbrain, those that fill the second arch arise primarily from rhombomere 4, and finally the caudal arches (III-VI) are populate by the post-otic NCCs generated by rhombomeres 6 and 7 (Lumsden et al., 1991; Schilling and Kimmel, 1994) (**Fig. 2**).

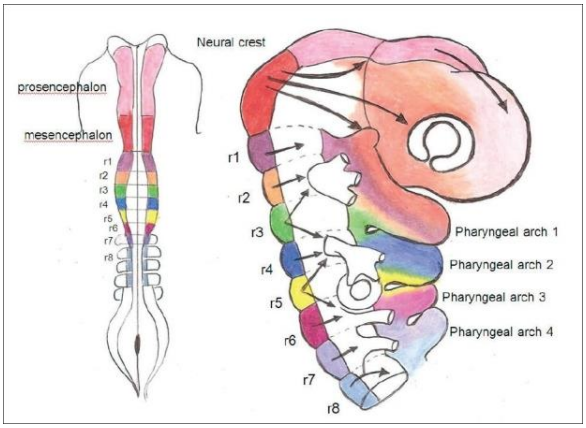

Fig. 2. Neural crest streams migrating from neural tube in formation to the head. (Figure from Carstens and Ewings, 2009)

The segregation of the NCCs into the streams is controlled through localized cell death. Rhombomeres 3 and 5 are depleted in NCCs production and, although these two hindbrain segments produce some NCCs, the majority of them from these rhombomeres die by apoptosis (Graham et al., 1993). Rhombomeres 3 and 5 constitute the so-called *neural crest free zones*. During normal development, jaw structures only form in the first arch, as well as the hyoid structure forms only in the second arch. Transplant experiments of the anterior hindbrain in the place of the mid hindbrain has shown that the NCCs produced by this tissue populate the second rather than the first arch with dramatic consequences on arch pattering: first arch structures developed in the second arch, while second arch form skeletal elements typical of the first arch (Noden, 1983). This suggests that NCCs acquire their positional information when they are within the neural tube and then transfer this information to the arches through their migratory capability. In fact, it seems that the prepatterned information contained in the hindbrain NCCs is associated with the expression pattern of *Hox* genes (Krumlauf, 1993). NCCs of the first arch do not express *Hox* genes at all, while second arch NCCs expresses Hox-a2 (Graham, 2003). *Hox* genes are conserved genes present in all animals, and involved in the specification of cephalic-

caudal axis and segment identity during early development, among which the formation and identity of the rhombomeres that constitute the hindbrain (Wilkinson, 1993). Therefore, *Hox* genes are essential both for the morphogenesis of the encephalon and to specify the rhomboencefalic NCCs. In this way, they can properly migrate into the corresponding branchial arches where they differentiate to give rise to the craniofacial structures (Trainor et al., 2002). *Hox* expression is activated by Retinoic Acid (RA) and regulated by growth and transcription factors like FGF8 (Ross et al., 2000).

2.2. Retinoic Acid pathway

RA, a metabolite of vitamin A, is a well-known morphogen in invertebrates and vertebrates (Morriss-Kay, 1992). RA is considered the main molecule involved in craniofacial morphogenesis in vertebrates with jaws (gnathostomes), and in activating the expression of a cascade of growth factors and then of genes controlling craniofacial development (Suzuki et al., 1999). Excess or deficiency of retinoids can induce craniofacial abnormalities (Kochhar, 2009), therefore the regulation of the amount of RA that is available to the embryo at specific times and to a given site is of critical importance.

The teratogenic effects of vitamin A excess in pregnant rats caused exencephaly, cleft palate, micrognathia, and eye defects (Cohlan, 1953). RA, available as a drug for severe cystic acne (Accutane), produced severe malformations in human newborns exposed during pregnancy, including reduced or absent ears, micrognathia, cleft palate, aortic arch abnormalities, and abnormalities of the central nervous system (Ross et al., 2000). Several animal studies have confirmed the teratogenic potential of RA excess, which produces overlapping defect patterns in many different animal species (monkeys, rats, mice, rabbits and hamsters). The malformations were those previously observed in humans. RA levels are tightly regulated by a combination of synthesis and degradation, and depends on the availability of its precursor, vitamin A (White and Schilling, 2008). All animals obtain form of vitamin A (retinol) from their diet in form of beta-carotene from plants and retinyl esters from animal sources. The major storage in embryos varies from species to species (Simões-costa et al., 2008). In placental mammals, retinol and retinyl esters are provided to the embryo through the maternal circulation. Retinol is secreted by the liver and transported in the blood at micromolar levels via serum retinol-binding-protein (RBP4) and is made available to the cells (including embryonic cells by maternal transfer) for potential conversion to RA (Quadro, 2004). In a RA-generating tissue, conversion of retinol to RA involves two steps: retinol is reversibly oxidized to retinaldehyde by either alcohol dehydrogenases (ADH) or retinol dehydrogenases (RDH), and retinaldehyde is irreversibly

oxidized to RA by retinaldehyde dehydrogenases (RALDH). RA is then released and taken up by surrounding cells. Some RA target cells express *cellular RA-binding-protein* (CRABP2) that facilitates uptake of RA and transport to the nucleus where RA binds the RA receptor (RAR) and retinoids X receptor (RXR) at the level of retinoic acid response element (RARE). The thus ternary complex formed regulates transcription of RA target genes (*Hox* genes) by modulating the binding of corepressors and coactivators. In no target cells, RA is sequester at cytoplasmic level by CRABP1 and delivered to CYP26 enzymes for degradation and excretion (Duester, 2008) (**Fig. 3**). In mammals there are three isoforms of CYP26 each with a specific spatial and temporal expression in the embryo: CYP26A1, expressed in the spinal cord and on rhombomere 2 at mouse stage E8.5 (MacLean et al., 2001); CYP26B1, expressed at the level of the heart and developing vasculature and at the level of rhombomeres 3 and 5 at mouse stage E8 and later in branchial ectomesenchyme; CYP26C1 expressed in rhombomeres 2and 4 at mouse stage E8-8.5, in the first branchial arch (MacLean et al., 2001; Reijntjes et al., 2005).

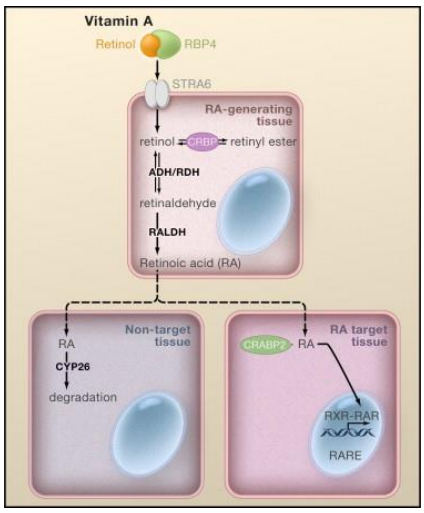

Fig. 3. Retinoic Acid synthesis and signalling. (Figure from Duester, 2008)

2.3. Hindbrain Pattering

One of the main functions of RA is in the developing hindbrain where it contributes to the anterior-posterior patterning (Morriss-Kay, 1992). In the mouse, the RA needed for this function is first produced at embryonic day 7.5 (E 7.5) in the trunk paraxial mesoderm by RALDH2 and diffuses into the adjacent central nervous system (Niederreither et al., 1999). The generation and diffusion of RA has been proposed to form a gradient that patterns the hindbrain into seven rhombomeres (r1-7) (White et al., 2007; Schilling et al., 2012). Because morphogens act at a

distance from their source of production, eliciting distinct cellular responses in a concentration-dependent manner (Rogers and Schier, 2011), they need to be robust and precise. Mechanism that enhance RA gradient robustness include: 1) tight feedback regulation of RA synthesis (recent evidence demonstrates that it also downregulates retinol dehydrogenase, RDH10, the enzyme that converts retinol to retinal (Strate et al., 2009)); 2) self-enhanced degradation with a negative feedback loop that regulates RA levels and compensate for changes in RA level (RA induces the expression of Cyp26A1 enzyme that specifically degrades RA (White et al., 2007)); 3) interactions between RA and other morphogens like the fibroblast growth factor (FGF) (Kudoh et al., 2002).

The FGF gradient is thought to be responsible for maintaining the cells of the posterior presomitic mesoderm in an immature state and to prevent them from activating their activation program (Dubrulle et al., 2001). Both RA and FGF gradient are produced in the posterior mesoderm during gastrulation, and induce posterior and suppress anterior expression of genes involved in rhombomeres specifications. FGF expression may drive the gastrulation movements that make the hindbrain field growing in size, and could activate the Cyp26 mRNA expression (del Corral and Storey, 2004).

However, RA activity during hindbrain development seems to be more complex and probably does not correspond to a simple concentration gradient of endogenous RA. Moreover, a gradient of RA has never been directly visualized, largely due to technical reasons. Sirbu et al. (2005) demonstrated in the mouse hindbrain the existence of dynamic shifting boundaries of RA activity: they showed that RA generated by RALDH2 in paraxial mesoderm initially travels as far anteriorly as presumptive r3 forming an early RA signalling boundary at r2/r3, just posterior to the RA-degrading enzyme Cyp26A1 expression domain. However, this boundary shifts posteriorly to the r4/r5 border as soon as Cyp26C1 is expressed in r4 (**Fig. 4**). Hence, the hindbrain utilizes the RA-degrading function of Cyp26A1 and Cyp26C1 to establish shifting boundaries of RA activity that induce both Hoxb1 and vHnf1, a repressor of Hoxb1. They also showed that the initial RA boundary at r2/r3 is independent of RA concentrations, as Cyp26A1 expression does is not substrate-dependent, while the shift to the r4/r5 boundary is RA-dependent, because Cyp26C1 expression in r4 is activated by the substrate itself. This study show that a stable RA gradient is not established across the hindbrain, but the initial gradient of RA entering the posterior hindbrain is converted by RA-degrading enzymes into RA boundaries that shift over time such that anterior tissues receive a short pulse of RA and posterior tissues receives a long pulse of RA.

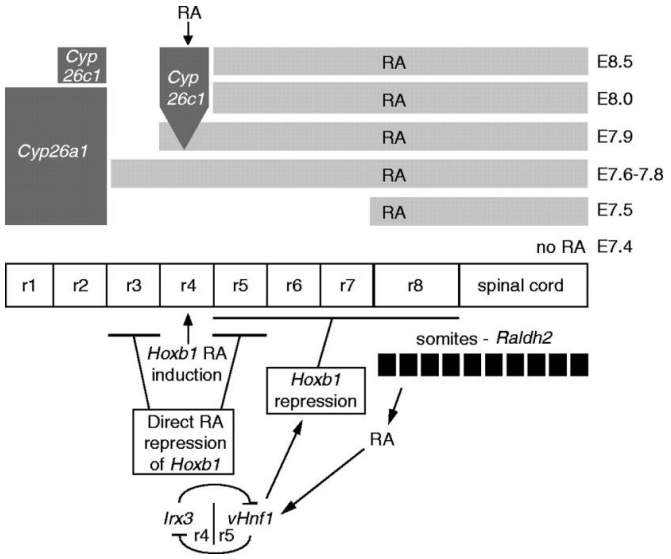

Fig. 4. Model of shifting RA boundaries during mouse hindbrain segmentation. Initially, RA forms an early anterior boundary at r2/r3 (next to the r2 border of Cyp26A1 expression), followed soon after by a late anterior boundary at r4/r5 (next to the r4 border of Cyp26C1 expression). RA acts firstly directly to induce Hoxb1 expression, then RA acts both directly and indirectly (through induction of vHnf1) to restrict Hoxb1 expression to r4. (Figure from Sirbu et al., 2005)

Thanks to its fine regulation, RA can form gradients that are roust, precise and capable of inducing multiple sharp boundaries of target gene expression (Hox genes) which give rise to a correct hindbrain segmentation. The correct NCCs migration from rhombomeres to branchial arches (and the subsequent correct craniofacial morphogenesis) is therefore established by the correctly establishment of the hindbrain RA gradient. By consequence, it is plausible that severe malformations of the face could result both by a generalized RA synthesis/degradation imbalance with altered amounts of RA in rhombomeres, and with a consequent ectopic expression of transcription and growth factors both in the hindbrain and rhomboencephalic NCC-derived tissues (Morriss-Kay, 1992; Osumi-Yamashita et al., 1994; Mark et al., 1995; Whiting, 1997; Schneider et al., 2001). The causes of local imbalance in RA content may be different: genetic risk factors, maternal infections during pregnancy, physical factors, or exposure to chemicals, including to chemical mixtures. There are many substances related to alterations in craniofacial development: exogenous retinoids, ethanol, some drugs (valproic acid, thalidomide, antimycotics) and pesticides (such as the class of the azoles fungicides).

RA excess due to exogenous RA exposure is related to the over- or ectopic- expression of homeotic genes, resulting in the homeotic transformation of any segmental region controlled by RA (somites, leading to vertebrae, or rhombomeres, leading to cranio-facial elements) (Mark et al., 1995). On the other hand, as the concentration of RA in embryonic tissues is controlled by

RA metabolism, it is likely that chemicals able to perturb ADH, ALDH or CYP26 functions may act as teratogens, by reducing or increasing the concentration of RA.

Inhibitors of the cytochrome P450- dependent RA catabolism, like the azole fungicide Fluconazole, are clinically used to increase plasma levels of RA (Schwartz et al., 1995). A similar mechanism has been suggested in order to explain the azole teratogenicity (Tiboni et al., 2009; Menegola et al., 2000, 2001). This hypothesis seems confirmed by the evidence that the embryonic normal morphology is restored after the co-exposure to azoles and to a specific RA production (Citral) (Schuh et al., 1993; Di Renzo et al., 2007).

As far as Eth is concerned, studies on mouse embryos exposed to ethanol showed interference with normal hindbrain RA controlled genes (*Hox*), suggesting an interference with RA metabolic enzymes (Dunty et al., 2002). Interaction between ethanol and RA is an intriguing hypothesis, but deserve confirmation studies.

3. AZOLE FUNGICIDES TERATOLOGY

Azole fungicides are a family of heterocyclic aromatic compounds with five atoms. Based on the number of nitrogen atoms, they are classified as imidazoles (two nitrogen atoms) and triazoles (3 nitrogen atoms) (**Fig. 5**).

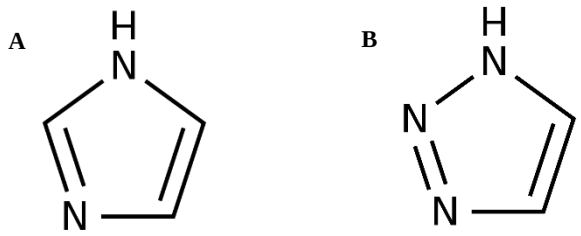

Fig. 5. Structure of the chemical groups characterizing the class of different azoles: (A) Imidazole; (B) Triazole.

Both imidazole- and triazole-derivatives are largely used in agriculture as well as in medicine as antifungal agents because of their capability to inhibit the P450 enzyme CYP51 (lanosterol 14α-demethylase), involved in the fungal wall formation (Vanden Bossche et al., 1984). The inhibitory action towards CYP51, which mediate the conversion of lanosterol to ergosterol, results in accumulation of lanosterol, changing the exact shape and physical properties of the fungal membrane, causing permeability changes and malfunction of membrane-imbedded proteins. The mechanism seems to be related to the interaction of the nitrogen atom with the central iron atom in the porphyrin system of cytochrome P450 (Zarn et al., 2002). The inhibitory potencies of these compounds is not limited to fungi. Inhibition has been observed in a number of mammalian cytochrome P450-dependent activities, including hepatic microsomal metabolism (Sheets and Mason, 1984), cholesterol and steroids metabolism (Loose et al., 1983; Mason et al., 1985), accounting for the possible interference of azoles with the metabolism of other drugs (Blum et al., 1991; Kantola et al., 2000). A concentration-dependent inhibition of the P450 cytochrome involved in the catabolism of RA (CYP26) has been reported *in vitro* and in patients with promyelocytic leukemia after treatment with the bis-triazole-derivative Fluconazole (Schwartz et al., 1995; Vanier et al., 2003). Due to their antifungal activities, more than 20 different compounds, including Fluconazole, are on the market for medical use, even during pregnancy, against superficial and deep mycosis for oral, topical, vaginal or systemic treatment of candidiasis and coccidioidal or cryptococcal meningitis (King et al., 1998; Kale and Johnson, 2005). About 40 different azole agrochemicals (including Cyproconazole, Triadimefon and

Flusilazole) are used worldwide against mildews and rust or cereal grains, fruits, vegetables and ornamentals accounting for several thousand per year (Giavini and Menegola, 2010).

Experimental studies demonstrated that the exposure, both *in vitro* and *in utero*, of rodent embryos to azole derivatives is able to alter hindbrain organization, NCC migration, ectomesenchyme compaction, and branchial arch and nerve morphogenesis, and to induce craniofacial alterations associated to axial, skeletal, and limb defects quite similar to those observed due to RA excess (Menegola et al., 2000, 2001, 2003, 2005a, 2005b, 2006a, 2006b; Di Renzo et al., 2007, 2011a, 2011b). *In vitro* exposed rat embryos showed specific malformation at the level of the branchial apparatus: hypoplasia of the first and second branchial arch or fusion of the branchial arches. The *in vivo* treatment of E8 mice pregnant females was related to cleft palate, skeletal craniofacial abnormalities and axial defects. The observed craniofacial malformations were at the level of skeletal structures derived from the first and second branchial arch: fusion, agenesis, ectopic elements and/or abnormal shape of the osseous or cartilaginous elements of the jaw, of the tympanic ring, of the zygomatic bone, of the middle ear ossicles. Malformations observed at the axial level consist of fusion of vertebrae or ribs, duplication of axles or morphological transformations of the same homeotic segments (Menegola et al., 2005b). Both the craniofacial and axial defects were similar to those described after RA in utero exposure. Since the antimycotic activity of the azole derivatives is based on their ability to inhibit CYP51, the hypothesis is that the effects related to the embryonic exposure to azole fungicides may depend by the inhibition of other embryonic CYP enzymes, such as the RA-degrading enzyme CYP26, that regulate the spatial-temporal distribution of RA. CYP26 is one of the cytochrome P450 specifically expressed in vertebrate embryos during development, with more than 61% identity identified in aminoacidic sequence of CYP26 in fish, chicken and mammals. Such conservation in the sequence supports a high conservation of functions (Stoilov et al., 2001; Abu-Abed et al., 2002). Similar to mammalian embryos, other vertebrate (the frog *Xenopus laevis*), and invertebrate (the ascidian *Phallusia mammillata* and *Ciona intestinalis)* embryos showed congenital malformations similar to those obtained in mammals after azole embryo exposure. (Groppelli et al., 2005; Pennati et al., 2006; Zega et al., 2009).

From the finding that the abnormalities observed both in mammals and non-mammals (amphibians and ascidiacea) are quite similar to those evoked by overexposure to morphogen RA, it can be extended that the inhibition of the CYP26 enzyme, responsible for the catabolism of RA, and the subsequent endogenous increase of the embryonic RA levels, is the possible mechanism of teratogenesis (Menegola et al., 2006a).

This hypothesis is supported by several indirect proofs:

1) some malformations induced by azole fungicides mimic those obtained with excess of RA (Menegola et al., 2005b);

2) Exposure of embryos to azole fungicides results in CYP26 overexpression (Tiboni et al., 2009);

3) azoles alter the rhombomeric structure of the hindbrain and the migration pattern of NCCs (Menegola et al., 2003, 2004);

4) exposure to some azoles alters the expression of specific genes controlled by RA as Krox20, TGFβ, CRABP1, Hoxb1, Hoxb2 (Massa et al., 2007; Di Renzo et al., 2009);

5) co-exposure to Triadimefon and subteratogenic doses of RA induces a synergistic effect (Menegola et al., 2004);

6) exposure to an inhibitor of RA synthesis (Citral) attenuates the teratogenic effects induced by triazole derivatives (Di Renzo et al., 2007).

3.1. Azole exposure in mixture and teratogenicity

The large use of azole fungicides both in agriculture and for pharmaceutical use makes concrete the possibility of simultaneous exposure to these compounds for humans and the occurrence of mixture effects. In this regard, the European Food Safety Authority (EFSA) asked the Panel on Plant Protection Products and their Residues (PPR Panel) to deliver a scientific opinion on risk assessment for a selected group of pesticides from the triazole group to test possible methodologies to assess cumulative effects from exposure to these pesticides on human health (EFSA, 2009). Currently, little information is still available regarding the embryo-toxicological effects deriving from exposure to mixtures of azoles. In their study of 2013, Menegola and co-workers showed that mixtures of no effect levels of Triadimefon, Imazalil, Fluconazole and mixtures of lower concentrations (derived from the Admissible Daily Intake, ADI) of Cyproconazole, Triadimefon, Triadimenol, Flusilazole, Tebuconazole, Imazalil with or without therapeutic doses of Fluconazole, produced an additive effect on post-implantation rat embryos, supporting the hypothesis that the individual tested substances share a same MoA (the inhibition of CYP26) and that the class of the azole fungicides constitute a common mechanism group (CMG).

3.2.Fluconazole

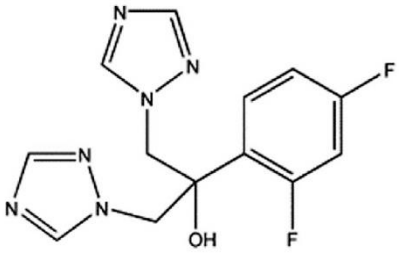

Fig. 6. Fluconazole structure

Among azoles, FLUCO (a bis-triazole derivative, **Fig. 6**) is a clinically used fungicides commonly dosed for treating a variety of mycoses and infections (Laverda et al., 1996; Mastroiacovo et al., 1996). Dose and administration period depend on type and severity of the infection: vaginal candidiasis is usually treated with a 150-mg single dose, while systemic mycoses are daily treated for several months with 400 mg FLUCO, respecting the total maximum daily recommended dose of 1600 mg. FLUCO excellent bioavailability has been reported after oral dosing and a linear pharmacokinetic has been demonstrated at doses of 200-400-800 mg/day (corresponding to a maximum plasma concentration of 33-163-229 μM) (Santos et al., 2010). As far as the use in pregnancy is concerned, the American Food and Drug Administration agency (FDA) recently changed the indications on the risk category in pregnancy for high dose fluconazole from category C (animal reproduction studies have shown an adverse effect on the foetus and there are no adequate and well-controlled studies in humans, but potential benefits may warrant use of the drug in pregnant women despite potential risks) to category D (there is positive evidence of human foetal risk based on adverse reaction data from investigational or marketing experience or studies in humans, but potential benefits may warrant use of the drug in pregnant women despite potential risks), while the pregnancy category for a single, low dose of fluconazole is category C (Sannerstedt et al., 1996).

Considering that teratogenic effects observed after *in vitro* exposure to FLUCO of whole postimplantation rodent embryos (Tiboni, 1993; Menegola et al., 2001) and after exposure of amphibian embryos (Groppelli et al., 2005) strictly resemble the alterations induced by RA excess in mammals (Menegola et al., 2003; 2004) and in frogs (Groppelli et al., 2005), and considering that the inhibitory activity of FLUCO on CYP26 enzyme accounts for the use of FLUCO in patients with acute promyelocytic leukaemia (Schwartz et al., 1995; Vanier et al., 2003; Van Wauwe et al., 1990), the proposed teratogenic mechanism for FLUCO is the

inhibition of CYP26 embryonic enzymes with the consequent increase in local RA levels. The observation in rodents embryos that the co-exposure to sub-teratogenic doses of both RA and FLUCO (62.5µM) leads to the same phenotype as the teratogenic doses of RA and FLUCO alone, definitively supported the hypothesis of local increase of RA as key event in FLUCO teratogenicity (Menegola et al., 2006; Menegola et al., 2004). Furthermore, exposure to FLUCO has been linked to altered gene expression of some CYP26 isoforms (increased expression of CYP26A1 and CYP26B1, but no changes in CYP26C1 expression) (Tiboni et al., 2009).

4. ETHANOL TERATOLOGY

Ethanol (**Fig. 7**) is a well-known teratogen agent in human population mainly taken by alcoholic beverages. Being a xenobiotic, its detoxification occurs at the hepatic level: it is oxidized, by the enzyme alcohol dehydrogenase (ADH), to acetaldehyde, which is again oxidized to acetate by the enzyme aldehyde dehydrogenase (ALDH).

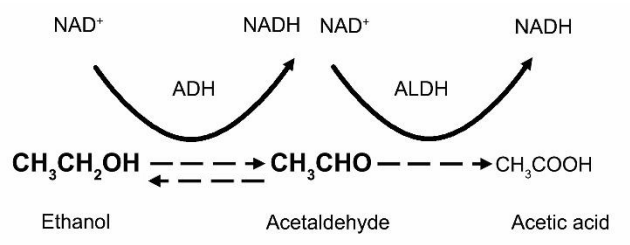

Fig. 7. Chemical reaction of Ethanol metabolism

The abuse of alcoholic substances involves a series of complications at the physiological, psychological and sociological level. Therefore, prevention and information programs to avert alcohol abuse and promote the responsible consumption of alcoholic beverages, play an important role both at social and individual level. Controlling alcohol intake is even more important for pregnant women, because of the dose-dependent teratogenic effects that ethanol can exert on embryos developing (Ornoy and Ergaz, 2010). For this reason, the general recommendations are to avoid completely the intake of alcohol during pregnancy. Both ethanol and its metabolite (acetaldehyde) are small non-ionized hydrophilic molecules able to cross easily the placenta. Waltman and Iniquez (1972) have shown that ethanol, administered intravenously to the mother at the time of delivery, traverses the placenta and, within 1 minute, is present in the bloodstream of the newborns.

Ethanol consumption during pregnancy can produce a wide range of physical, cognitive, and behavioural disabilities in newborns classified in a recognised syndromic picture named as foetal alcohol spectrum disorder (FASD) (Abel and Hannigan, 1995). The most severe form, that includes morphological abnormalities, is defined as foetal alcohol syndrome (FAS) (de Sanctis et al., 2011; Joya et al., 2012; Memo et al., 2013) and is characterized by microcephaly, flat midface with short palpebral fissures, low nasal bridge with short nose and long smooth or flat phyltrum (de Sanctis et al., 2011). In studies on postimplantation rat embryos exposed *in vitro* to Eth, the reported malformations are mostly neural tube defects, rotation and cardiac abnormalities and hypoplasia of the first branchial arch (Giavini et al., 1992; Deltour et al., 1996;

Duester, 1998; E. Menegola et al., 2001; Kot-Leibovich and Fainsod, 2009). FAS pathogenesis has been deeply investigated and the altered pathway, by which Eth acts as teratogen, comprise:

- Action on neural crest cells. In a study on *Xenopus laevis* NCCs after exposure with ethanol, Shi and colleagues found abnormalities in the migration of these cells, and abnormalities at the level of pigmentation and the trunk. Increasing the dose of alcohol, the NCCs migration decreased until they entirely ceased (2% ethanol) (Shi et al., 2014). The *Xenopus laevis* NCCs behaviour in culture was also studied: the NCCs showed abnormalities when treated with ethanol, such as a reduction of the number of migration cells and disorganization of their migration pattern (Czarnobaj et al., 2014).
- Increased levels of apoptosis among NCCs (Kotch and Sulik, 1992; Ewald and Shao, 1993; Holownia et al., 1997; Ikonomidou, 2000; Climent et al., 2002; Light et al., 2002; Kilburn et al., 2006).
- Impaired signalling by transcription factors or growth factors, including RA (Miller and Kuhn, 1995; Smith, 1997; Sulik, 2005; Yelin et al., 2005; Zhou et al., 2011).
- Metabolic stress (including oxidative stress) (Kotch et al., 1995).

The characterization of the mechanism by which ethanol exerts its teratogenic effects is difficult due the pleiotropic nature of its action. It is not possible to study all the processes simultaneously involved, but it is possible to explore some of them in order to better understand the mechanisms, the main target and the developmental stage of effect (Kiecker, 2016).

5. STATE OF THE ART ON THE RISK ASSESSMENT FROM EXPOSURE TO MIXTURES OF CHEMICALS

In the last years, the effects on human health and environment after exposure to different multiple chemicals have become an item of concern. These effects are known as “mixture effects”. The European Parliament pointed the attention to the need to consider the risk assessment of chemical mixtures within the context of EU (European Union) legislation on chemicals.

The risk assessment of exposure to mixtures and the estimation of potential interactions between chemicals are very complex problems. They are also problems of great importance since human exposure, both in the living environment both in the workplace, is characterized by the simultaneous presence of a multiplicity of chemical substances. It should be emphasized that, despite the availability in the literature of numerous toxicological studies on the interactions between chemical agents, the current knowledge about the mechanisms of interaction between chemicals is rather limited and has gaps. A European Commission has been asked to assess how and whether relevant existing legislation adequately addresses risk from exposure to multiple chemicals from different sources and pathways, and on this basis to consider appropriate modifications, guidelines and assessment methods (European Commission, 2009).

First, it is appropriate to define what a mixture, the risk and the risk assessment are:

- MIXTURE: any combination of two or more chemicals, regardless of source and spatial or temporal proximity, that may jointly contribute to actual or potential effects in a receptor population (EPA, 1986).
- RISK: chance of harmful effects to human health or to ecological systems resulting from exposure to an environmental stressor that may be a physical, chemical or biological entity.
- RISK ASSESSMENT: it is the probability of the adverse health effects that may occur after exposure to a chemical, physical or biological entity.

The risk assessment is carried out through the analysis of three key moments:

1) HAZARD IDENTIFICATION: the process to identify the types of adverse health effects that can be caused by exposure to a stressor, and to characterize the quality and weight of evidence supporting this identification. For this purpose, the study of the toxicokinetic properties (absorption and distribution of the substance and/or of its metabolites) and the study of the toxicodynamics property (interaction among the substance and the target of

the toxic effect) of the tested chemical are needed. It is possible to understand the qualitative and quantitative aspects related to absorption, bioaccumulation potential, distribution, metabolism and elimination.

2) RISK CHARACTERISATION: the assessment of the significance of the toxic effects to the human species by applying the formula ADI = NOAEL / SF where
   ADI = (*Admissible Daily Intake*) is the dose, expressed in mg/kg of body weight, which can be taken daily by an individual for the entire lifetime without risk to health.
   NOAEL = (*No Observed Adverse Effect Level*) is the amount of a substance that does not cause adverse toxic effects. It is a value obtained from experimental studies and epidemiological observations.
   SF = (*Safety Factor*) It is the factor used to transform the NOAEL in ADI and depends on the nature of the toxic effect, on the type of the at-risk population and on the quality of the toxicological information available.
3) Human exposure assessment based on theoretical or analytical data.
   The final stage of the process is the comparison of the knowledge gained during the risk characterization process with data collected on human exposure. The greater the distance between the ADI and the exposure value, the higher the confidence level and then lower the probability that individuals should run into a risk for health.

The 95% of the resources in toxicology was devoted to studies on single chemicals (Groten, 2000). Actually, since humans and all other organisms are typically exposed to multi-component chemical mixtures present in the surrounding environmental media (water, air, soil), in food or in consumer products (European Commission, 2009), the exposure to chemical mixtures is the rule rather than the exception. For this reason, the hazard identification, the exposure assessment and risk characterization should focus on mixture, rather than on the single compounds. As consequence, the interest of scientists and regulators in the toxicology and in the potential risk of combined exposures is growing and the risk assessment caused by exposure to chemical mixtures is suggested as an integral part of protecting public health (Feron et al., 1998; Groten, 2000). In 1986 the United State Environmental Protection Agency (EPA) published the Guidelines for the Health Risk Assessment of Chemical Mixtures (EPA, 1986). Recently, the Agency for Toxic Substances and Disease Registry (ATDSR) proposed studies on chemical mixtures as one of six priority research areas identified in its environmental public health agenda (De Rosa et al., 2004).

The major aims of research programs on the toxicology of chemical mixtures are: 1) to introduce the concepts of joint action and interaction and risk assessment of chemical mixtures; 2) to explore methods to predict and to identify hazardous combinations of chemicals relevant to humans (Feron and Groten, 2002).

To study the toxicity of chemical mixtures successfully and to assess their potential risk properly, the first step is to understand the basic concepts of joint action and interaction of chemicals. The toxicological effects of combinations of chemicals can be described as independent, additive or due to interaction (Wilkinson et al., 2000; Feron and Groten, 2002; Moretto, 2008).

The effects are **independent** (*Simple dissimilar action*) when the mechanism/ MoA and possibly, but not necessarily, the nature of and sites of the toxic effects differ between the chemicals in a mixture, and one chemical does not influence the toxicity of toxicity of another. The effects of the exposure are the combination of the effects that each compound would have caused when give alone (response-addition).

The **additive** effect (*Simple similar action*) is a non-interactive process, which occur when all the chemicals in a mixture act by the same MoA and differ only in their potencies. The effect of the exposure to the mixture is equivalent to the effect of the sum of the potency-corrected doses of each compound in the mixture (dose-addition). The principle of dose-addiction means that mixture effects are to be expected even when each chemicals is present below the No Observable Adverse Effect Level (NOAEL), because it is assumed that all chemicals in the mixture behave as if they were a dilution of one other (European Commission, 2009). Compounds acting with similar MoA are said to belong to a CMG. EFSA (*European Food Safety Agency*), according to EPA, proposed several criteria to identify a CMG regarding the pesticides (EPA, 2002; EFSA, 2009). A preliminary identification of substances that might cause a common toxic effect is based on chemical structure (core molecular structure, functional groups or their metabolic precursor) and on the mechanism of pesticide action, since it is assumed that substances that share similar chemical structure or the same mechanism of action can cause a similar toxic effect. Subsequently, a first refinement of the grouping can be performed by definitively identifying those substances that cause a common toxic effect. Then the toxic MoA by which each substance causes a common toxic effect is determined.

All other forms of joint action deviating from the two classes of combined toxicity that are described above, fall within the group of **interactions**. The combined effects can be stronger (synergistic, potentiating, supra-additive) or weaker (antagonistic, inhibitive, sub-additive) than would be expected on the basis of dose-addition for CMG compounds (Moretto, 2008).

All three basic principles are theoretical. Actually, one will most likely have to deal with these concepts simultaneously, especially when mixtures consist of more than two compounds and when the targets (individuals rather than cells) are more complex (Groten, 2000). It is therefore crucial to distinguish between simple and complex mixtures, according to which it will also change the risk assessment method. A *simple mixture* is defined as a mixture that consists of a relatively small number of chemicals (ten or less), the composition of which is qualitatively and quantitative known (Feron et al., 1998). Typical examples are a cocktail of pesticides or a combination of medicines. A complex mixture is defined as a mixture that consists of tens, hundreds or thousands of chemicals, the composition of which is qualitatively and quantitative not fully known (Feron et al., 1998). Examples are welding fume, drinking water a workplace atmosphere and wood dust.

There are limited number of studies in literature on toxic effects from combinations of compounds at doses below their individual NOAEL, although the levels of human exposure to many different chemicals are generally low and below the NOAELs. The major concern is therefore the possibility of a mixture effect even when these substances are present at low concentrations. In agreement with Jonker et al. (1996), Moretto (2008) collected the most relevant data of *in vivo* and *in vitro* studies with mixtures whose components have doses or concentrations at or below the effect level and obtained that:

a) Mixtures of compounds sharing the same MoA show dose-additivity at low doses;
b) Mixtures of compounds sharing the same MoA generally show dose-additivity, although all possible combined affects may occur;
c) Mixtures of compounds not sharing the same MoA do not show dose-additivity at doses below the NOAEL;
d) Mixtures of compounds not sharing the same MoA show all possible combined effects at higher doses

These studies indicate that the type of combined action observed at clearly toxic-effect-levels does not predict what will happen at no-toxic-effect-levels, including levels below the NOAEL. Therefore, what happens at no-toxic-effect-levels is what counts in assessing the potential health risk of human exposed to mixtures.
Humans are exposed to an almost infinite number of possible combinations of chemicals. Is therefore required some form of initial filter that allows to focus on the potentially dangerous

mixtures. The EPA Guidelines of 2002 suggest to investigate a few mixtures considered "high priority" and to use those data for extrapolation to other environmental mixtures considered similar. The Commission proposed a number of criteria to focus and identify mixtures of potential concern:

1) Human exposure at significant levels;
2) Chemicals that are produced and/or marketed as multiple substances or commercial mixtures that contain several active ingredients and/or potentially dangerous substances;
3) Evidence for potential serious adverse effects for one or more chemicals at the likely exposure levels;
4) Likelihood of frequent or large scale exposure of the human population or the environment to the mixture;
5) Persistence of chemicals in the body and/or in the environment;
6) Evidence for potential interaction at levels of human and environmental exposure;
7) Predictive information on the action of such substances;
8) Particular attention to the mixtures with one or more components, which are assumed not to have a threshold effect.

Examples of mixtures considered high priority are diesel fuels, mixtures of PCBs (polychlorinated biphenyls) for which there is a large amount of toxicity data concerning commercial mixtures, PAH (polycyclic aromatic hydrocarbons), heavy metals, and pesticides. Exposure to multiple residues of pesticides derived from food is a common event in the general population. According to EU data, 53-64% of the food samples did not contain pesticide residues at detectable levels, 32-42% contained residues below the maximum residue levels (MRLs); 14-23% of the samples with residues contained more than one active ingredient (CEC, 2007). Therefore, exposure to mixture of pesticides occurs as a consequence of intake of food items containing multiple residues. Workers in productive industries, farmers and the consumers of agricultural products may be those who are most at risk of exposure. Hence, there is a reason for conducting the risk assessment of exposure to mixture of pesticides, keeping in mind that doses to which people are exposed are relatively low.

Once given priority to a mixture, we need to focus on the methods to be developed to extrapolate the exposure and toxicity estimates. The EPA's 2002 guidance distinguishes between specific risk assessments methods for complex mixtures and for simple mixtures.

For complex mixtures, particularly those that consist of commonly, produced commercial or industrial mixtures (e.g. diesel fuels), the preferred method is the use of mixture toxicity data

considered in its totality. With the release of the mixtures in the environment, however, the components of the mixture can be altered. Then, the mixture for which there are toxicological data can no longer be identical in composition to the mixture released into the environment.
For simple mixtures, the approach based on the risk assessment of the single mixture components can be used. The EPA Guidelines of 2002 suggest, in the absence of adequate information on the presence of chemical interactions, to assume a situation of non-interaction and recommend the use of the models of dose additivity if the MoA are identical or similar. To ensure an appropriate level of protection in the absence of adequate data or when the MoA are different, it is still preferable to use an approach based on dose additivity which will not underestimate the toxicity of the mixture. There are different methods used for the calculation of dose additivity. The best known is the TEF (*Toxic Equivalency Factor*), widely used for the evaluation of mixtures of dioxins. Other methods are the RPF (*Relative Potency Factor*) and the HI (*Hazard Index*). Despite the dose additivity has proved effective in predicting and evaluating the toxicity of mixtures, recent studies suggest that the similarity of molecular initiating events (MIEs) is not an essential requirement to induce additive effects, because mixtures composed of chemicals with different MIEs can exhibit mixture effects too, probably acting on the same biological pathway (EFSA, 2013). Recently, it has been argued that grouping criteria based solely on chemical similarity or similar mechanisms may lead to unrealistically narrow groupings, with the exclusion of chemicals that also might contribute to combination effects (Boobis et al., 2011). This is in recognition of emerging evidence that biological effects can be similar, although the molecular details of toxicological mechanisms may profoundly differ in many respects (Kortenkamp, 2007).

The analysis of the methodologies for mixtures risk assessment allowed us to highlight the main limitations and weaknesses of these approaches, highlighting which are the aspects to be improved and which need further study in the future. Analysis reveals three main problems: 1) there are little toxicological data on most of the mixtures of chemicals; 2) the majority of the available data only covers the evaluation of binary interactions between substances; 3) there are few studies on chronic exposure to low concentrations, despite it represents the most common situation for environmental exposures.

The large current gaps are:

- It is ignored in such places, how often and to what extent, humans and the environment are exposed to certain mixtures and how the exposure may change over time.

- The composition, especially of complex mixtures, is never known at all.
- For many substances, we do not have reliable information on the mode of action. Moreover, it is very difficult to know all the modes of action that may arise in different types of organisms of a complex biological community.
- It is difficult to predict the interaction (strengthening, synergism) of chemicals in mixtures, in particular the long-term effects. In addition, the generalized use of models of non-interaction (dose or response additivity) does not take account of the possibility of interactions.
- We do not consider the fact that both the mechanisms of action and the mechanism of interaction of the chemicals are dose dependent with different effects and/or possible interactions at different dose ranges.

The last one is a particularly critical point, as most of the studies on mixtures available in literature are experiments of exposure to high doses on a reduced number of components of the mixture. Actually, most of the human and environmental exposures occur at low doses and in the presence of complex mixtures (CEC, 2007).

Despite gaps in knowledge and data, a better systematic in evaluating the toxicity of mixtures is possible. The next steps of the scientific challenge to the toxicology of mixtures are:

- To better understand humans and environmental exposure to mixtures by monitoring and by mathematical modelling in order to be able to predict the risk.
- To establish criteria for defining the "relevant" components of a mixture, which do not take into account only the concentration but also of the contribution to the general toxicity.
- To establish the criteria under which characterize or predict a mode of action.
- To define the conditions that can lead to potentiation or synergy situations, and to determine which the probability of their occurrence is.

The assessment of exposure to chemical mixtures is certainly a very complex issue. Especially considering that, although methodologies for the identification of priority mixtures and for the risk assessment are available, there are serious gaps in knowledge and in data that limits the ability to assess properly the mixtures.

To reached the hoped more systematic evaluation of the toxicity of mixtures, in the context of EU regulations, the European Commission will issue some technical guidelines in order to:

- Promote a consistent approach to the assessment of priority mixtures;

- Promote the development of knowledge about the chemical mixtures to which human populations and the environment are actually exposed;
- Fill gaps in knowledge, especially regarding the mode of action of chemicals and of prediction of the interactions.

In general, risk assessment of combined exposure to mixtures poses several challenges to scientists, risk assessor and risk manager, such as the need for assessing an ever-increasing number of chemicals, while reducing animal use, costs and time required for chemical testing (EFSA, 2013). Although the evaluation of the teratogenic risk of chemicals should be based primarily on tests of treated animals (*in vivo* exposure), in recent years we are trying to develop and validate alternatives to *in vivo* testing, such as testing *in vitro* or *in silico* or the application of integrated approaches at different levels. Those approaches can also contribute to the improvement and the reduction of conventional tests on the animal model (Landesmann et al., 2013). Therefore, a mechanistic approach and the development of integrated models are crucial to assessing mixtures' risks.

6. ALTERNATIVE MODELS IN DEVELOPMENTAL TOXICICTY EVALUATION

As society progresses through the second decade of the 21st century, there is increased need to develop new ideas and new information in the practice of toxicology and risk assessment. In addition, there is a societal pressure to reduce the use of animals; hence, greater emphasis is put on alternative methods to assist in making decisions regarding risk assessment. Together with the need for toxicity evaluations for the large number of chemicals in commercial use, new *in vitro* and *in silico* technologies and computational system biology to complement, and eventually replace, whole animal testing need to be introduced or, when already in place, their use greatly increased (Moretto et al., 2015).

6.1. ANIMAL MODELS

6.1.1. Whole Embryo Culture (WEC)

The rodent whole embryo culture technique was first introduced in 1960s by the pioneering research of Denis New (New, 1978). WEC is a technique by which postimplantation embryos are removed to an *in vitro* environment capable of supporting normal growth and development from pre-somite to the limb bud stages of organogenesis. This method gave to embryologist and teratologists an unprecedent degree of access to the developing embryo: they could for the first time directly observe, treat, and manipulate embryos in order to characterize the pathogenesis of teratogenic agents and elucidate mechanism of action (Ellis-Hutchings and Carney, 2010). New's work on WEC started with chick embryo model, which unfortunately did not allow more detailed manipulations, which required separation of the embryo from the yolk sac. The use of chicken embryo was finally replaced in the early 1960s by the use of rodent embryos: rats (*Rattus norvegicus*) and mice (*Mus musculus*) are the most used in experimental studies of developmental biology and still constitute the major animal models for mammals. The choice of these rodent species was critical in that the embryos, at the beginning of their development, form a transient visceral yolk sac that is closely apposed, but not physically attached to the maternal system. So that the embryo and the amnion enclosed within the visceral yolk sac could be explanted intact, hence the name "whole" embryo culture (Ellis-Hutchings and Carney, 2010). The culture of postimplantation rat embryos from 9.5 days *post coitum* (late gastrula/early neurula stage) allows to support embryonic development for a duration of 48 hours at which the embryo reaches the phylotypic stage (period in which all the vertebrate embryos have the same

features) (**Fig. 8**). It is possible to prolong the culture for additional 12 hours maximum in which, however, the development is slower compared to the *in utero* development.

With the ability to culture postimplantation embryos *in vitro*, came the need to devise quantitative end points for evaluating the effects of treatment on various aspect of development. Standards end points included viability (presence of a heartbeat and blood cells circulating through the vitelline vessels) and growth, as measured by somite count and crown-rump length. In addition, quantitative morphological scoring system were devised in which a suite of developmental landmarks were assigned numerical scores reflecting their progression of development (Nigel A. Brown and Fabro, 1981).

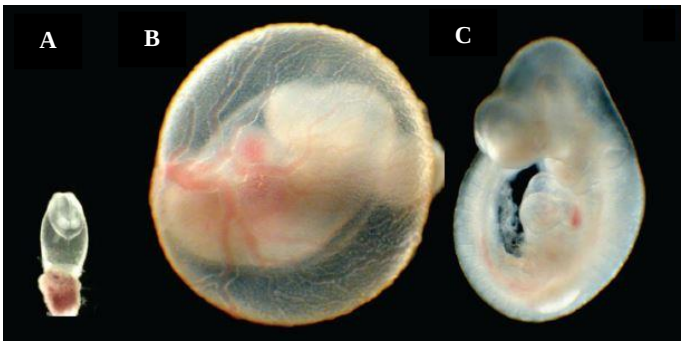

Fig. 8. Development of postimplantation rat embryos in WEC: **A:** gestational day 9.5 rat embryo used at the start of culture. **B:** rat embryo cultured for 48 hours in enclosed visceral sac. **C:** rat embryo cultured for 48 hours after removing of extra-embryonic membranes, left side view. (Figure from Flick and Klug, 2006)

WEC, as an *in vitro* technique, has ethical, financial and scientific advantages over *in vivo* tests. It is suitable for the assessment of a very wide range of different teratogenic agents including drugs, pesticides, environmental chemicals, nutritional excesses and deficiencies, and physical factors. It also has been used to asses many different types of research question, including: (1) to distinguish between maternally-mediated effects apart from direct actions on the conceptus, (2) identifying which features of chemical structure drive teratogenic potency within a given class of compounds, and (3) elucidating the toxicokinetic determinants of teratogenicity. Finally, the use of the WEC allows embryos to be chosen at constant and optimal stages, permits continuous exposure at selected concentrations, and makes it possible to stop the development at selected critical stages (Ellis-Hutchings and Carney, 2010).

The impact of WEC on the field of teratology has been enormous and there are a number of different applications and discoveries that could exemplify WEC contributions to this field:

- Identification of proximate teratogen, which in many cases is not the administered compounds, but a metabolite (Nagano et al., 1981; Yonemoto et al., 1984; Horton et al.,

1985; Clarke et al., 1991; Dorman et al., 1995; Carney et al., 1996; Andrews et al., 1998; Klug et al., 2001).

- Study of mother temperature changes associated with influenza or hypoglycaemia (Cockroft and New, 1978).
- Mechanistic studies of teratogenicity induced by oxidative stress produced by radiation (Manda et al., 2007), nitric oxide (Lee and Juchau, 1994), alcohol (Kotch et al., 1995) and thalidomide (Hansen et al., 1999; Parman et al., 1999).
- Study of alteration in the expression of left-right polarity (Fujinaga et al., 1990).
- Study of the direct effects on the embryo of nutrient excess or deficiency, as well as the interference with embryonic nutrition as a mode of teratogenic action. It is with retinoids that there is a direct link between WEC and human reproduction since there is a good correlation between rat embryo studies *in vitro* and *in vivo* and clinical malformations (Morriss and Steele, 1974, 1977; Steele et al., 1987; Klug et al., 1989).
- Study of the pathogenic pathway involved in teratogenic processes induced by exposure to triazole derivatives and mixture of fungicides (E. Menegola et al., 2006; Menegola et al., 2013).

WEC is also useful to molecular techniques such as whole mount in situ hybridization and whole mount immunohistochemistry to assess gene and protein expression, respectively (Ellis-Hutchings and Carney, 2010).

WEC technique has been also validated by the European Centre for the Validation of Alternative Methods (ECVAM) in 2001 (Anon, 2002) as a screening and/or prioritization tool for pharmaceutical, agricultural, and industrial chemicals.

6.1.2. Ascidian Embryo Teratogenesis Assay (AET)

Ascidians are marine sessile, filter-feeding organisms ubiquitous through the world and belonging to the sub-phylum Urochordata or Tunicata. Phylogenetic analysis, performed comparing the sequences of 5S and 18S ribosomal ribonucleic acid (rRNA), recognized the sub-phylum Urochordata as the sister group of vertebrates and there is a big gap between ascidians and other invertebrates (Delsuc et al., 2006). As adults, ascidians are sessile filter feeders and the entire body is invested with a thick covering: the tunic, from which the name "tunicate" is derived. One of the major constituents of the tunic is cellulose (Satoh, 1994). Indeed, these animals are the only known metazoan able to synthesize cellulose, a capability probably acquired through a lateral transfer of genes from bacterial genome (Passamaneck and Di Gregorio, 2005). Particularly, ascidian embryos display striking similarities to vertebrate ones as they develop through a swimming, tadpole like larva, which represents a simple prototype of the chordate body plan (Passamaneck and Di Gregorio, 2005), comprising a hollow neural tube lying dorsal to a rod-like notochord (Satoh, 1994).

The solitary ascidian *Ciona intestinalis* is one of the most cosmopolitan and studied species. The tadpole larva consists of only ~2,600 cells, which constitute all the organs including epidermis, central and peripheral nervous system, endoderm and mesenchyme in the trunk, notochord and muscles in the tail (Satoh, 2003). In addition, early embryos are well suited for experimental analysis; in fact, they are relatively transparent with an overall dimension of 200 µm. The blastomeres are large and easy to manipulate. Ascidian embryogenesis is rapid, taking ~18 hours from fertilization to the development of a free-swimming tadpole at 18°C, and the entire life cycle takes 3 months, which facilitates genetic analyses. *C. intestinalis* genome has been sequenced and it consists of ~16.000 genes, approximately half the number present in the human genome (Dehal, 2002). The small size of this genome provides further advantages for understanding genome organization and gene function (Passamaneck and Di Gregorio, 2005). Finally, transgenic DNA can be introduced into developing embryos using microinjection or even simple electroporation methods, which allow the simultaneous transformation of hundreds, even thousands, of synchronously developing embryos (Satoh, 2003).

One peculiar characteristic of the late tailbud and larval phases is the detection in trunk region of some migrating cells called Neural Crest Like Cells (NCLCs) supposed to be the precursor of the neural crest cells (NCCs), traditionally considered as a vertebrate innovation (Jeffery, 2007). In ascidians, NCLCs were first described in *Ecteinascidia turbinata*, where clusters of cells displayed long distance migration from the dorsal midline during embryo development (Jeffery

et al., 2004). Subsequently, NCLCs were identified in several ascidian species, including both colonial and solitary ones (Jeffery, 2006). In *C. intestinalis* hatching larvae, these scattered cells are localized lateral and posterior to the sensory vesicle. In swimming larvae, these cells appeared to migrate anteriorly toward the developing oral siphon (Jeffery et al., 2008). The most striking similarity between ascidian NCLCs and vertebrates NCCs is their common role in pigment cell development. These resemblances support the possibility that the ascidian and vertebrate cells had a common origin during chordate evolution, perhaps originating from a primordial neural crest cell with a primary role of generating body pigment cells. While maintaining their primary function in ascidians as well as in vertebrates, in the vertebrates' lineage the primordial neural crest cell subsequently evolved many additional fates (Jeffery, 2006).

During embryogenesis of ascidians, RA is a crucial morphogen too (Stoilov et al., 2001; Nagatomo and Fujiwara, 2003). It was seen, in fact, that excess of RA can induce deficiency mainly in the anterior neural tissues, such as the adhesive organ (papillae) with sensory neurons, forebrain containing sensory organ pigment cells (De Bernardi et al., 1994; Katsuyama et al., 1995) and pharyngeal gill slits (Hinman and Degnan, 1998). In addition, Nagatomo et al. identified *Ciona* homologs of the RA pathway enzymes RALDH2 and CYP26. The Ciona homolog of RALDH2, Ci-RALDH2, was expressed in a few muscle-lineage blastomeres in the middle gastrula. Strong expression was then restricted to the anterior-most three muscle cells on each side of the tailbud embryo. The *Ciona* CYP26 homolog, Ci-CYP26, was expressed in the anterior neural tissues and presumptive papilla region in the middle gastrula. The non-overlapping expression domains of Ci-RALDH2 and Ci-CYP26 look similar to those in vertebrates, although the expression of both genes was restricted to a small number of cells in *Ciona* embryos (**Fig. 9**) (Nagatomo and Fujiwara, 2003). Moreover, treatment with RA upregulate Ci-CYP26 expression, slightly downregulate Ci-RALDH2 expression and shifts anteriorly the expression of CiHox-1 (homolog of the vertebrate RA target gene Hox-1) in the tailbud embryo (Katsuyama et al., 1995; Nagatomo and Fujiwara, 2003). The Ci-CYP26 expression in neck region, as well as CiHox-1 expression, may be induced by endogenous RA. These data suggest that a role for RA-dependent Hox codes in specifying the antero-posterior identities was probably present at the base of chordates (Campo-Paysaa et al., 2008).

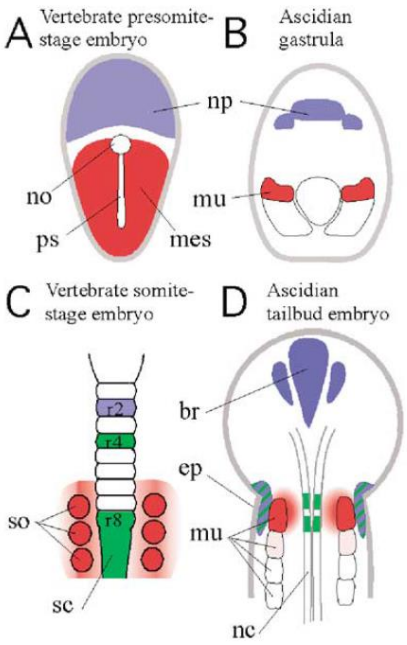

Fig. 9. Gene expression pattern in gastrulae and tailbud embryos of vertebrates and ascidians. All illustrations are dorsal view and the anterior is to the top. Expression of CYP26, RALDH2 and Hox-1 is indicated in blue, red and green, respectively. Putative secretion and diffusion of RA is also indicated in red. **A:** Vertebrate presomite-stage embryo. **B:** Ascidian gastrula. **C:** Vertebrate somite-stage embryo. **D:** Ascidian tailbud embryo. br, brain; ep, epidermis; mes, mesoderm; mu, muscle; nc, nerve cord; no, node; np, neural plate; ps, primitive streak; sc, spinal cord; so, somite. (Figure from Nagatomo and Fujiwara, 2008)

Thanks to their cosmopolitan distribution, basic body plan (Satoh, 2003) and key phylogenetic position (Delsuc et al., 2006), ascidian larvae have been proposed as an excellent alternative experimental system for investigating the mechanisms underlying the development of chordates (Passamaneck and Di Gregorio, 2005; Sasakura et al., 2012), and therefore of vertebrates, and for applying embryo-toxicity tests (Cima et al., 1996; Zega et al., 2009; Matsushima et al., 2013).

Ascidian embryos have been proposed as suitable models to evaluate embryotoxicity related to xenobiotic exposure (Pennati et al., 2006; Zega et al., 2009). Previous studies reported that ascidian larvae exposed to different azole fungicides showed characteristic malformations resembling those elicited by RA (Pennati et al., 2006; Groppelli et al., 2007; Zega et al., 2009). In both the analysed species, *Phallusia mammillata* and *Ciona intestinalis*, azole-induced malformations affected the anterior region of the trunk, in which the sensory vesicle appeared reduced and the pigmented organs were severely altered. Moreover, the development of the adhesive papillae, the anterior most organs, was impaired. Similarly, larvae exposed to RA displayed truncation of the anterior structures and malformed sensory vesicle (Hinman and Degnan, 1998; Nagatomo and Fujiwara, 2003; Kanda et al., 2009). This observation suggests that, similarly to what proposed in vertebrates, in ascidians the teratogenic action of azoles depends on perturbation of RA pathway (Pennati et al., 2006; Groppelli et al., 2007; Zega et al., 2009).

6.2. *IN SILICO* MODELS

Strategies for the safety evaluation of combined exposures and complex chemical mixtures, and models facilitating the interpretation of findings in the context of risk assessment of mixtures have become increasingly important. Key to further maturation of mixture toxicology is the development of integrated approaches between experimental toxicology, biomathematics, biology, bioengineering, pharmacology and model developing to ensure parallel and coordinated research in this challenging area of toxicology (Groten et al., 2001). In addition, ethical, scientific, and economic needs are driving the reduction of toxicity testing in animals, with the eventual aim of complete replacement. An integrated testing strategy is any approach to the evaluation of toxicity which serves to reduce, refine or replace an existing animal procedure, and which is based on the use of two or more of the following: physicochemical data, *in vitro* data, human data (epidemiological, clinical case reports), animal data (where unavoidable), computational methods and biokinetic models (Blaauboer et al., 1999).

However, the knowledge about the relationships between the administered dose of a chemical and its effects still presents gaps. To fill those gaps, two solutions are available: (1) increasing the complexity of *in vitro* systems to reproduce tissues and interactions between them or (2) using computational (*in silico*) modelling to simulate numerically the behaviour of the complex systems, starting from *in vitr*o data to provide model parameter values. Those solutions are complementary in the sense that some, even if limited, amount of mathematical modelling will be needed anyway to scale up the results of *in vitro* assays to a whole body. Conversely, better *in vitro* systems will provide better input data to mathematical models (Quignot et al., 2014). *In silico* methods to predict toxicity of chemicals have been widely used in environmental sciences for over 40 years, and provide a simplistic representation of a system (hence the complexities of interactions ad processes within an organism cannot be fully characterized) based on that the activity effected by a chemical is a consequence of its physico-chemical and structural properties. Hence, knowledge of a chemical's properties (or knowledge of related chemicals) can be used to make predictions on activity (Madden et al., 2014).

One challenge in this field arises from the need to have models for dosimetry (the delivery of active forms of the test molecules/metabolites to target tissues) and for responses (the manner in which the molecular and cellular interactions of toxic compounds cause perturbations leading to an adverse response) (Andersen et al., 2005). The models for dose - response are conveniently dichotomized as pharmacokinetic (PK) and pharmacodynamic (PD) models. PK or toxicokinetics describes quantitatively the fate of molecules in the body; PD or toxicodynamics

focuses on their effects (therapeutic or toxic) at the biological target level. It is classical to differentiate PK from PD, but they form a continuum and may feedback one on each other. Obviously, PK conditions PD, since the timing and intensity of effects on a given target depend on the concentration time course of the active chemical species (parent molecule or metabolites) at that target site (Quignot et al., 2014). To have confidence in predictions from PK and PD models, these models need to be biologically realistic. Physiologically based (PB) models, both PBPK and PBPD models, assume then a central role in quantitative extrapolation from *in vitro* data. PBPK models investigate variables such as the rates of absorption, distribution, excretion, and biotransformation of chemicals and their metabolites. In toxicology research and chemical risk assessment, they are used to make more accurate predictions of target tissue dose for different exposure situations (Andersen, 1995). One risk assessment goal is co-ordination of PBPK models to create biologically based dose–response (BBDR) models that predict expected incidence of adverse responses for varied exposure situations (Andersen et al., 2005).

Another trend is the development of systems biology models for predictive toxicology and for efficient quantitative *in vitro* to *in vivo* extrapolations (QIVIVE) (Geenen et al., 2012; Hamon et al., 2015). Systems biology models are characterized by synergistic integration of theory, computational modelling, and experiments. This new discipline has provided a framework for investigating the interactions between the separate parts of biological systems in order to understand its functioning (Kitano, 2002). An important part of systems biology is therefore collecting the experimental data of components of a system into a mathematical model (Alberghina and Westerhoff, 2005) and integrating that model over time. The information gained from modelling is of particular relevance. Firstly, comparisons between experimental observation and the mathematical model behaviour can link knowledge of system components to explanations of system behaviour. Secondly, *in silico* experiments can be carried out on the model to test the effects of perturbations on the system and to identify the processes that control the system. These experiments may either be only feasible using a computer, or are faster and cheaper than laboratory experiments (Bakker et al., 2000).

Biological systems are highly complex due to both the number of components present and the nonlinear interactions between them (Kitano, 2002). In order to understand emergent properties of the system, the interactions between the components must be studied. For toxicology, using models in terms of rate equations and balance equations, together culminating in ordinary differential equations (ODEs), would be beneficial as it is a well-understood formalism, fast and

mathematically robust. In the ODE methodology, the biochemistry of the reactions is essentially translated into mathematics. The biological system and the corresponding network of chemical reactions are described in terms of a set of balance equations with reaction stoichiometries indicating which metabolite is produced or consumed in which reaction, plus a set of reaction rate equations. The ODEs resulting from the combination of these two sets are then solved using numerical methods. Enzymes or transporters catalyse most processes in biological systems. Examples of well-known and popular equations used to describe enzyme-catalysed reactions are Michaelis–Menten kinetics and Hill equation, which express the dependence of the reaction rates on the concentrations of the small molecules in the systems (Cornish-Bowden, 1979).

In the past, modelling has been unattractive to experimental biologists due to the necessity to acquire extensive programming and mathematic knowledge. This should no longer be the case. There are a number of software packages to perform several mathematical tasks and to make modelling more user-friendly. One of those is GNU MCSim, which is a numerical simulation and Bayesian statistical inference tool for algebraic or differential equation systems. GNU MCSim was created specifically to perform Monte Carlo analyses in an optimized, and easy to maintain environment (Bois, 2009).

In addition, the accumulation through the years of experimental data on structure and function of proteins, and on the relationship between them, features an extensive database, from which general rules have been derived. The database may indeed be used to predict the properties of incompletely characterized to entirely uncharacterized proteins based on current biochemical knowledge using computational procedures. The *molecular docking*, for example, is a computer simulation technique used to predict the preferred orientation of one molecule (such as a small-size ligand) relative to a second molecule (such as a protein) when they are bound in a complex. This knowledge is then used to evaluate the strength of association, or binding affinity, using suitable statistical scoring functions (Gianazza et al., 2016). *Molecular Operating Environment* (*MOE*) is a leading drug discovery software platform, which allow the *molecular docking* investigations (Chemical Computing Group, Montreal, Quebec, Canada). *MOE* integrates visualization, modelling and simulations, as well as methodology development, in one package. *MOE* scientific applications are used by biologists, medicinal chemists and computational chemists in pharmaceutical, biotechnology and academic research.

7. AIM OF THE WORK

Exposure of the embryo to environmental chemicals (pesticides, air and water pollutants) can result in congenital malformations or developmental defects such as oro-facial cleftings. Unfortunately, the human embryo is not usually exposed to a single substance, but to many substances simultaneously. In fact, evaluating the toxicity of mixtures of multiple chemicals is one of the major objectives of today's toxicology, despite the effect of exposure to a mixture is still difficult to understand.

The EPA Guidelines of 2002 suggest to investigate a few mixtures considered "high priority" and recommend the use of the models of dose additivity in the absence of adequate information on the presence of chemical interactions. However, recent studies suggest that the similarity of molecular initiating events (MIEs) is not an essential requirement to induce additive effects, because mixtures composed of chemicals with different MIE can exhibit mixture effects too, probably acting on the same biological pathway and contributing to the same adverse outcome (EFSA 2013). In addition, it has been argued that grouping criteria based solely on chemical similarity or similar mechanisms may lead to unrealistically narrow groupings, with the exclusion of chemicals that also might contribute to combination effects (Boobis et al., 2011). This is in recognition of emerging evidence that biological effects can be similar, although the molecular details of toxicological mechanisms may profoundly differ in many respects (Kortenkamp, 2007). It appears evident that a clear and efficient test strategy for risk assessment of mixtures is still lacking. Furthermore, there is an increasing societal need to reduce animal testing.

To arrive in the future to the creation of a realistic overall picture of human exposure to mixtures, the development of integrated approaches between *in vitro* and *in silico* techniques and computational systems biology able to predict the effects of mixtures starting from the concentrations of their individual components will be essential.

Mechanistic studies of some teratogenic agents such as retinoids, ethanol and some pesticides of the class of the azoles fungicides suggested that they could exert their teratogenic action by interfering with the same pathway. From literature data, it is clear that ethanol (Eth) and azoles can lead to the same adverse outcome (craniofacial abnormalities after embryonic exposure) probably acting with different MIEs both potentially converging on Retinoic Acid (RA) metabolic pathway, altering the RA production (Eth) and the RA catabolism (azoles) (Menegola et al., 2000, 2001, 2003, 2005a, 2005b; E. Menegola et al., 2006; Menegola et al., 2006b; Di

Renzo et al., 2007, 2011a, 2011b; Deltour et al., 1996; Dunty Jr. et al., 2002; Kot-Leibovich and Fainsod, 2009; Kane et al., 2010).
Data previously obtained described specific teratogenic effects (reduction and fusion of branchial arches mediated by altered hindbrain segmentation and neural crest migration) in postimplantation rat whole embryos cultured *in vitro* in presence of some azole fungicides alone or in binary mixtures. Results showed a clear concentration-response effect for single fungicides while co-exposure resulted in an additive effect. The observed additive effect of the binary mixture supports the hypothesis that the tested individual substances share the same mode of action (inhibition of CYP26 enzymes involved in retinoic acid, RA, catabolism with subsequent local increase in endogenous RA levels) and that azole fungicides constitute a common mechanism group.

Considering these premises, the aim of my work is to investigate our hypothesis through the development of an *in silico* model, validated by *in vitro* experiments, useful to simulate and predict the effects on embryo development after co-exposure to different classes of substances with independent mode of action (MoA) but acting on the same pathway and potentially contributing to the same adverse outcome.

For this purpose, three parts were considered.

- In the first part, post-implantation rat embryos were cultured using the *in vitro* technique Whole Embryo Culture (WEC) in presence of RA, Fluconazole (FLUCO), ethanol (Eth) and mixtures of FLUCO and Eth, in order to draw the toxicity dose-response curves.
  FLUCO was chosen because it is a well-known azole fungicide whose mode of action is the inhibition of CYP26 enzymes involved in RA catabolism, whereas Eth was chosen because it is a well-known teratogen which probably affects the RA metabolic pathway by altering its production. To better characterize the contribution of each component to the observed effects, the mixtures will be obtained with the "fixed + moving" approach, in which embryos were exposed to the no effect concentration of one chemical ("fixed") and increasing concentrations of the other chemical ("moving"). So that, it would be possible to test the feasibility of using *in vitro* methods to refine cumulative assessment groups and to assess the outcome of combined exposures. In particular to confirm or discount the dose-additivity hypothesis for compounds having different mode of action but potentially contributing to the same adverse outcome.

An additional mixture obtained co-exposing embryos to the no effect concentrations of both RA and Eth was also performed. Data from the single substances and mixtures will be compared with those obtained for RA.

- In the second part, the mechanisms of action which we assume at the basis of the observed effects were evaluated through the development of a system biology model able to simulate both the formation of a RA gradient in the rat embryo hindbrain and its perturbation after exposure to azole fungicides, to Eth and their binary mixtures, starting from the concentration of the single substances. The model was developed using an integrated approach combining mathematical modelling, molecular docking and *in vitro* experiments.

  RA data (percentage of malformations at the branchial apparatus) from *in vitro* experiments were used to fit an empirical RA concentration-response model. The parameters for FLUCO and Eth were adjusted according to the fit to the previous experimental data and their affinities for CYP26 or ADH7 were computed following a computational approach based on molecular docking. Predictive simulations for the mixtures were then performed.

  To confirm the feasibility of the model, predictions of the effects of previous different mixtures of azoles were finally performed.

- The use of alternative models in toxicology has been strictly recommended to evaluate the potential effects of the co-exposure of chemicals in a mixture (EPA, 2002). Considering the data obtained in non-mammalian species, in the last part of this work the evaluation of the effects after co-exposure to FLUCO and Eth were performed using the ascidian *Ciona intestinalis* embryo model as a new alternative teratological screening test (AET, Ascidian Embryo Teratogenicity assay).

  Therefore, through comparative teratological analysis, it would be possible to reduce more and more the use of mammal models.

8. LEGEND OF ABBREVIATIONS

ADH	=	Alcohol dehydrogenases
AET	=	Ascidian embryo teratogenicity assay
AO	=	Adverse outcome
AOP	=	Adverse outcome pathway
BMD	=	Bench mark dose
CMG	=	Common mechanism group
CNS	=	Central nervous system
CRABP	=	Cellular RA-binding-protein
CYPRO	=	Cyproconazole
Eth	=	Ethanol
FASD	=	Foetal alcohol spectrum disorder
FGF	=	Fibroblast growth factor
FLUCO	=	Fluconazole
FLUSI	=	Flusilazole
FON	=	Triadimefon
KE	=	Key event
LAOEL	=	Lower observed adverse effect level
MIE	=	Molecular initiating event
MoA	=	Mechanism of action
MOE	=	Molecular operating environment
NCC	=	Neural crest cell
NOAEL	=	No observed adverse effect level
ODE	=	Ordinary differential equation
PBPK	=	Physiologically-based pharmacokinetic model
RA	=	Retinoic acid
RALDH	=	Retinaldehyde dehydrogenases
WEC	=	Whole embryo culture

PART 1:

PERTURBATION OF THE RETINOIC ACID PATHWAY

Introduction

Retinoic Acid (RA), a Vitamin A derivative, is a well-known morphogen in invertebrates and vertebrates and it is essential for normal embryonic development (Morriss-Kay, 1992; Ross et al., 2000). It is also known that the excess or deficiency during pregnancy can induce abnormalities in mammalian embryos and that the developing hindbrain and branchial region are particularly sensitive target tissue resulting in craniofacial defects (Maden and Holder, 1992; Kochhar, 2009). Studies *in vitro* on rodent embryos, showed that excess of RA influences craniofacial development in a stage-dependent manner causing alteration in the identity of branchial arches, cranial ganglia and rhombomeres at morphological and molecular levels (Lee et al., 1995).

Various studies demonstrated that the exposure, both *in vitro* and *in utero*, of rodent embryos to a number of azole derivatives is able to induce branchial malformations similar to those induced by excess of RA (Menegola et al., 2000, 2001, 2003, 2005a, 2005b; E. Menegola et al., 2006; Menegola et al., 2006b; Di Renzo et al., 2007, 2011a, 2011b). Considering these data and considering that a concentration-dependent inhibition of CYP26, involved in the catabolism of RA, has been reported *in vitro* and in patients with promyelocytic leukemia (Schwartz et al., 1995; Vanier et al., 2003), the proposed teratogenic mechanism for the azole fungicides is the inhibition of CYP26 embryonic enzyme with the consequent increase in local RA levels (Menegola et al., 2006a). The observation in rodents embryos that the co-exposure to sub-teratogenic doses of both RA (0.025 µM) and Fluconazole (FLUCO) (62.5 µM) leads to the same phenotype as the teratogenic doses of RA and FLUCO alone, definitively supported the hypothesis of local increase of RA as key event in FLUCO teratogenicity (Menegola et al., 2004; E. Menegola et al., 2006). Furthermore, the observed additive effects previously obtained by our research group after exposure to mixtures of azoles supports the hypothesis that all the tested individual substances share the same mode of action and that the class of the azole fungicides constitute a common mechanism group (Menegola et al., 2013).

Ethanol (Eth) is a well-known teratogen agent whose consumption during pregnancy can produce a wide range of physical, cognitive, and behavioural disabilities in newborns classified in a recognised syndromic picture named as foetal alcohol spectrum disorder (FASD) (Abel and Hannigan, 1995). In studies on postimplantation rat embryos exposed *in vitro* to Eth, the reported malformations are mostly neural tube defects, rotation and cardiac abnormalities and hypoplasia

of the first branchial arch (Giavini et al., 1992; Deltour et al., 1996; Duester, 1998; E. Menegola et al., 2001; Kot-Leibovich and Fainsod, 2009). The characterization of the mechanism by which ethanol exerts its teratogenic effects is difficult due the pleiotropic nature of its action. It is not possible to study all the processes simultaneously involved, but it is possible to explore some of them in order to better understand the mechanisms, the main target and the developmental stage of effect (Kiecker, 2016). One of the potential mechanisms, by which Eth acts as teratogen, is RA content impairment (Deltour et al., 1996; Kot-Leibovich and Fainsod, 2009; Kane et al., 2010). Early studies suggest that ethanol functions as a competitive inhibitor of the enzymatic conversion of retinol to RA, thereby lowering the overall levels of RA in the embryo (Duester, 1998). However, the exposure to ethanol could have also the opposite effect on RA level in the embryo: alcohol consumption is known to induce the enzymes involved in its catabolism and is related to the mobilisation of retinol stored in mother's liver, leading to increased retinoid exposure of the embryo (Kiecker, 2016). An effect of ethanol on the concentrations of RA likely would have a large impact on processes governed by vitamin A, including cranio-facial morphogenesis.

To verify the teratogenic mechanism exert by RA, FLUCO and Eth, post-implantation rat embryos were exposed to increasing concentration of RA (0.025, 0.0375, 0.05, 0.125, 0.25 µM), to increasing concentrations of Eth (17-42.5-85-127 mM), to increasing concentrations of FLUCO (62.5-125-250-500 µM), or co-exposed to binary mixtures of FLUCO and Eth, in order to draw its toxicity dose-response curve. Data from the single substances and mixtures were finally compared with those obtained for RA. *Whole mount* immunostainings were also performed at the end of the culture period in order to evaluate the distribution of CRABP1 (marker of neural crest cells at the phylotypic stage), CYP26A1, CYP26B1, CYP26C1 and ADH7.

Materials and methods

Materials and compound preparation

The medium used for the extraction of embryos from the uteri was sterilized Tyrode solution (Sigma); the medium used for the postimplantation whole embryo culture was undiluted heat inactivated rat serum added with antibiotics (penicillin 100 IU/mL culture medium and streptomycin 100µg/mL culture medium, Sigma). All-trans RA (Sigma, Italy), dissolved in DMSO, FLUCO (98%, Sigma), freshly dissolved in distilled water, and Eth (99.8%, Sigma) were used as test substances.

The primary antibody, used in order to specifically mark neural crest cells, was the mouse monoclonal anti-CRABP1 (ABR, Italy), diluted 1:500 in PBS; antibodies against CYP26a1, CYP26b1 and CYP26c1 (SantaCruz Biotechnology Inc, Italy) respectively diluted 1:100, 1:50, 1:100 in PBS. The secondary antibody was the anti-mouse or anti-rabbit-Ig-peroxidase (Fab fragment, Boehringer, Italy), diluted 1:40 in PBS. The staining was performed with the substrates 4-Cl-1-naphthol and 0.006% oxygen peroxide (Sigma, Italy).

Selection of compound concentrations

The concentrations of RA (0.025-0.0375-0.05-0.125-0.25 µM) were those used in previous published experiments, 0.025 µM being the No Observed Adverse effect Level (NOAEL), 0.5 µM the concentration teratogenic for 100% of embryos (Menegola et al., 2004). Groups of control + DMSO (5 µl DMSO per bottle) were also performed.

The concentrations of FLUCO (62.5-125-250-500 µM) were those used in previous published experiments, 62.5 µM being the No Observed Adverse effect Level (NOAEL), 500 µM the concentration teratogenic for 100% of embryos (Menegola et al., 2001). The concentration of Eth were 17-42.5-85-127.5 mM. The lower tested concentration of Eth is the well known not teratogenic concentration for postimplantation rodents embryos cultured *in vitro*, suggested for the use of Eth as solvent in postimplantation rodent embryo cultures (1µL/mL culture medium, corresponding to 0.1%, 17.35mM) (Kitchin and Ebron, 1984). Rat embryos were exposed to Eth alone (17-42.5-85-127 mM), to FLUCO alone (62.5-125-250-500 µM), or co-exposed to the NOAEL of Eth (17mM) and to different concentrations of FLUCO or were co-exposed to the NOAEL of FLUCO (62.5 µM) and to different concentrations of Eth. A control group (CONT) and a group of Eth 17 mM + RA 0.025 µM were also performed.

Embryo culture

Virgin female CD:Crl rats (Charles River, Calco, Italy), housed in a thermostatically maintained room (T = 22 ± 2 °C, relative humidity = 55 ± 5%) with a 12 h light cycle (light from 6.00 a.m. to 6.00 p.m.), free access to food (Mucedola, Milano, Italia) and tap water *ad libitum*, were caged overnight with males of proven fertility. The morning of a positive vaginal smear was considered day 0 of gestation. Embryos were explanted from pregnant rats at day 9.5 *post coitum* (p.c.) under aseptic conditions. Embryos at stage 1-3 somites (late gastrulation/ early neurulation) were selected and cultured according to the New's method (1978), modified by Giavini et al. (1992) in 20 ml glass bottles (5 embryo/bottle), containing 5 mL culture medium. The bottles, inserted in a thermostatic (37.8 °C) roller (30 rpm) apparatus, were periodically gas equilibrated according to Giavini et al. (1992). After 24 and 48 h of culture, embryos were morphologically examined and specifically processed for the whole mount immunostaining. At least three replications (bottles) were performed for each group.

Whole-mount immunostaining

Embryos were immunostained according to the method described by Wei et al. (1999). After 48 h of culture and morphological examination, embryos destined to immunostaining were fixed in Dent's fixative (1:4 in volume dimethyl sulfoxide: methanol) overnight at −20 °C. Stained cells appeared dark brown through the dissecting microscope. Images obtained from embryos of different groups were compared.

Acridine orange

In order to visualize apoptotic cells, the embryos exposed to Eth and to FLUCO were immediately stained with the vital dye acridine orange (Sigma, Italy; 5 mg/ml PBS), according to the method described by Abrams et al. (1993), washed in PBS, and viewed under a fluorescence microscope (EX = 450±490 nm; LP= 520 nm).

Morphological examination

To evaluate the development degree and any morphological abnormality in the different groups, embryos were examined under a dissecting microscope and yolk sac diameter, crown-rump and head length and somite number were recorded. A morphological score was determined according to Brown and Fabro (1981) and any abnormality recorded. The percentage of abnormal embryos was determined. Data were statistically analysed using ANOVA followed by Tukey's test and using χ^2 test. The level of significance was set at $p < 0.05$.

Results

Effects of exposure to RA on rat embryo development

At the end of 48 h in culture, the morphometric parameters (VYS diameter, crown-rump length, head length, somite number, total score), recorded as means ± standard deviations, were similar to the values reached by the control group indicating the absence of a general toxicity. Only the somite number of the RA 0.125 µM group resulted different from CONT. The 60% of the embryos from RA 0.25 µM group were plurimalformed; for this group somite number was not recorded. (**Tab. 1.1**). In the control group no abnormalities has been observed (**Fig. 1.3 A-A'**). By contrast, concentration-related abnormalities at different districts were observed in embryos exposed to RA (**Tab. 1.2**). RA 0.0375 µM was identified as the no effect level (NOAEL) for encephalon and otic vesicle district, as it did not cause a significant increase of abnormalities, while RA 0.05 µM could be considered the NOAEL for the posterior districts level, comprising somites, caudal and flexion abnormalities. On the contrary, all the tested concentrations resulted effective for branchial arch abnormalities; RA 0.025 was the LOAEL for this parameter (**Fig. 1.1, Fig. 1.3 C-D**).

Effects of co-exposure to FLUCO and Eth on rat embryo development.

At the end of 48 h in culture, the morphometric parameters (VYS diameter, crown-rump length, head length, somite number, total score), recorded as means ± standard deviations, were similar in all considered groups indicating the absence of a general toxicity (data not shown).

ETH

Eth at 17 mM was ineffective in inducing any developmental abnormality at the branchial arches district. At this concentration, were recorded only sporadic extra-branchial abnormalities (microcephaly). By contrast, concentration-related and specific branchial dysmorphogenic effects (fused or abnormal branchial arches) and severe extrabranchial abnormalities (swollen hindbrain and severe flexion anomalies (hook-shaped tail)) were described in Eth 42.5-127.5 mM-exposed groups (**Tab. 1.3, Fig. 1.2A, Fig. 1.3 B-B'**). Groups exposed to Eth 127.5 mM showed a high percentage of plurimalformed embryos (**Tab. 1.3**).

FLUCO

Groups exposed to FLUCO 125–250–500 µM showed specific abnormalities only at the level of the branchial apparatus (fused or abnormal branchial arches) and the effects were FLUCO

concentration-related (**Tab. 1.4, Fig. 1.2B**). In particular, FLUCO 500 µM caused the 100% of embryos with branchial arch malformations. Those data confirmed the branchial apparatus as the main target of the teratogenic effects induced by FLUCO. FLUCO 62.5 was identified as the no effect level (NOAEL), as it did not cause a significant increase of abnormalities.

FLUCO moving + Eth fixed

The co-exposure to the sub-teratogenic Eth concentration for branchial abnormalities (17 mM) and increasing concentrations of FLUCO (62.5-125-250-500 µM) induced a worsened malformative picture, showing in these groups a very significant increase of percentage of malformed embryos in comparison to groups exposed to FLUCO alone. In mixture with Eth, FLUCO 62.5 µM was an effective concentration (37.5% abnormal embryos). The abnormalities were those specifically induced by FLUCO (**Tab. 1.5, Fig. 1.2A, Fig. 1.3 E-E'**).

Eth moving + FLUCO fixed

The co-exposure to the NOAEL FLUCO concentration (62.5 µM) and increasing Eth concentrations (17-42.5-85 mM) enhanced the incidence of branchial arch malformations (fused or abnormal branchial arches) while the typical effects induced by Eth in the extrafaringeal regions (hook-shaped tail, swollen hindbrain, plurimalformations) where enhanced by FLUCO only in Eth 85 mM group (**Tab. 1.6, Fig. 1.2B**). In mixture with FLUCO, also the lower tested concentration (Eth 17 mM) was highly teratogenic (47.4% abnormal embryos).

Effects of co-exposure to RA and Eth on rat embryo development.

An additional mixture obtained co-exposing embryos to the lowest concentrations of both RA (0.025 µM) and Eth (17 mM) was also performed. The RA 0.025 µM plus Eth 17 mM group was highly effective, with the 100% of the embryo showing branchial arches and extra branchial abnormalities (swollen hindbrain and microcephaly) (**Tab. 1.7**).

Immunostaining

CRABP1

The immunostaining of CRABP1 was used as a biomarker for the visualisation of NCCs.

After 24 h in culture, CRABP1 positive cells were visible at the level of the welding edges of the neural tube and at the level of rhombomeres 2, 4 and 6 in embryos with normal phenotype (**Fig. 1.4**). Embryos with altered phenotype, presented a properly immunostaining of the welding edges of the anterior neural tube, but showed specific defects in the hindbrain segmentation: the NCCs were located in not well delimited rhombomeres, characterized by less clear boundaries and a weak and diffuse colouring (**Fig. 1.5**).

After 48 h of culture, embryos with normal phenotype showed visible immunostained areas at the level of the frontonasal region, at the level of the welding edge of the neural tube, at the level of the otic vesicle and at the level of the pharyngeal arches with three distinct migratory flows from the rhomboencephalon to the branchial arches (where the ectomesenchyme appeared condensed) (**Fig. 1.4**). Embryos with branchial altered phenotype showed a continuous immunostained mass migrating from the hindbrain to the branchial apparatus (**Fig. 1.5**).

CYP26s

The immunostaining of CYP26A1, CYP26B1 and CYP26C1 was used to evaluate the expression sites of the enzyme in the different embryonic districts. The expression of each isoform partially overlap the expression of CRABP. With some differences at the level of the limits of expression, CYP26A1, CYP26B1, CYP26C1were expressed at the level of frontonasal region, around the otic and optic vesicle, at the welding edges of the anterior neural tube, at the first branchial arch and at the caudal region. The immunostaining on embryos with abnormal branchial arch formation (reduced branchial arches) revealed no differences on protein distribution among different groups in comparison to normal embryos (**Fig. 1.4, Fig. 1.5**).

ADH7

The immunostaining of ADH7 was used to evaluate the expression sites of the enzyme in the different districts of the embryos exposed to Eth.

After 24 h in culture, ADH7 positive cells were visible at the level of the closing edge of the neural tube and at the level of the NCCs migration flows to the branchial arches (**Fig. 1.4**)

After 48 h in culture, in embryos with normal phenotype the immunostained cells were mainly located around the otic and optic vesicles, at the level of the first branchial arch and at the level of the frontonasal region. Immunostained cells are also visible at the level of the welding edge of the neural tube and the level of the developing trigeminal ganglion. In groups with altered phenotype, the expression sites of ADH7 in the embryonic district was unchanged (**Fig. 1.5**).

Acridine Orange

The vital staining with acridine orange allows to highlight the territories in apoptosis in the different embryonic districts, thanks to the intense fluorescence of cells with fragmented DNA.
In embryos with normal phenotype, the presence of physiological apoptotic areas at the level of the otic vesicle, the maxillary process and weakly at the level of the first gill arch and frontonasal region was observed. In embryos treated with the highest concentrations of Eth, a widespread massive apoptosis in the craniofacial region was observed. FLUCO induced apoptosis at the level of the pharyngeal region only at the highest concentration tested and in mixture with ethanol. Considering that apoptosis was induced only in groups exposed at the highest concentration, the cell death was not considered as the first event involved in the induction of the teratogenic effects.

Discussion

Exposure to RA

The teratogenic potential of RA on post implantation rat whole embryo culture was confirmed by the present study. The alteration recorded shown that the effects of RA exposure have multiple targets at different body level (encephalon, the branchial apparatus, the otic vesicle and the caudal region), consistent with literature (Klug et al., 1989; Lee et al., 1995; Menegola et al., 2004). Anyway, the enhancing of the extra-pharyngeal malformations (hook-shaped tail, swollen hindbrain, microcephaly, plurimalformed embryos) was present only at the higher RA concentrations, while the branchial arches district was selectively affected at each concentration tested. The abnormalities were concentration-related with a significant increase of fusions at the level of the branchial arches (most severe than reductions).

Exposure to FLUCO+Eth

From morphological examination it was observed that both Eth and FLUCO could induce alterations at the pharyngeal region: exposure to FLUCO leads to severe and specific malformations at the level of the branchial arches (reductions or fusions), while exposure to Eth commonly leads to less severe pharyngeal malformations (reduction of branchial arches) but also induces extra-pharyngeal malformations and plurimalformations. Those data confirmed the branchial apparatus as the main target of the teratogenic effects induced by FLUCO as previously observed (Menegola et al., 2000, 2001, 2003, 2004, 2006b).

After exposure to Eth, extra-pharyngeal malformations were observed: caudal anomalies (hook-shaped tail, which likely indicates alterations in the caudal neurulation), swollen hindbrain and reduced prosencephalon. High concentrations of Eth have been related to a high percentage of plurimalformed embryos.

As regards the mixtures, a significant effect was observed in all FLUCO groups co-exposed to the sub-teratogenic concentration of Eth (17 mM), in comparison to those exposed to FLUCO alone. The most impressive effects were those on the FLUCO NOAEL (62.5 µM) group, that resulted effective for nearly 40% of embryos after Eth co-exposure.

In all Eth groups co-exposed with FLUCO NOAEL (62.5 µM), a significant increasing of fusions at the level of the branchial arches was observed (exposure to Eth alone causes this type of malformation only sporadically). In mixture with FLUCO, Eth 17 mM cannot be considered the NOAEL as it was an effective concentration (47.4% abnormal embryos). In addition, the co-exposure caused the enhancing of the extra-pharyngeal malformations (hook-shaped tail, swollen

hindbrain, plurimalformed embryos) at the higher Eth concentrations. Furthermore, RA and Eth showed synergistic effects because when given simultaneously at subteratogenic concentrations, they produced a severe teratogenic effect with the 100% of malformed embryos.

Immunostaining

Whole mount immunostaining for CRABP1 allowed to correlate the defects at the branchial arches induced by both Eth and FLUCO with severe alterations in the migration and specification pattern of the neural crest cells (NCCs). In addition, a correspondence between expression sites of CYP26 isoforms and ADH7 with the expression sites of CRABP1 has been recorded, further confirming that the target structures of the teratogenic effect are the NCCs and the same for each molecule. In fact, there are no differences of expression signals between embryos with normal and altered phenotype: what changes is the localization of the immunostained target tissues, which follows the anomalous migration of the NCCs.

A correspondence between expression sites of ADH7 and apoptotic areas (branchial arches, frontonasal region, otic and optic vesicle and neuroepithelium) was also detected in embryos exposed to effective concentrations of Eth. The specificity in inducing massive cell death only in limited target tissue, allows to hypothesize that Eth could exert his teratogenic potential on molecules specifically expressed in the affected tissue, instead of a general cellular homeostasis imbalance (Kotch et al., 1995; Wentzel and Eriksson, 2009). Anyway, the apoptotic effect is not observable at lower doses but appears only at the higher ones where other causes (oxidative stress) can concur to the development of the observed effects. For this reason, these results were not considered relevant to the adverse outcome pathway (AOP) outline. These data support the hypothesis that these alterations, induced by altered RA levels, are a part of a more complex mechanism that ultimately lead to severe foetal malformations of the NCC-derived cranio-facial structures (Morriss-Kay, 1992; Osumi-Yamashita et al., 1994; Mark et al., 1995; Whiting, 1997; Schneider et al., 2001).

The different structure targets of effect of Eth and FLUCO could be justified by their different mode of actions (MOA).

Eth is a well-known teratogenic agent, able to induce facial dysmorphogenesis and reduced I.Q. (Kotch and Sulik, 1992; Sulik, 2005). The effective teratogenic concentrations commonly used in whole embryo cultures to generate alcohol-related abnormalities are 44-88 mM (corresponding to 0.25-0.5%) (Zhou et al., 2011). The Eth-related pathogenesis and MoA seem to be multifactorial, mostly related to disrupted cell-cell interactions, impaired cell proliferation

and enhanced cell death in target districts, including neural crest and the branchial apparatus (Wentzel and Eriksson, 2009). Potential MoA comprise RA content impairment (Deltour et al., 1996; Duester, 1998; Kot-Leibovich and Fainsod, 2009; Kane et al., 2010; Kiecker, 2016).

As far as the mechanism of action of FLUCO is concerned, evidence suggests that azole-fungicides could exert their embryotoxic effects by inhibiting the embryonic enzymes involved in RA catabolism (CYP26), increasing RA signalling in tissues expressing these enzymes. Several indirect studies suggested that FLUCO might interfere with endogenous embryonic RA levels: 1) the similarities between phenotypes of RA and FLUCO treated embryos, the similar effect of RA or FLUCO treatment on hindbrain patterning (Menegola et al., 2004); 2) the additive effects as treatment with sub-teratogenic doses of both RA and FLUCO leading to the same phenotype as the teratogenic dose of RA or FLUCO alone (Menegola et al., 2004); 3) the inhibitor of RA synthesis Citral is able to attenuate the frequency and severity of branchial arch abnormalities induced by FLUCO in embryos cultured *in vitro* (Di Renzo et al., 2007); 4) the evaluation of CYP26 expression in mouse embryos exposed *in utero* to FLUCO at neurulation stages showed that FLUCO exposure was associated, in total embryo extracts, to an up-regulation of cyp26a1, cyp26b1, whereas no significant change was identified for the cyp26c1 isoform (Tiboni et al., 2009).

The mixture effect of the co-exposure to azole fungicides and Eth has never been investigated until now, but it seems that the co-exposure to FLUCO and Eth is able to induce mixture effects, with the selective enhancement of branchial abnormalities. In particular, the fix sub-teratogenic concentration of one chemical in the culture medium resulted active in influencing the branchial embryotoxicity of the other ones *in vitro*. Considering that the altered district are those colonized by RA and that they are the unique districts expressing both the RA metabolic and catabolic enzymes, it could be hypothesized that both the molecules concur to increase the RA levels in specific responsive embryonic tissues, probably altering different steps in the same pathway.

Finally, our data focus the attention on the effects of mixtures of different mode of action molecules. Albeit the classical theories on mixture toxicity indicate the common mechanism as the main criterion for mixture effects, recent studies suggest that the MoA similarity is not an essential requirement to induce additive effects, because mixtures composed of chemicals with diverse modes of action can exhibit mixture effects too (P. on P. P. P. and their R. (PPR) EFSA, 2013). Recently, it has been argued that grouping criteria based solely on chemical similarity or

similar mechanisms may lead to unrealistically narrow groupings, with the exclusion of chemicals that also might contribute to combination effects (Boobis et al., 2011). This is in recognition of emerging evidence that biological effects can be similar, although the molecular details of toxicological mechanisms may differ profoundly in many respects (Kortenkamp, 2007). This could be the case of Eth-FLUCO mixture, in which the biological effect induced by the local increase of RA levels could be evocated by different molecular actions.

Our data support the need of a cumulative risk assessment not only for chemicals grouped on the base of similarities in chemical structure or derived from mechanistic considerations but also for chemicals differently acting on the same biological pathway.

Tables and Figures

Table 1.1. Numbers of somites from embryos exposed to increasing RA concentrations (µM) expressed as means ± standard deviations.

NUMBER OF SOMITES AFTER 48 H OF CULTURE					STATISTICS vs. CONT
GROUP	**EXAMINED**	(M	±	DS)	
CON	22	23.33	±	0.58	
RA 0.0375	8	23.25	±	0.50	
RA 0.05	14	23.25	±	0.75	
RA 0.125	18	20.55	±	1.51	**

Table 1.2. Evaluation of the teratogenic effects, as detected at term of the culture period, of the exposure to RA at increasing concentrations. The observed teratogenic effects were at the level of both branchial and extrabranchial districts.

	CONTROL	RA 0.025 µM	RA 0.0375 µM	RA 0.05 µM	RA 0.125 µM	RA 0.250 µM
TOTAL EXAMINED	22	22	14	14	19	5
PLURIMALFORMED EMBRYOS, %	0	0	0	0	5.26	60
TOTAL EXAMINED WITHOUT PLURI	22	22	8	14	18	5
EMBRYOS WITH BA ABNORMALITIES (FUSED AND/OR REDUCED BA), % **	0	aa 9.09	aabb 25.00	aabbcc 78.57	aabbccdd 94.44	aabbccdde 100
EMBRYOS WITH FUSED BA, % **	0	0	0	aabbcc 57.14	aabbccdd 77.78	aabbccddee 100
EMBRYOS WITH REDUCED BA, %	0	aa 9.09	aabbcc 25	aabbcc 57.14	aab 22.22	bbccddee 0
EMBRYOS WITH EXTRABRANCHIAL ABNORMALITIES, % **	0	0	aabb 75	aabb 85.71	aabbc 88.88	aabbccddee 100

Post hoc analysis performed if overall test showed that there is a significant linear trend among the ordered categories (** p<0.01, chi-square test)

aa p<0.01 vs. CONTROL;

b p<0.05 vs. RA 0.025 µM;

bb p<0.01 vs. RA 0.025 µM;

c p<0.05 vs. RA 0.0375µM;

cc p<0.01 vs. RA 0.0375µM;

dd p<0.01 vs RA 0.05 µM;

ee p<0.01 vs RA 0.125

Table 1.3. Evaluation of the teratogenic effects, as detected at term of the culture period, of the exposure to Eth at increasing concentrations. The observed teratogenic effects were at the level of both branchial and extrabranchial districts.

	CONTROL	Eth 17 mM	Eth 42.5 mM	Eth 85 mM	Eth 127.5 mM
TOTAL EXAMINED	36	30	11	15	11
EMBRYOS WITH BA ABNORMALITIES (FUSED AND/OR REDUCED BA), % **	0	0	aabb 72.72	aabb 80	aabbccdd 100
EMBRYOS WITH FUSED BA, %	0	0	0	6.67	0
EMBRYOS WITH REDUCED BA, % **	0	0	aabb 72.72	aabb 80	aabbccdd 100
EMBRYOS WITH EXTRABRANCHIAL ABNORMALITIES, % **	0	aa 10	aabb 27.27	aabbcc 53.33	aabbccdd 100

Post hoc analysis performed if overall test showed that there is a significant linear trend among the ordered categories (** $p<0.01$, chi-square test)

aa $p<0.01$ vs. CONTROL;

bb $p<0.01$ vs. Eth 17 mM;

cc $p<0.01$ vs. Eth 42.5 mM;

dd $p<0.01$ vs. Eth 85 mM

Table 1.4. Evaluation of the teratogenic effects of the exposure to FLUCO at increasing concentrations. The teratogenic effects observed at the end of the culture period were specifically at the level of the branchial apparatus.

	CONTROL	FLUCO 62.5 µM	FLUCO 125 µM	FLUCO 250 µM	FLUCO 500 µM
TOTAL EXAMINED	36	15	9	18	10
			aabb	aabbcc	aabbccdd
EMBRYOS WITH BA ABNORMALITIES (FUSED AND/OR REDUCED BA), % **	0	0	44.44	72.22	100
EMBRYOS WITH FUSED BA, % **	0	0	0	aabbcc 33.33	aabbccdd 100
EMBRYOS WITH REDUCED BA, % **	0	0	aabb 44.44	aabb 38.89	ccdd 0
EMBRYOS WITH EXTRABRANCHIAL ABNORMALITIES, %	0	0	0	0	0

Post hoc analysis performed if overall test showed that there is a significant linear trend among the ordered categories (** $p<0.01$, chi-square test)

aa $p<0.01$ vs. CONTROL;

bb $p<0.01$ vs. FLUCO 62.5 µM;

cc $p<0.01$ vs. FLUCO 125 µM;

dd $p<0.01$ vs. FLUCO 250 µM

Table 1.5. Evaluation of the effects of the co-exposure to Eth (at the fixed concentration level, 17 mM) and FLUCO (at moving concentrations). The observed teratogenic effect was specifically at the level of the branchial apparatus.

	CONTROL	Eth 17 mM	Eth 17 mM + FLUCO 62.5 µM	Eth 17 mM + FLUCO 125 µM	Eth 17 mM + FLUCO 250 µM	Eth 17 mM + FLUCO 500 µM
TOTAL EXAMINED	36	30	19	18	18	9
EMBRYOS WITH BA ABNORMALITIES (FUSED AND/OR REDUCED BA), % **	0	0	aabb 47.37	aabbcc 72.22	aabbccdd 94.44	aabbccddee 100
EMBRYOS WITH FUSED BA, % **	0	0	aabb 26.31	aabbcc 50	aabbccdd 72.22	aabbccddee 100
EMBRYOS WITH REDUCED BA, % **	0	0	aabb 47.37	aabbcc 22.22	aabbcc 22.22	ccddee 0
EMBRYOS WITH EXTRABRANCHIAL ABNORMALITIES, %	0	10	5.26	0	16.67	0

Post hoc analysis performed if overall test showed that there is a significant linear trend among the ordered categories (** $p<0.01$, chi-square test)

aa $p<0.01$ vs. CONTROL

bb $p<0.01$ vs. Eth 17 mM

c $p<0.05$; cc $p<0.01$ vs. Eth 17 mM + FLUCO 62.5 µM

dd $p<0.01$ vs. Eth 17 mM+ FLUCO 125 µM

ee $p<0.01$ vs. Eth 17 mM + FLUCO 250 µM

Table 1.6. Evaluation of the effects of the co-exposure to FLUCO (at the fixed concentration level, 62.5 µM) and Eth (at moving concentrations). The observed teratogenic effects included branchial and extrabranchial districts.

	CONTROL	FLUCO 62.5 µM	FLUCO 62.5 µM + Eth 17 mM	FLUCO 62.5 µM + Eth 42.5 mM	FLUCO 62.5 µM + Eth 85 mM
TOTAL EXAMINED	36	15	19	8	10
EMBRYOS WITH BA ABNORMALITIES (FUSED AND/OR REDUCED BA), % **	0	0	aabb 47.37	aabbcc 87.5	aabbccdd 100
EMBRYOS WITH FUSED BA, % **	0	0	aabb 26.31	aabb 25	aabbccdd 100
EMBRYOS WITH REDUCED BA, % **	0	0	aabb 47.37	aabbc 62.5	ccdd 0
EMBRYOS WITH EXTRABRANCHIAL ABNORMALITIES, % **	0	0	5.26	aabb 12.5	aabbccdd 100

Post hoc analysis performed if overall test showed that there is a significant linear trend among the ordered categories (** $p<0.01$, chi-square test)

aa $p<0.01$ vs. CONTROL;

bb $p<0.01$ vs. FLUCO 62.5 µM

c $p<0.05$; cc $p<0.01$ vs. FLUCO 62.5 µM + Eth 17 mM

dd $p<0.01$ vs. FLUCO 62.5 µM + Eth 42.5 mM

Table 1.7. Evaluation of the effects of RA and of the co-exposure to Eth and RA (at concentrations ineffective for branchial development). The clear effect of the mixture supports the hypothesis of a contribution of Eth in RA pathway deregulation.

	SOLVENT CONTROL GROUP (DMSO 1µL/mL)		POSITIVE CONTROL (RA 0.25 µM)		Eth 17 mM	RA 0.025 µM	Eth 17 mM + RA 0.025 µM
TOTAL EXAMINED	10		10		30	8	12
							aaccdd
EMBRYOS WITH BA ABNORMALITIES (FUSED AND/OR REDUCED BA), %	0		100		0	0	100
EMBRYOS WITH FUSED BA, %	0		100		0	0	bb 0
EMBRYOS WITH REDUCED BA, %	0		0		0	0	aabbccdd 100
EMBRYOS WITH EXTRABRANCHIAL ABNORMALITIES, %	0		100		10	0	aaccdd 100

Statistical analysis was performed in order to compare data obtained in mixture group with controls (DMSO, RA 0.25) and with the single exposure to Eth or RA 0.025 µM.

aa $p<0.01$ vs. SOLVENT (DMSO);

bb $p<0.01$ vs. POSITIVE CONTROL (RA 0.25 µM);

cc $p<0.01$ vs. Eth 17 mM;

dd $p<0.01$ vs. RA 0.025 µM.

Figure 1.1. Histograms showing the branchial arch abnormalities (%) collected on embryos exposed to increasing RA concentrations.

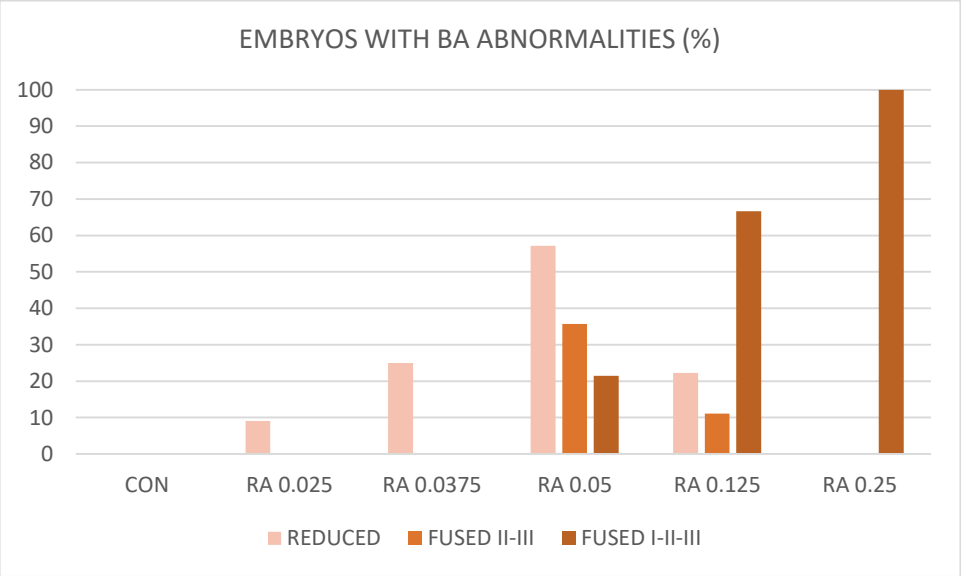

Figure 1.2. Histograms showing embryos with branchial arches abnormalities (%) after exposure to Eth and Eth moving + FLUCO fixed (A), or FLUCO and FLUCO moving + Eth fixed (B).

A)

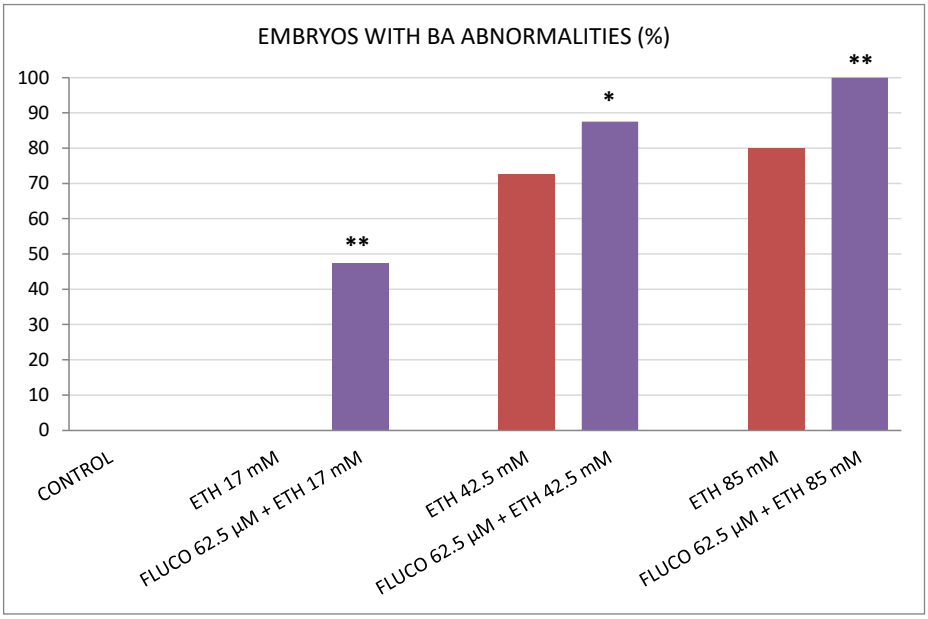

B)

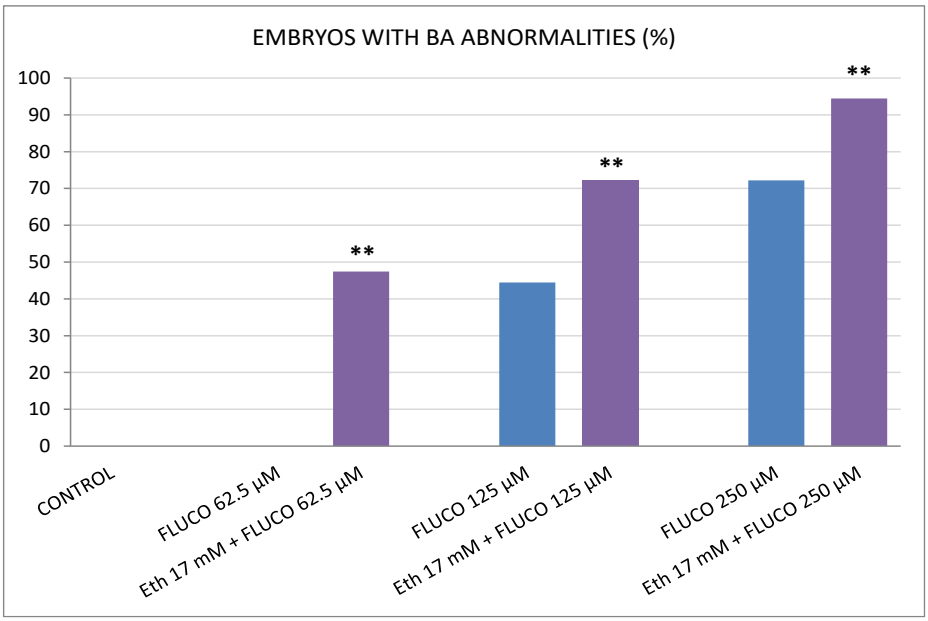

Figure 1.3. Morphology of the different observed phenotypes after 48 h of culture (Magnifications: 20X, 40X).

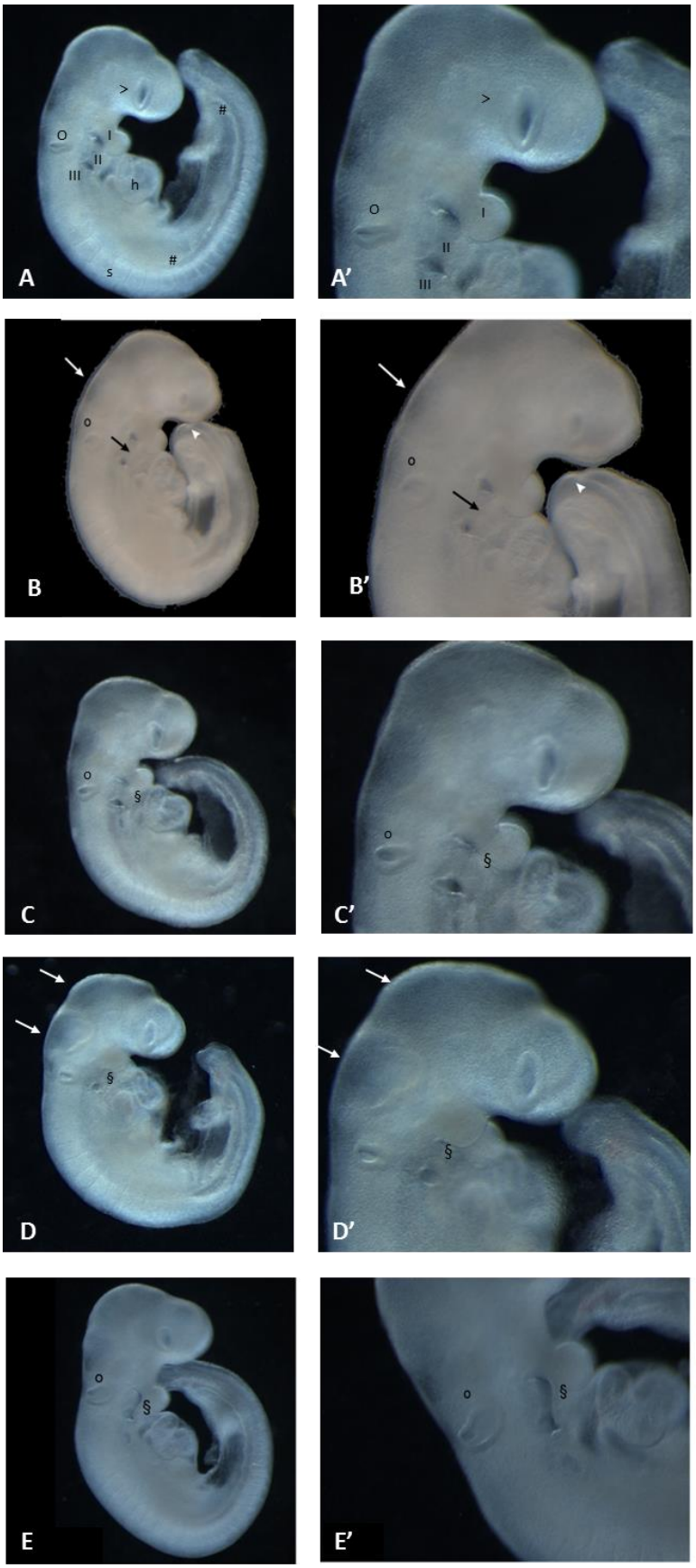

Figure A, A': Morphology of an embryo with NORMAL phenotype after 48 h of culture (Control + DMSO). Note the dorsal region of the embryo with the embryonic axial structures (somites, s) and the anterior and posterior limb bud (#), ventrally the heart (h), the cephalic region with the optic (>), the otic (o) vesicles and the branchial apparatus with the first (I), second (II), and third (III) separated branchial arches.

Figure B, B': Morphology of an embryo with REDUCED branchial arches after 48 h of culture (Eth 42.5 mM). Note the swollen hindbrain (white arrow), the reduction of the second branchial arch (black arrow) and the hook-shaped tail (white arrowhead) with a severe developmental delay of the posterior neuropore.

Figure C, C': Morphology of an embryo with a PARTIAL FUSION of the branchial arches after 48 h of culture (RA 0.05 µM). The embryonic structures appear normal except for the partial fusion between the first and the second branchial arch (§).

Figure D, D': Morphology of an embryo with FUSED branchial arches after 48 h of culture (RA 0.125 µM). Note the swollen midbrain and hindbrain (white arrows). The hindbrain is short and the branchial arches are fused in a single structure (§).

Figure E, E': Morphology of an embryo with TOTAL FUSION of the branchial arches after 48 h of culture (FLUCO 250 µM + Eth 17 mM). Note the total fusion between the branchial arches in a continuous structure (§).

Figure 1.4. Embryos with normal phenotype after 24 h or 48 h of culture immunostained to detect the NCC marker (CRABPI) or the enzymes involved in RA oxidization (CYP26) or production (ADH) (Magnifications: 32X, 20X).

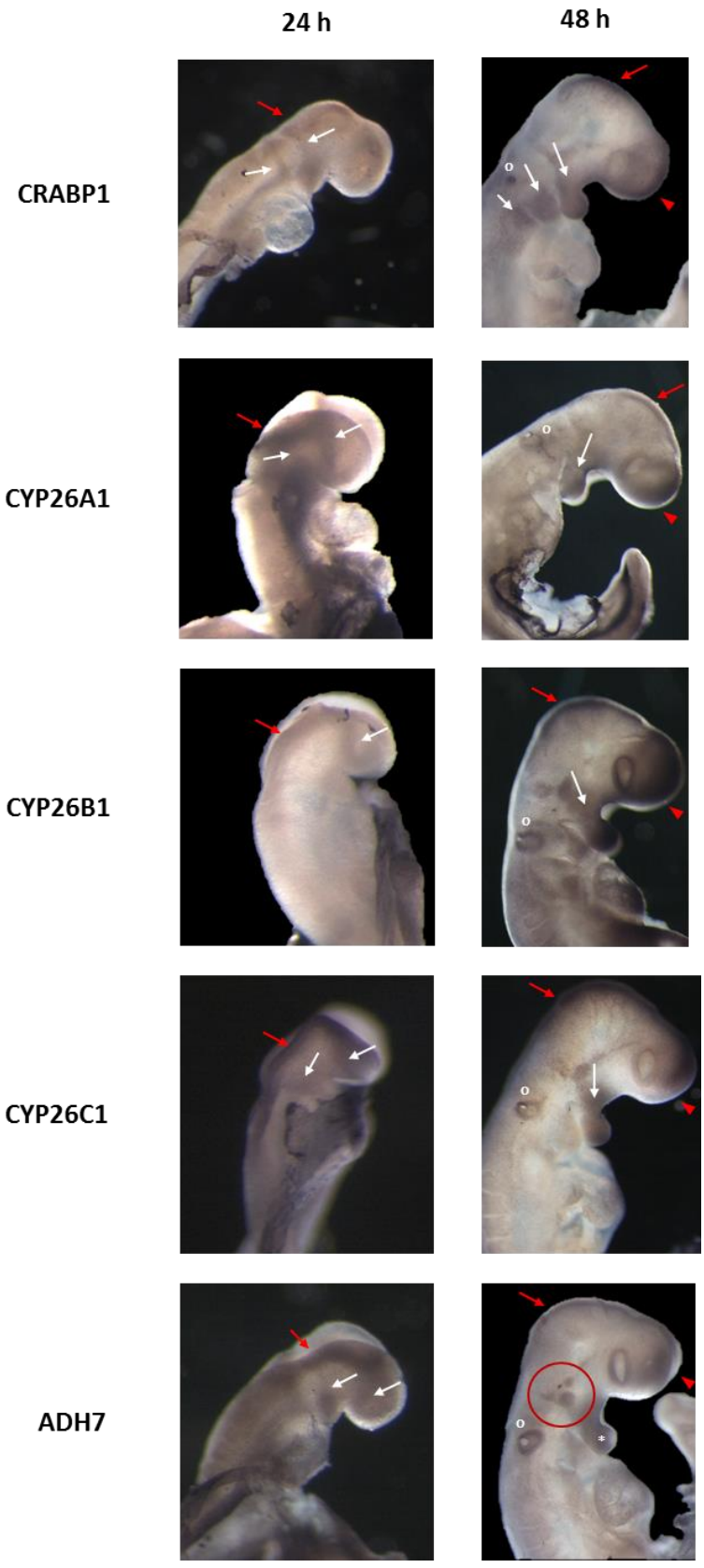

Left images: Lateral view of embryos with normal phenotype after 24 h of culture. Note, for each antibody, the well immunostained welding edge of the neural tube (red arrow), and the migration streams of the NCCs from specific rhombomeres to the branchial arches (white arrows).

Right images: Lateral view of embryos with normal phenotype after 48 h of culture. For CRABP1, note the immunostained areas at the level of the frontonasal region (red arrowhead), at the welding edges of the neural tube (red arrow), at the level of the otic vesicle (o) and at the level of the branchial arches with three separate streams (white arrows), indicating the successful migration of NCCs.
CYP26 isoforms are expressed, with some minor differences, in the frontonasal region (red arrowhead), at the level of the margin of the optic and otic vesicle (o), at the level of the closing edge of the encephalon (red arrow), at caudal level and in the branchial region (white arrows).
Note the expression of ADH7 at the level of the trigeminal ganglion (red circle) with the ophthalmic branch, at the level of the first branchial arch (*), around the otic (o) and optic vesicles, in the frontonasal region (red arrowhead) and at the level of the welding edge of the neural tube (red arrow).

Figure 1.5. Comparison between embryos showing the normal phenotype or reduced branchial arches after 48 h of culture immunostained with the different antibodies (Magnification: 20X).

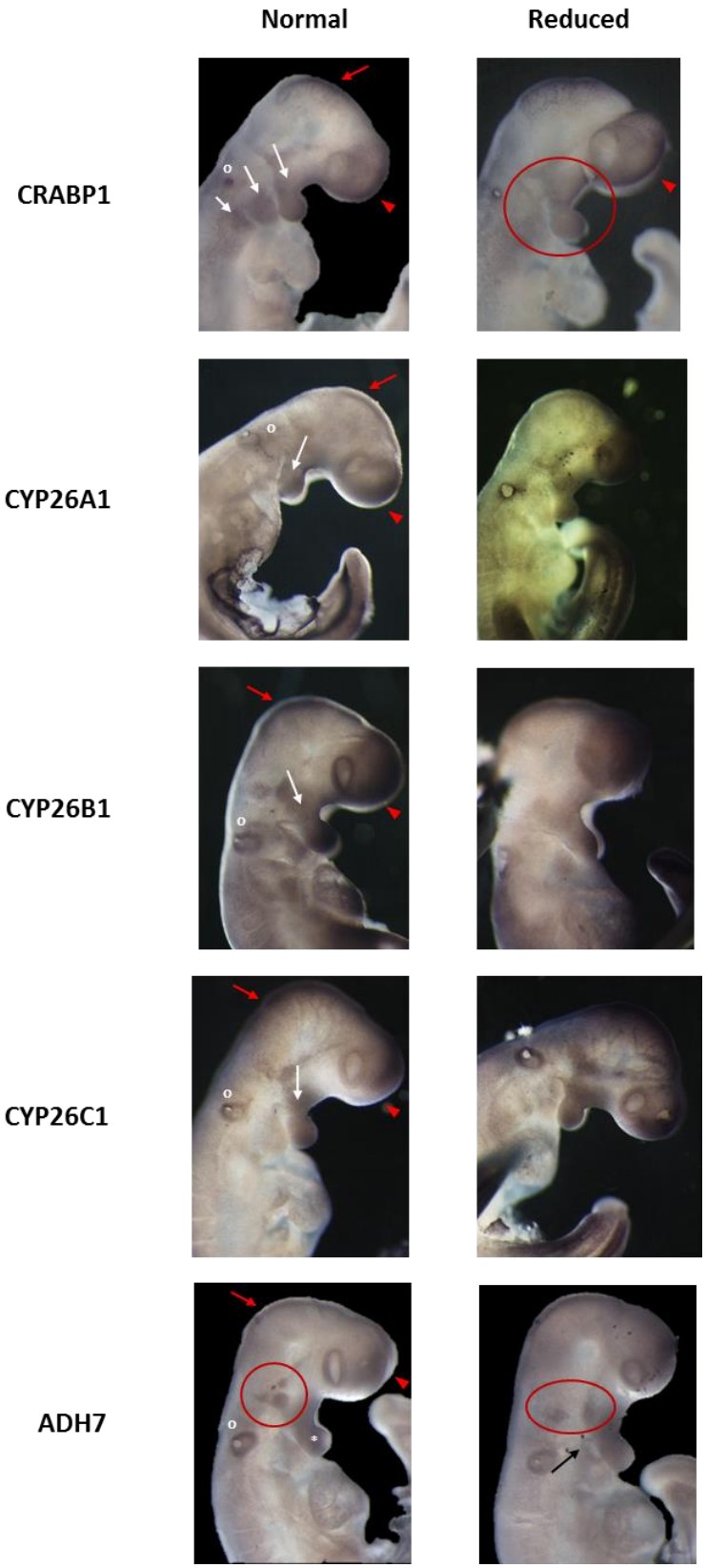

Lateral view of embryos with normal and reduced branchial arches phenotype after 48 h of culture.

CRABP1: In embryos with branchial abnormalities (reduced branchial arches) note the immunostained areas at the level of the frontonasal region (red arrowhead), at the welding edges of the neural tube (red arrow), and in the continuous mass (red circle) at the level of the fusion between the second and the third branchial arch.

CYP26: Note as in embryos of equal developmental stage with reduced branchial arches, there is no difference about immunostained areas compared to normal phenotypes.

ADH7: Note the reduction of the second branchial (black arrow) arch and the delayed development at the level of the structure of the trigeminal ganglion (red circle).

PART 2:

DEVELOPMENT OF AN INTEGRATED SYSTEM BIOLOGY MODEL FOR PREDICTING MIXTURE OF CHEMICALS ACTING ON THE SAME PATHWAY

Introduction

In the last years, the effects on human health and environment after exposure to different multiple chemicals have become an item of concern. These effects are known as “mixture effects”. The study of risk assessment of exposure to mixtures of chemicals is a problem of great importance since humans and all other organisms are typically exposed to multi-component chemical mixtures, present in the surrounding environmental media (water, air, soil), in food or in consumer products (Feron et al., 1998; Groten, 2000). Despite the availability of numerous toxicological studies in the literature on the interactions between chemicals, the current knowledge of the mechanisms of interaction between chemicals is rather limited. One of the major aims of research programs on the toxicology of chemical mixtures is to explore methods to predict and to identify hazardous combinations of chemicals relevant to humans. To arrive in the future to the creation of a realistic overall picture of human exposure to these substances, the development of mathematical models to predict the effects of mixtures starting from the concentrations of their individual components will be essential (Feron and Groten, 2002). Key to further maturation of mixture toxicology is the development of integrated approaches between experimental toxicology, biomathematics, biology, bioengineering, pharmacology and model developing to ensure parallel and coordinated research in this challenging area of toxicology (Groten et al., 2001). In addition, ethical, scientific, and economic factors are driving the reduction of toxicity testing in animals, with the eventual aim of complete replacement.

Retinoic acid (RA), a metabolite of vitamin A (retinol, RO), is a well-known morphogen in invertebrates and vertebrates embryo produced by ADH7 and degraded by the enzyme CYP26 isoforms (CYP26A1, CYP26B1, CYP26C1) of the cytochrome P450 family (Morriss-Kay, 1992). RA is considered the main molecule involved in craniofacial morphogenesis. It activates a cascade of expressions of growth factors and genes controlling craniofacial development (Suzuki et al., 1999). The generation and diffusion of RA has been proposed to form a gradient that patterns the hindbrain into seven rhombomeres (r1-7) (Richard J. White et al., 2007; Schilling et al., 2012). Because morphogens act at a distance from their source of production, eliciting distinct cellular responses in a concentration-dependent manner (Rogers and Schier, 2011), their action needs to be robust and precise. The self-enhanced degradation of RA is a mechanism that enhances RA gradient robustness. RA induces the expression of CYP26a1 that specifically degrades RA (White et al., 2007), inducing a negative feedback loop to regulate RA levels. Despite that control, severe malformations of the face can result from either a generalized RA imbalance or from an ectopic localization of RA in rhombomeres (with a subsequent ectopic

expression of growth factors and genes in the hindbrain and rhomboencephalic NCC-derived tissues (Morriss-Kay, 1992; Osumi-Yamashita et al., 1994; Mark et al., 1995; Whiting, 1997; Schneider et al., 2001). There are several possible causes of imbalance in RA concentrations and many substances are able to alter craniofacial development: valproic acid, thalidomide, retinoids, ethanol and some drugs and pesticides such as the class of the azoles fungicides (Morriss and Steele, 1974, 1977; Steele et al., 1987; Klug et al., 1989; Kotch et al., 1995; Hansen et al., 1999; Parman et al., 1999; Menegola et al., 2013).

Azoles are synthetic antifungal compounds, derived from triazole or imidazole, sold annually to thousands of tons for the purpose of plant protection (Hof, 2001). Their large use in agriculture and presence as residues in food carry the potential for human exposure. In addition to environmental exposure, humans can be exposed to some azole fungicides for the treatment of local or deep fungal infections (Zarn et al., 2002; EFSA, 2009). The specific teratogenic effect of some azole fungicides has been investigated using postimplantation rat whole embryo culture. Embryos exposed to single azoles develop abnormal branchial structures related to the abnormal hindbrain segmentation and abnormal neural crest cell (NCC) migration and compaction (Menegola et al., 2000, 2001, 2003, 2005a, 2005b, 2006a, 2006b; Di Renzo et al., 2007, 2011a, 2011b). The postulated mechanism of action was the inhibition of CYP26 enzymes involved in RA degradation during early embryonic development, with the consequent increase in local RA concentration (Menegola et al., 2006a; Marotta and Tiboni, 2010).

Humans could be exposed simultaneously to azole fungicides acting with the same mode of action (MoA). Since in standard human risk assessment, chemicals thought to exhibit their effects through common mechanisms are assumed to show dose-additivity and are grouped together (cumulative risk assessment), our hypothesis is that mixtures of azole fungicides could show dose-additivity too. In fact, data previously obtained by Menegola and colleagues (2013) described an increase of the teratogenic effects (reduction and fusion of branchial arches) in postimplantation rat whole embryo culture *in vitro* in presence of mixtures of azole fungicides, including fluconazole (FLUCO), triadimefon (FON), flusilazole (FLUSI) and cyproconazole (CYPRO), compared to single exposures. In order to test the hypothesis that the *in vitro* responses to mixtures of azoles, causing craniofacial malformations, could be derived under the assumption of dose-additivity on the basis of the concentration–response curves of each individual compound, we modelled the outcome of mixture of azoles basing on benchmark dose (BMD) and relative potency factor (RPF) approaches. The predicted effects were compared with the results obtained *in vitro*. Deviation from additivity was calculated as ratio of observed versus

expected effect size (Boobis et al., 2011). Experimental data on branchial abnormalities caused by the individual compounds were retrieved and analysed with PROAST which can analyse ordinal data: all tested azoles are teratogenic at micromolar (μM) concentrations, but characterized by different potencies (**Fig. 2.1**).

Teratogenic potency in WEC of different azoles		
conazole	BMD10 (μM)	95% confidence lower value
Imazalil (IMA)	4.4	1.7
Flusilazole (FLUSI)	6.0	4.3
Triadimefon (FON)	19.8	10.1
Triadimenol (NOL)	23.1	15.0
Cyproconazole(CYPRO)	26.0	14.7
Tebuconazole (TEBU)	46.2	17.1
Fluconazole (FLUCO)	72.2	31.5

Figure 2.1. Table indicating the teratogenic potency in whole embryo culture (WEC) of different azoles.

Results showed a clear concentration-response effect for single fungicides while in the co-exposure, regarding branchial arch abnormalities, there are no significant deviations from concentration–additivity. The observed additive effect of the binary mixture supports the hypothesis that the tested individual substances share the same MoA and that azole fungicides can be grouped together for risk assessment as regards craniofacial malformations (Menegola et al., 2013).

Ethanol (Eth) can also alter craniofacial morphogenesis in the developing conceptus. Eth is commonly consumed in alcoholic beverages during pregnancy, even though it is a known teratogen. The teratogenic effects of Eth have been well investigated, but its specific molecular initiating events (MIEs) have not yet been completely clarified. One of the potential mechanism by which Eth could act as teratogen, is the possible interference with ADH7, a key enzyme for the synthesis of RA from RO.

Recent studies (EFSA, 2013) suggest that the similarity of MIEs is not an essential requirement to induce additive effects, because mixtures composed of chemicals with different MIE can exhibit additivity too, probably acting on the same biological pathway and contributing to the same adverse outcome.

In order to test the hypothesis that also the *in vitro* responses to mixtures of azoles and Eth could be derived under the assumption of dose-additivity on the basis of the concentration–response curves of each individual compound, the outcome of mixture of FLUCO and ETH was modelled

based on bench mark dose (BMD) and relative potency factor (RPF) approaches. The predicted effects, derived under the dose-additivity hypothesis, were compared with the results obtained *in vitro* in the first part/chapter of this work. The co-exposure to Eth and FLUCO at their NOAELs resulted effective, inducing almost 40% branchial arch abnormalities. In addition, a significant enhancement of teratogenic effects were observed in the other groups co-exposed to FLUCO and Eth in comparison to the single exposure. As for mixtures of azoles, regarding branchial arch abnormalities, there are no significant deviations from concentration–additivity. Whereby, the present data suggest that FLUCO and Eth, limited to the branchial pathogenesis, could produce additive effect affecting the same pathway but with different MoA.

To investigate the mechanisms of action which we assume at the basis of the observed effects, the aim of this work was to obtain an *in silico* model, validated by *in vitro* experiments, useful to simulate and predict the probability of cranio-facial malformations of co-exposure substances with independent MoA but acting on the same pathway and potentially contributing to the same adverse outcome. The model was developed using an integrated approach combining mathematical modelling, computer simulations of molecular docking and *in vitro* experiments.

Part of this project was developed inside the EuroMix project, funded by the Horizon 2020 framework program of the European Union. The overall objective of the EuroMix project is to establish and to disseminate new, efficient, validated test strategies for the toxicity of chemicals in a mixture aiming to deliver refined information for future safety assessment of chemicals. This includes exposure assessment via multiple exposure routes.
Specific objects are:

- Determine a refined grouping strategy for cumulative assessment groups.
- Establish criteria for prioritization of chemicals for carrying out mixture testing.
- Verify the reliability of *in silico* methods and *in vitro* bioassays against *in vivo* animal tests.
- Determine how to extrapolate the results of *in vitro* bioassays and *in silico* models to humans.
- Develop harmonized tools and models for performing realistic assessment of chemical mixtures.

Materials and methods

In vitro experiments

We generated all the teratological data used in this study as reported in the first part/chapter of this work. Only the frequencies of malformations of the branchial arches (**Tab. 2.1**) were considered here.

In silico molecular modelling

Comparative Modelling

The sequences of the three isoforms of CYP26 (CYP26A1, CYP26B1, CYP26C1) were selected from Uniprot - Protein Knowledgebase database (http://www.uniprot.org/), (entry UniProt ID: Q8VIL0, G3V7X8, D4AAL3, respectively), and used as query sequences for searching homolog template sequences with a solved 3D structure in the Protein Data Bank *via* BLASTP (https://blast.ncbi.nlm.nih.gov/Blast.cgi?PAGE=Proteins). The crystal structure of Cyanobacterial CYP120A1 (entry PDB: 2VE3) was selected and then a multiple alignment was then performed using Clustal W (http://www.ebi.ac.uk/Tools/msa/clustalo). The alignment between target sequences and template proteins was subsequently manually adjusted. Comparative modelling of the three isoforms was carried out with the MOE Homology Model program (Molecular Operating Environment, release 2013.08, by Chemical Computing Group Inc., Montreal, QC, Canada), using default settings and MMFF94x as force field. All models were refined down to a Root Mean Square (RMS) gradient of 0.01 kcal/mol/Å^2. The quality of the final models was checked with the MOE Protein Geometry module to make sure that the stereochemical quality of the proposed structure was acceptable.

Binding site analysis

The binding site of each CYP26 isoform was identified through the MOE Site Finder program, which uses a geometric approach to calculate putative binding sites in a protein, starting from its 3D structure. This method is not based on energy models, but only on alpha spheres, which are a generalization of convex hulls (Edelsbrunner et al., 1995). The prediction of the binding sites confirmed the binding sites defined for RA, imported from its CYP120A1 co-crystallised structure during the homology modelling procedure.

Molecular docking

Molecular docking of azoles and ethanol was performed on CYP26a1, CYP26b1 and CYP26c1 isozymes. *In silico* screening was carried out with the MOE Dock program, part of the MOE Simulation module, and was divided in two step: placement and refinement. For the first one, "Triangle Matcher" (the best method for standard and well-defined binding sites) was selected as placement methodology. For the second one, "Induced fit" was used. Thirty complexes were generated for each tested ligand, and only five were kept after refinement.

In silico dissociation constant evaluation

For each ligand, the best poses binding the heme group (according to the GBVI/WSA dG scoring parameter) were selected for computing affinity. The estimated binding affinities were calculated through the MOE Quickprep module, in which the complexes are refined through a set of specific MOE molecular mechanics procedures aimed at the relaxation of ligands in the receptor-binding site. During these steps, protein side-chain atoms and ligand atoms were left free to move. The dissociation constants (*Ki*) were then computed through the binding free energy, as estimated *via* the GBVI/WSA dG scoring function, according to the following equation: $Ki = e^{\Delta G/RT}$, where *R* represents the gas constant and *T* the absolute temperature (300 K), and expressed as *pKi* values (-Log10 of *Ki*).

Mathematical modelling of RA gradient disruption

The model described the formation of RA during the early development of a rat embryo hindbrain (between days 9.5 and 10 *post coitum*, which is the sensitive window to azole fungicides), and its perturbation after exposure to FLUCO, Eth and their binary mixtures.

According to our model, the synthesis of RA is catalyzed by ADH7, whose production is induced by RO and Eth. RA is assumed to be catabolised by CYP26A1. The inhibitory effect exerted on CYP26 isoforms by FLUCO and to a lesser extent by Eth has been reported in the first chapter of this work. In addition, the level of CYP26a1 mRNA in the hindbrain is up-regulated by FGF and of RA (Reijntjes et al., 2005). The CYP26 enzymes plays a central role in protecting the developing embryo from supra-physiological levels of RA. In particular, the crucial role of CYP26a1 during development is underlined by the notion that *Cyp26a1*-/- mutant embryos show abnormal hindbrain specification, abnormal neural crest cell migration and abnormal anterior branchial arches (Sakai, 2001; Abu-Abed et al., 2002; Uehara et al., 2007).

Previous studies indicates that *Cyp26a1* is initially expressed in the anterior neural plate during gastrulation (Kudoh et al., 2002) and that it first establishes the anterior boundary of the RA signal at r2–r3 (Sirbu, 2005). *Cyp26a1* is also required for exogenous RA treatments to rescue RA-deficient embryos (Hernandez et al., 2007). Furthermore, exposure to FLUCO has been linked to an increased expression of CYP26A1 (Tiboni et al., 2009). Thus, Cyp26a1 seems to have a key role in the hindbrain, distinct from that of the other two isoforms Cyp26b1 or Cyp26c1 (which are not induced in the nervous system by RA) as the major RA-degrading enzyme (White et al., 2007).

Considering both the essential role of Cyp26a1 during the initial phases of the embryonic development, and the complexity of ODEs (*ordinary differential equations*) system to describe temporal-dependent CYPs' isoforms expression, in the present model only the dissociation constant related to cyp26a1 was considered.

Kinetics equations

The following equations are based on those reported in Goldbeter et al., 2007. The variables are the concentrations of FLUCO, Eth (*ETH*), ADH (*ADH*), RA (*RA*), RO, *cyp26a1* mRNA (*mRNA*), CYP26A1 protein (*CYP26*) and FGF protein (*FGF*). The time evolution of these variables a distance *x* from the starting of the RA signal at the bottom of the hindbrain is governed by the following set of kinetic equations:

$$\frac{dADH(t)}{dt} = k_{syn\_ADH} - k_{\deg\_ADH} \cdot ADH(t) + k_{trs\_by\_ETH} \cdot \left(\frac{ETH^2}{k_{i\_ETH\_ADH}{}^2} + \frac{RO}{k_{i\_RO} + RO} \right) \cdot ETH \qquad (1)$$

Parameters k_{syn_ADH} and k_{deg_ADH} measure respectively the rate of synthesis and the first order degradation rate of ADH. In our hypothesis, ADH is induced by ETH: $k_{trs\_by\_ETH}$ measure the transcription rate of ADH induced by ETH, while $k_{i\_ETH\_ADH}$ and k_{i_RO} measure the affinity for ADH respectively by ETH and RO.

$$\frac{dRA(t)}{dt} = k_{syn\_by\_ADH} \cdot ADH(t) \cdot \left(\frac{RO}{k_{i\_RO} + RO} \right) \cdot \left(1 - \frac{x}{L} \right) - CYP26 \cdot \left(k_{met\_RA} \cdot RA(t) \right.$$
$$\left. - k_{met\_FLUCO} \cdot \left(\frac{\frac{FLUCO}{k_{i\_FLUCO} + FLUCO}}{\frac{RA(t)}{k_{i\_RA} + RA(t)}} \right) - k_{met\_ETH} \cdot \left(\frac{ETH}{k_{i\_ETH} + ETH} \right) \right) - k_{\deg\_RA} \cdot RA(t) \qquad (2)$$

Parameters $k_{syn\_by\_ADH}$ and k_{met_RA} measure respectively the rate of synthesis of RA by ADH and the first order degradation rate of RA by enzyme CYP26, while k_{deg_RA} represents the rate of non-specific degradation of RA besides that catalysed by CYP26. k_{i_FLUCO} and k_{i_ETH} represent the affinity constant for CYP26 respectively for FLUCO and ETH, while k_{met_FLUCO} and k_{met_ETH} represent the rate of FLUCO and ETH degradation. We consider the parallel linear gradients $(1 - x/L)$ in the rate of synthesis of RA by ADH enzyme, and in the amount of FGF protein (White et al., 2007). L is the number of the hindbrain cells ($L = 50$) at the considered stage, while x is the cell considered for the prediction in the model which correspond at the middle of the hindbrain ($x = 25$).

$$\frac{dmRNA(t)}{dt} = k_{trs} + v_{\max} \cdot \frac{RA^2(t)}{k^2_{act} + RA^2(t)} \cdot \frac{FGF(t)^2}{k^2_{act} + FGF^2(t)} - k_{\deg} \cdot mRNA(t) \qquad (3)$$

The k_{trs} parameter measure the transcription constant of CYP26 mRNA and V_{max} represent the maximum rate of transcription of CYP26 mRNA by RA. Parameters k_{act} and k_{deg} represent respectively the CYP26 activation by RA constant and the first order degradation rate of CYP26 mRNA.

$$\frac{dCYP26(t)}{dt} = k_{trd} \cdot mRNA(t) - k_{\deg} \cdot CYP26(t) \qquad (4)$$

Parameters k_{trd} and k_{deg} represent respectively the CYP26 translation constant and the first order degradation rate of CYP26 protein.

$$\frac{dFGF(t)}{dt} = k_{syn} \cdot \left(1 - \frac{x}{L}\right) - k_{\deg} \cdot FGF(t) \qquad (5)$$

Parameters k_{trd} and k_{deg} represent respectively the FGF translation constant and the first order degradation rate of FGF protein.

In these kinetic equations, we assume that the regulatory effects of ETH on ADH and of RA and FGF on *cyp26* mRNA obey cooperative kinetics, described by Hill functions with cooperativity degree 2.

In order to predict malformation risk with the model, the above equations were solved by numerical integration to obtain RA concentrations at the center of the hindbrain (x = 25). To predict the probability of malformation as a function of (excess) RA concentrations we used a *multistage* model:

$$P = 1 - \exp\left(-Q0 - Q1 \cdot RA_{x=25}\right) \qquad (6)$$

Parameter values and model calibration

We used our experimental data on branchial arch malformation frequencies following 48 h of exposures to RA, Eth and FLUCO (**Tab. 2.1**). The measured counts of malformations were assumed to be binomially distributed with a probability p given by the multistage equation of the model. The priors were set to uninformative uniform distribution. Most model parameters were set on the basis of the values reported in Goldbeter et al., 2007, or derived from the molecular affinity calculations. The remaining model parameters were numerically estimated via Bayesian calibration (Bois, 2009). Each parameter value is reported in **Tab. 2.2**.

Independent data on malformation rates in WEC as a function of RA concentration (after 48h) were used to calibrate the parameters Q0 and Q1 of the multistage equation of the model. Markov-chain Monte Carlo (MCMC) simulations were performed with GNU MCSim version 5.5.0 (http://www.gnu.org/software/mcsim). Two MCMC chains were run in parallel for 10,000 iterations. Plots were produced with R, version 2.14.0 {R Development Core Team (2011) R:http://www.R-project.org/}.

Results

Molecular docking

All the tested azoles show affinities in the range of those calculated for RA, for the three CYP26 isoforms (**Fig. 2.2**). The affinities are consistent with the azoles' teratogenic profiles and potencies. A correlation between CYP26A1 affinity and teratogenic potency is observed, except for TEBU. TEBU effects (less than expected considering CYP26A1 affinity) could be lowered by the higher affinity of TEBU for CYP26B1 isoform, not involved during hindbrain patterning and facial morphogenesis.

Literature shows, in fact, that:

- Cyp26a1-/- mutant embryos show abnormal hindbrain specification, abnormal neural crest cell migration and abnormal anterior branchial arches (Sakai, 2001; Abu-Abed et al., 2002; Uehara et al., 2007).
- Cyp26b1-/- embryos have normal hindbrain patterning and show abnormal neural crest migration only at the level of posterior branchial arches (Maclean et al., 2009).
- Cyp26c1-/- mutant embryos are normal, even if Cyp26a1/c1 double null mutants exhibit a worsening on hindbrain patterning and neural crest cells anomalies (Uehara et al., 2007).

Mathematical model calibration

The empirical RA concentration-response model (in the figure below) was fitted on the basis of the previous experimental data of percentage of branchial arch malformations caused by increasing RA concentrations. The calibration of the multistage model with the RA-malformation data gives the resulting parameter: Q_0 = -0.364297; Q_1 = 0.0202369.

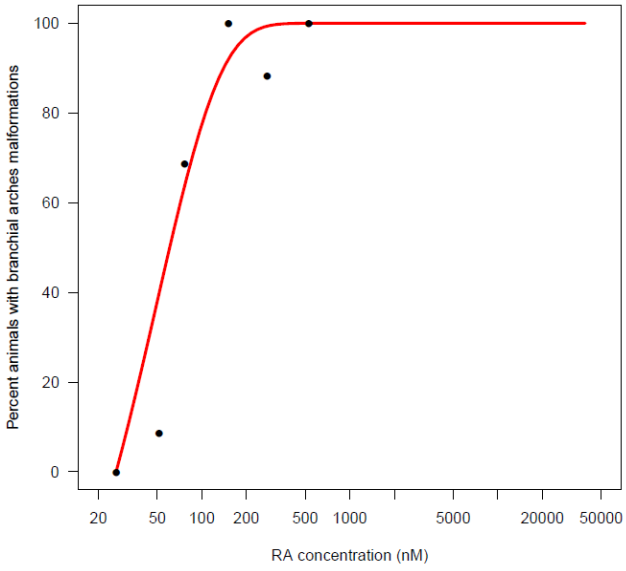

Fig. 2.3 A-B shows the fitted dose-response curve for Eth and for FLUCO on the basis of the experimental data of percentage of branchial arch malformations. The data are well reproduced. **Fig. 2.3 C-D** show the predicted relationship between concentrations of Eth or FLUCO and the concentration of RA in the center of the hindbrain. FLUCO is much more potent at increasing RA concentration than Eth. The uncertainty resulting from the unavoidable measurement errors and modelling approximations is reflected by the grey areas, which correspond to the 95% confidence interval for the probability prediction curves (dark grey) and for the data themselves (light grey). Remember that the data are binomially distributed with a probability given by the predicted curve; the limited sample size of the data leads to increased uncertainty and to discrete confidence bounds (hence the staircase aspect of the data confidence intervals. The red bars indicate the lower and upper bounds of the 95% confidence interval.

Fig. 2.3 E-F show pure model predictions of the percentage of branchial arch malformations after co-exposures to FLUCO and Eth. For comparison with the predictions, actual experimental data are superimposed to the curve (they were not used in the calibration process and just serve as validation). The malformation data are somewhat underestimated by model predictions, but they fall within the 95% confidence intervals of the model predictions. Note the strong interaction effect between FLUCO and Eth: 17 mM Eth or 62.5 µM of FLUCO alone have no effect, but induce consistently about 40% malformations when given together.

Discussion

One of the major aims of research programs on the toxicology of chemical mixtures is to predict and identify hazardous combinations of chemicals relevant to humans. To come to a realistic overall picture of human exposure to these substances, the development of mathematical models to predict the effects of mixtures starting from the concentrations of their individual components will be essential (Feron and Groten, 2002).

Azole fungicides and ethanol can affect cranio-facial morphogenesis during the early development of an embryo and this is well documented in *in vitro* exposure experiments (Giavini et al., 1992; Abel and Hannigan, 1995; Deltour et al., 1996; Duester, 1998; Menegola et al., 2001, 2006a; Kot-Leibovich and Fainsod, 2009; Marotta and Tiboni, 2010). In addition, data obtained by Menegola and colleagues (2013) in postimplantation rat whole embryo cultured *in vitro* in presence of mixtures of azole fungicides show that the co-exposure resulted in an additive effect. The postulated mechanism of action for the azole fungicides class is the inhibition of CYP26 enzymes (involved in RA degradation during early embryonic development), with subsequent increase in RA local content. On the other hand, one of the potential mechanism by which Eth could act as teratogen, is the possible interference with ADH7, a key enzyme for the synthesis of RA. Recent studies suggest that the similarity of MIEs is not an essential requirement to induce additive effects, because mixtures composed of chemicals with different MIE can exhibit mixture effects too, probably acting on the same biological pathway and contributing to the same adverse outcome (EFSA, 2013).

Our starting hypothesis was that FLUCO and Eth, limited to the branchial pathogenesis, could produce additive effect affecting the RA pathway despite they act with different MoA. The first conclusion of our experimental work is that FLUCO and Eth could not act only additively, but synergistically. No-effect concentrations of FLUCO and Eth alone (17 mM and 62.5 µM respectively) induce consistently about 40% malformations when given together, as can be observed on **Fig. 2.3**.

We went further and developed an integrated approach combining pathway modelling, molecular docking and *in vitro* experiments, to predict for mixture effects and for the estimations of the RA levels in rat hindbrain after FLUCO and Eth co-exposure starting from the concentrations of the individual substances. The model seems to confirm the accuracy of the hypothesized pathogenic pathway: in fact, experimental data and model predictions have a promising agreement.

The Bayesian approach used for calibrating the model parameters permitted us to take into account both uncertainty and variability in experimental data, which is an asset for the relevance of the predictions. The previous obtained *in vitro* experimental data allowed us to finely calibrate and cross-validate the model, which was able to simulate both the formation of a RA gradient in the rat embryo hindbrain and its perturbation after exposure to Eth, to FLUCO and their binary mixtures.

To verify the accuracy of the model, we simulated the effects of binary mixtures of azole fungicides (cyproconazole, CYPRO; triadimefon, FON; flusilazole, FLUSI) previously studied in our laboratory. We modified the kinetic equation (2), which describe the time evolution of RA concentration along the hindbrain, adding the CYPRO, the FON and the FLUSI CYP inhibition terms:

$$\frac{dRA(t)}{dt} = k_{syn\_by\_ADH} \cdot ADH(t) \cdot \left(\frac{RO}{k_{i\_RO} + RO} \right) \cdot \left(1 - \frac{x}{L} \right) - CYP26 \cdot \left(k_{met\_RA} \cdot RA(t) \right.$$

$$- k_{met\_FLUCO} \cdot \left(\frac{\frac{FLUCO}{k_{i\_RA} + FLUCO}}{\frac{RA(t)}{k_{i\_RA} + RA(t)}} \right) - k_{met\_CYPRO} \cdot \left(\frac{\frac{CYPRO}{k_{i\_CYPRO} + CYPRO}}{\frac{RA(t)}{k_{i\_RA} + RA(t)}} \right)$$

$$- k_{met\_FON} \cdot \left(\frac{\frac{FON}{k_{i\_FON} + FON}}{\frac{RA(t)}{k_{i\_RA} + RA(t)}} \right) - k_{met\_FLUSI} \cdot \left(\frac{\frac{FLUSI}{k_{i\_FLUSI} + FLUSI}}{\frac{RA(t)}{k_{i\_RA} + RA(t)}} \right)$$

$$\left. - k_{met\_ETH} \cdot \left(\frac{ETH}{k_{i\_ETH} + ETH} \right) \right) - k_{\deg\_RA} \cdot RA(t)$$

We calibrated the new parameters (the different k_{met}) of the model with data on branchial arch malformations caused by the single azole (**Tab. 2.3**), in the same Bayesian framework as for FLUCO and Eth (see material and methods section). Predictive simulations for mixtures were then performed. The corresponding parameters are reported in **Tab. 2.4**.

Fig. 2.4 show the model predictions for binary mixtures of CYPRO + FON 7.8 µM (**A**), FON + FLUSI 3.125 µM (**B**) and FLUSI + FON 12.5 µM (**C**). The model appears to be reasonably predictive also for the mixture's effects after different azoles co-exposures. That model and the postulated MoA can also predict rather well the effects of mixtures of azoles.

The model is not perfect though, and the predicted effects somewhat underestimated the experimental results. This may be due to the fact that we only considered action of the azoles on the CYP26A1 isoform while at least three isoforms are expressed or partially co-expressed in early embryonic tissues (including branchial arches) (White and Schilling, 2008).

It is also known from literature that morphogenic gradients during hindbrain development are more complex and probably do not correspond to a simple concentration gradient of endogenous RA. Sirbu et al. (2005) demonstrated the existence of dynamic shifting boundaries of hindbrain RA activity: they showed that RA generated by RALDH2 in paraxial mesoderm initially travels as far anteriorly as presumptive r3 forming an early RA signalling boundary at r2/r3 just posterior to the RA-degrading enzyme Cyp26a1 expression domain. However, this boundary shifts posteriorly to the r4/r5 border to the expression of Cyp26c1 in r4 (**Fig. 2.5**).

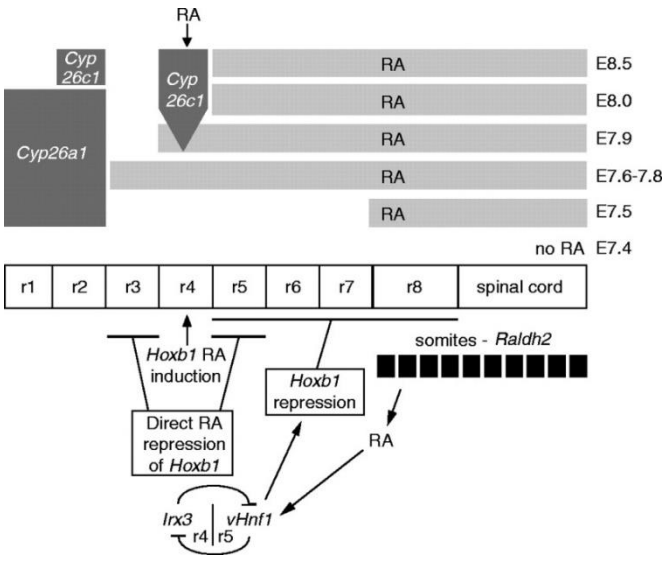

Figure 2.5. Model of shifting RA boundaries during mouse hindbrain segmentation. Initially, RA forms an early anterior boundary at r2/r3 (next to the r2 border of Cyp26a1 expression), followed soon after by a late anterior boundary at r4/r5 (next to the r4 border of Cyp26c1 expression). Moreover, RA acts directly to induce Hoxb1 expression and then RA acts both directly and indirectly (through induction of vHnf1) to restrict Hoxb1 expression to r4. (Figure from Sirbu et al., 2005).

Cyp26a1 is initially expressed in the anterior neural plate during gastrulation (Kudoh et al., 2002) and forms a boundary at presumptive r2/r3 (Pennimpede et al., 2010). This is followed by the later expression of Cyp26A1 in r2 and Cyp26C1 in r2 and r4 (Fujii, 1997; Abu-Abed et al., 2002; Tahayato et al., 2003; Uehara et al., 2007). *Cyp26a1*-/- mutant embryos show abnormal hindbrain specification, abnormal neural crest cell migration and abnormal anterior branchial arches (Sakai, 2001; Abu-Abed et al., 2002; Uehara et al., 2007). Sakai et al. (2001) showed using an RA-responsive lacZ transgene that RA signalling expands anteriorly into prospective r2 and r3 in *Cyp26a1*-/- mutants. Thus, Cyp26a1 acts as a local antagonist of RA signalling. In addition, *Cyp26a1*-/- mutants seems to be more sensitive to RA than wild types. Expansion of the posterior hindbrain caused by low doses of exogenous RA (5 nM) in mutants resembles wild-type embryos treated with much higher doses (Hernandez et al., 2007). This suggests that Cyp26a1 protects the embryo from elevated RA. Consistent with this idea, injection of high levels of retinal posteriorizes embryos lacking Cyp26a1 expression. Cyp26a1 is also required for exogenous RA treatments to rescue RA-deficient embryos (Hernandez et al., 2007). Thus Cyp26a1 seems to have a key role in the developing hindbrain to precisely restrict the field of endogenous RA signalling (White and Schilling, 2008).

In contrast to Cyp26a1, Cyp26b1 expression appears later and in a more dynamic pattern in the hindbrain in mice initially in r3 and r5 and later in r2–6 (MacLean et al., 2001). These patterns suggest that Cyp26b1 creates a new sink for RA within the central hindbrain (r3–5) at the end of gastrulation that eventually covers all but the most posterior rhombomeres. Loss-of-function *Cyp26b1*-/- mutations in mice cause abnormalities in the limbs and craniofacial skeleton as well as a loss of germ cells from the testis, but no major hindbrain defects (MacLean et al., 2007).
Cyp26c1 is also expressed in the hindbrain in mouse. Cyp26c1 expression initially appears in the head mesenchyme at E7.5 (Uehara et al., 2007), and is then expressed after gastrulation in r4 earlier than does that of Cyp26b1 at r3 and r5 (MacLean et al., 2001; Sirbu, 2005). These patterns suggest that Cyp26c1, like Cyp26b1, forms a sink for RA within the central rhombomeres (r2– 6) of the hindbrain that both reduces RA within cells that express it and helps shape gradients of RA in adjacent cells. Cyp26c1-deficient mice are viable and have no overt anatomical abnormalities. However, *Cyp26a1*-/- *Cyp26c1*-/- double mutants have severely posteriorized hindbrains and die during embryogenesis (Uehara et al., 2007) (**Fig. 2.6**).

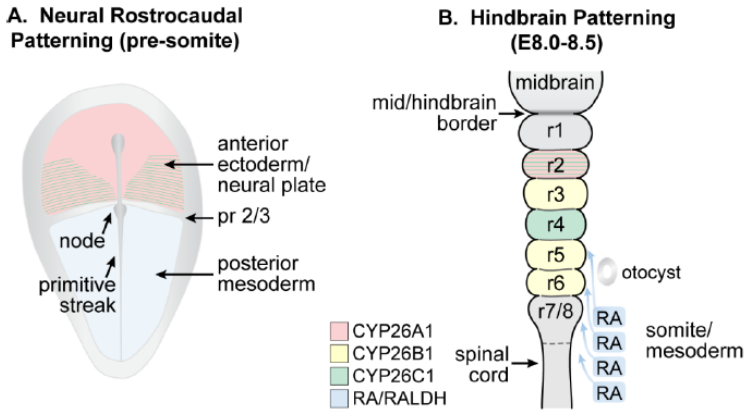

Figure 2.6. Schematic representation of the complementary RALDH2 retinoic acid (RA)-synthesizing and CYP26A1 RA-metabolizing activities during early embryo patterning (**A**) and hindbrain development (**B**). (**A**) RA generated by RALDH2 in the posterior mesoderm forms an early anterior boundary of activity in the neural plate at presumptive rhombomere (pr) 2/pr3, whereas Cyp26A1 and Cyp26C1 are expressed rostral to the pr2 border. (**B**) By E8.0 to E8.5, RA is being expressed by the somites and anterior presomitic mesoderm, and acts on the overlying hindbrain and spinal cord. The activity of the CYP26 enzymes regulate access of the neuroepithelium to RA (Clagett-Dame and Knutson, 2011).

Hence, the hindbrain utilizes the RA-degrading function of Cyp26s isoforms to establish shifting boundaries of RA activity. Sirbu et al. also showed that the initial RA boundary at r2/r3 is independent of RA activity, as Cyp26a1 expression does not require RA, but that the shift to an r4/r5 boundary is dependent upon RA to activate Cyp26c1 expression in r4. Their study showed that a stable RA gradient is not established across the hindbrain, but the initial gradient of RA entering the posterior hindbrain is converted by CYP26s isoforms into RA boundaries that shift over time such that anterior tissues receive a short pulse of RA and posterior tissues receives a long pulse of RA. This is essential for the specification of both rhombomeres and rhombomeric neural crest cells (NCC) migrating to the corresponding branchial region (Trainor and Krumlauf, 2000). These results provide strong evidence that the combined action of all three Cyp26s, differentially expressed in embryonic tissues, are required to pattern the A-P axis of the hindbrain.

All these subtle effects are not described by our model. To develop and validate a more sophisticated model we would need data on RA and other morphogens concentration in the hindbrain as a function of time and xenobiotic exposure concentrations. This could be the subject of further research. It may start from the development of branchial arches morphogenesis model, which could describe the triggering of NCCs migration.

Results from molecular docking showed that all the tested azoles have high affinities for all the three CYP26 isoforms and that the affinities are consistent with the different azole teratogenic profiles and potencies. The possibility of a different affinity of different azoles for the expressed

CYP26 isoforms could explain the underestimation of the predicted effects when compared to experimental results and it should be taken in account for a future improvement of the model. Moreover, azole-related inhibition of other CYP enzymes expressed in embryos at early stages such as CYP51, CYP2S1, and CYP11A1, all involved during the synthesis of cholesterol, steroids, and other lipids (Choudhary et al., 2003) could also be considered.

In any case, our model, despite the limitations discussed above, has several potential mechanistic or predictive applications for the risk assessment of exposures to mixtures of azoles acting with the same MoA or exposure to mixtures of Eth and azoles, which probably act with different MoA on the RA pathway. We also demonstrated that molecular docking could be a useful tool to screen molecules potentially interfering with CYP26 activity.

This *in silico* tool, developed by integrating different approaches, could be the starting point in the EuroMix project context to deliver refined safety assessment of mixtures of chemicals acting in the framework of a skeletal malformation AOP.

Tables and Figures

Table 2.1. Frequencies of malformations at the branchial arches in embryos exposed to Eth, FLUCO and FLUCO+Eth.

	Dose	N_malformed	N_observed
Retinoic Acid (µM)	0	0	22
	0.025	2	23
	0.05	11	16
	0.125	19	19
	0.25	15	17
	0.5	28	28
Ethanol (mM)	0	0	19
	17	0	15
	26	1	12
	34.7	2	12
	42.5	4	14
	85	12	15
	127	2	2
Fluconazole (µM)	0	0	19
	62.5	0	15
	125	4	9
	250	13	18
	500	10	10
FLUCO + ETH 17 mM	0	0	15
	62.5	6	16
	125	13	18
	250	17	18
	500	9	9
ETH + FLUCO 62.5 µM	0	0	15
	17	9	19
	42.5	7	9
	85	10	10

Table 2.2. Model parameter values.

RA pathway parameters

Parameter	Description (Units)	Value
RA	Amount of RA (nM)	26 [a]
k_syn_by_ADH	RA transcription by ADH constant (nM/min)	3.61022 [b]
k_met_RA	RA metabolized constant (1/(nM * min))	0.01667
k_deg_RA	RA degradation constant	0
k_trs_CYP26_base	CYP26 transcription constant (0.365 nM/min)	0.00608333
vmax_trs_CYP26_by_RA	Maximum rate of transcription of CYP26 by RA (7.1 nM/min)	0.118333
CYP26_mRNA	Amount of cyp26 mRNA (nM)	4
CYP26	Amount of CYP26 (nM)	14.28
k_act_CYP26_by_RA	CYP26 activation by RA constant (nM)	7.083839
k_deg_CYP26_mRNA	CYP26 mRNA degradation constant (1 min^$^{-1}$)	0.01667
k_trd_CYP26	CYP26 translation constant (1 min^$^{-1}$)	0.01667
k_deg_CYP26	CYP26 degradation constant (0.28 min^-1)	0.00466667
FGF	Amount of FGF (nM)	2.45
k_syn_FGF	FGF synthesis constant (min^$^{-1}$)	0.083333
k_deg_FGF	FGF degradation constant (1 min^$^{-1}$)	0.016667
k_inh_CYP26_by_FGF	CYP26 inhibition constant by FGF	1
k_i_RA	RA affinity constant to CYP26	85

Retinol parameters

Parameter	Description (Units)	Value
RO	Amount of Retinol (nM)	150 [c]
k_syn_ADH	ADH synthesis constant (nM/min)	0.016666667
k_deg_ADH	ADH degradation constant (1 min^$^{-1}$)	0.00234742 [b]
k_i_RO	RO affinity constant to ADH (nM)	49 [d]
ADH	Amount of ADH (nM)	7.1

Ethanol parameters

Parameter	Description (Units)	Value
ETH	Initial amount of Ethanol (mM)	0
K_i_ETH	ETH affinity constant to CYP26 (nM)	2.05 [e]
k_met_ETH	ETH metabolized constant	0.0058433 [f]
k_trs_ADH_by_ETH	ADH transcription constant by ETH (nM/min)	0.000380705 [f]
k_i_ETH_ADH	ETH affinity constant to ADH (mM)	36 [d]

Fluconazole parameters

Parameter	Description (Units)	Value
FLUCO	Initial amount of fluconazole (µM)	0
K_i_FLUCO	FLUCO affinity constant to CYP26 (nM)	0.142 [e]
k_met_FLUCO	FLUCO metabolized constant	0.00368049 [f]

[a] Duester, 2008.
[b] fitted with MatLab.
[c] Horton and Maden, 1995.
[d] Chase et al., 2009.
[e] molecular docking.
[f] Bayesian-numerically evaluated .

Figure 2.2. Cyp26's isoforms crystallographic structure (A: CYP26A1, B: CYP26B1, C: CYP26C1) and table of the affinities for different azoles. The affinities are consistent with different azole teratogenic potencies.

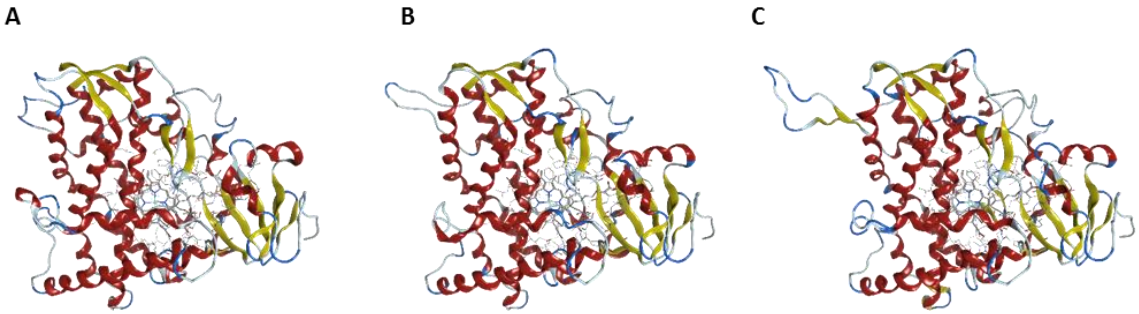

CYP26A1		CYP26B1		CYP26C1	
Compound	pKi	Compound	pKi	Compound	pKi
FLUSI	7.720	TEBU	7.466	TEBU	7.849
TEBU	7.613	CYPRO	7.326	IMA	7.161
IMA	7.495	FLUCO	7.175	CYPRO	7.087
Retinoic Acid	7.425	FLUSI	6.925	Retinoic Acid	7.028
CYPRO	6.953	FON	6.844	FLUCO	6.954
FON	6.845	Retinoic Acid	6.785	FON	6.840
NOL	6.655	IMA	6.550	FLUSI	6.837
FLUCO	6.601	NOL	6.511	NOL	6.763
ETH	3.174	ETH	2.348	ETH	2.988

Figure 2.3. Experimental data vs fitting and model predictions.

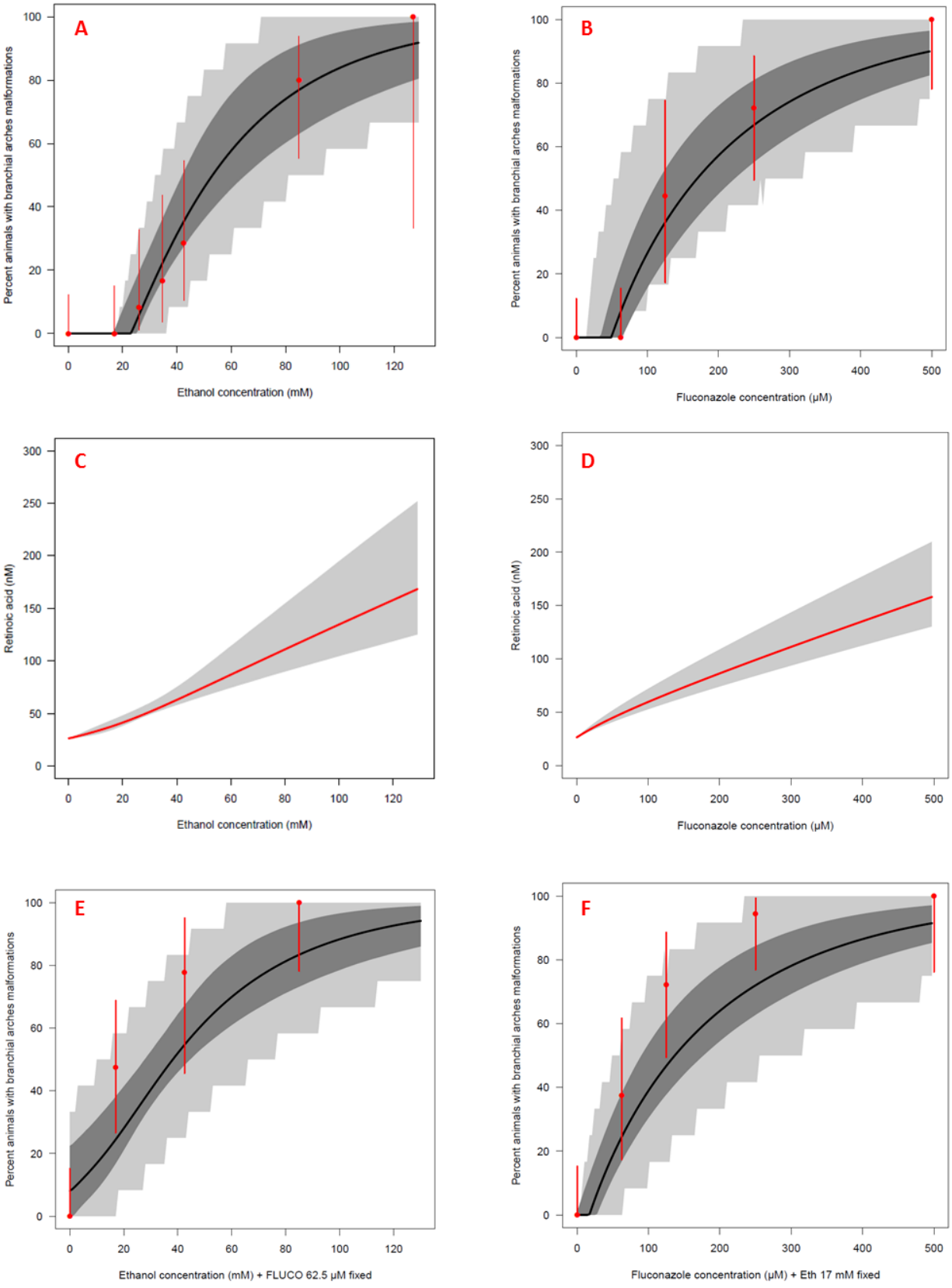

Table 2.3. Frequencies of malformations at the branchial arches in embryos exposed to cyproconazole, triadimefon, flusilazole and their binary mixtures.

	Dose	N_malformed	N_observed
Cyproconazole (µM)	0	0	9
	7.8	4	14
	15	8	9
	31.5	7	7
	250	3	3
Flusilazole (µM)	0	0	18
	1.5625	0	10
	3.125	5	11
	6.25	9	9
	9.375	5	5
Triadimefon (µM)	0	0	9
	6.25	0	8
	7.8	5	12
	12.5	3	11
	15	6	10
	25	8	8
	31.5	6	7
	50	7	7
	250	4	4
CYPRO + FON 7.8	0	0	9
	7.8	9	11
	15	3	3
FON + FLUSI 3.125	0	0	22
	6.25	10	10
	12.5	11	12
	25	8	8
	50	7	7
FLUSI + FON 12.5	0	0	22
	1.5625	4	7
	3.125	11	12
	6.25	6	6
	9.375	6	6

Table 2.4. Model parameter values for cyproconazole, triadimefon and flusilazole.

Cyproconazole parameters

Parameter	Description (Units)	Value
CYPRO	Initial amount of cyproconazole (μM)	0
K_i_CYPRO	CYPRO affinity constant to CYP26 (nM)	0.108 [e]
k_met_CYPRO	CYPRO metabolized constant	0.062215 [f]

Triadimefon parameters

Parameter	Description (Units)	Value
FON	Initial amount of triadimefon (μM)	0
K_i_FON	FON affinity constant to CYP26 (nM)	0.148 [e]
k_met_FON	FON metabolized constant	0.0412004 [f]

Flusilazole parameters

Parameter	Description (Units)	Value
FLUSI	Initial amount of flusilazole (μM)	0
K_i_FLUSI	FLUSI affinity constant to CYP26 (nM)	0.091 [e]
k_met_FLUSI	FLUSI metabolized constant	0.170554 [f]

[e] molecular docking.
[f] Bayesian-numerically evaluated .

Figure 2.4. Experimental data vs model predictions for CYPRO, FON and FLUSI mixtures.

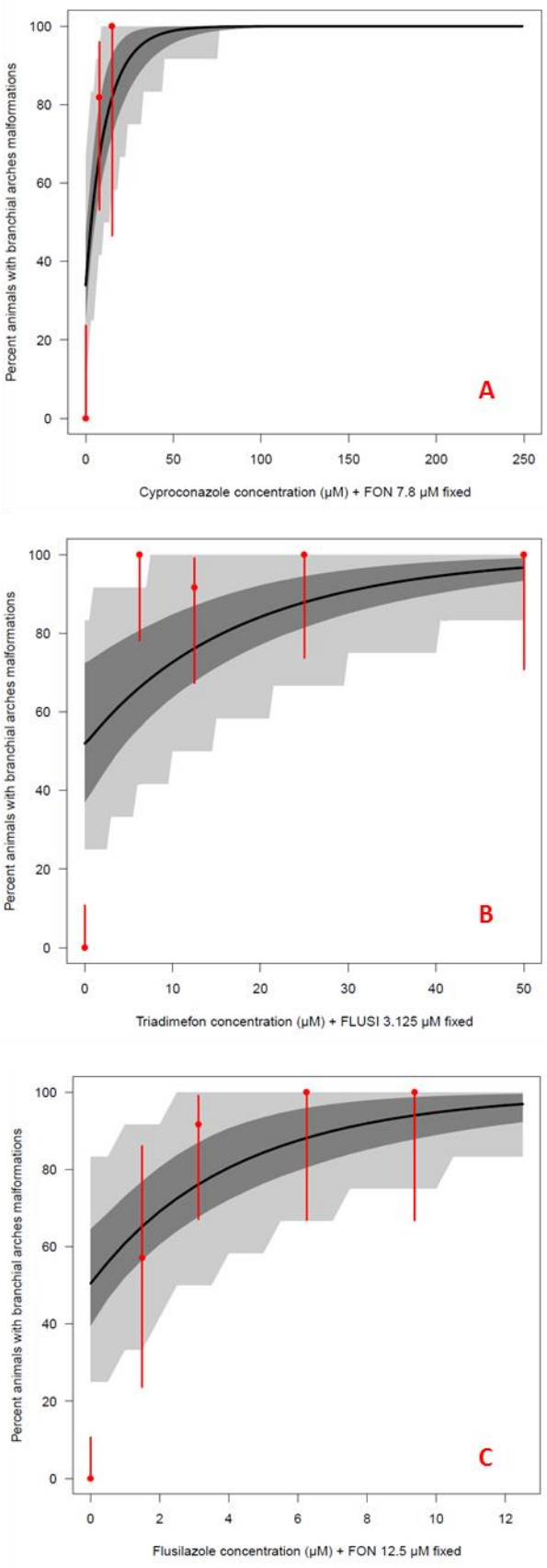

PART 3:

THE MIXTURE EFFECT OF CO-EXPOSURE TO ETHANOL AND FLUCONAZOLE: A STUDY IN AN ALTERNATIVE DEVELOPMENTAL MODEL, THE ASCIDIAN *CIONA INTESTINALIS* (AET)

Introduction

Ascidians are marine sessile, filter-feeding chordate organisms belonging to the Subphylum Urochordata, which has been recognized as the sister group of vertebrates (Delsuc et al., 2006). Particularly, ascidian embryos display striking similarities to vertebrate ones as they develop through a swimming, tadpole like larva, which represents a simple prototype of the chordate body plan (Passamaneck and Di Gregorio, 2005). Recently, ascidian embryos have been proposed as an excellent alternative experimental system for investigating the mechanisms underlying the development of chordates (Passamaneck and Di Gregorio, 2005; Sasakura et al., 2012), and therefore of vertebrates. They have also been used to outline the embryotoxic profile of numerous xenobiotics, including retinoic acid and certain azoles (De Bernardi et al., 1994; Cima et al., 1996; Nagatomo et al., 2003; Pennati et al., 2006; Groppelli et al., 2007; Zega et al., 2009; Matsushima et al., 2013). Previous studies reported that ascidian larvae exposed to different azole fungicides showed characteristic malformations resembling those elicited by retinoic acid (RA) (Pennati et al., 2006; Groppelli et al., 2007; Zega et al., 2009). In both the analysed species, *Phallusia mammillata* and *Ciona intestinalis*, azole-induced malformations were specifically at the anterior region of the trunk, in which the sensory vesicle appeared reduced and the pigmented organs were severely altered. Moreover, the development of the adhesive papillae, the anterior most organs, was impaired. The observation that the affected structure are in ascidians those controlled by RA (Nagatomo et al., 2003) and the evidence that the same alterations are produced by exogenous RA exposure (Hinman and Degnan, 1998; Nagatomo and Fujiwara, 2003; Nagatomo et al., 2003; Kanda et al., 2009) suggest that, similarly to what proposed in vertebrates (Menegola et al., 2003; Di Renzo et al., 2009; Marotta and Tiboni, 2010), also in ascidians the teratogenic action of azoles could depend on perturbation of RA pathway (Pennati et al., 2006; Groppelli et al., 2007; Zega et al., 2009)..

The use of alternative models in toxicology has been strictly recommended to evaluate the potential effects of the co-exposure of chemicals in a mixture (EPA, 2002). Considering the data obtained in ascidian species after azoles exposure, the aim of the last part of this work is to evaluate the ascidian *Ciona intestinalis* embryo model as a new alternative teratological screening test (AET, Ascidian Embryo Teratogenicity assay). The effects after exposure to FLUCO and Eth alone or in mixture will be compared with those obtained after exposing *C. intestinalis* embryos to increasing concentration of RA.

Materials and methods

Animals and embryos maintenance

Adults of *C. intestinalis* were collected by the fishing service of the Roscoff Biological Station (France) for what concern exposure to FLUCO and FLUCO+Eth fixed; or collected from the lagoon of Chioggia (Padova) for what concern exposure to RA, to Eth and to Eth+FLUCO fixed.

Animals were maintained in aquaria filled with artificial sea water (Instant Ocean, salinity 32‰) at 16° C and provided with circulation system as well as mechanical, chemical and biological filters. Constant light condition was preferred to promote gamete production.

Gametes of at least three adults were collected from dissected gonoducts and *in vitro* cross fertilization was performed in Petri glass dishes containing artificial sea water with Hepes (ASWH; pH 8). Embryos were maintained at 16 °C until they reached the hatching larva stage (22 hours post fertilization (hpf), Hotta et al., 2007).

Materials and compound preparation.

All-trans RA (Sigma, Italy), dissolved in DMSO, FLUCO (98%, Sigma), freshly dissolved in ASWH, and Eth (99.8%, Sigma) were used as test substances. All chemicals were of reagent grade and freshly prepared. The concentrations of RA (0.1, 0.2, 0.5, 1 µM) were those used in previous published experiments (De Bernardi et al., 1994; Nagatomo and Fujiwara, 2003). Groups of control + DMSO were also performed. The concentrations of FLUCO (0, 7.8, 15.75, 31.5, 250 µM) were chosen based on previous works (Groppelli et al., 2007) focusing on lower doses to identify the NOAEL (*No Observed Adverse Effect Level*), plus a high dose as positive control. The concentration of Eth were 1.7, 8.5, 17, 42.5, 85 mM. Groups of control (CONT) were also performed. Each treatment solution was dissolved in 10 mL of ASWH.

Embryo exposure

C. intestinalis embryos at early neurula stage (7 hpf) were exposed for 15 h, until control embryos reached the larval stage, to RA (0.1, 0.2, 0.5, 1 µM), to Eth alone (1.7, 8.5, 17, 42.5, 85 mM), to FLUCO alone (0, 7.8, 15.75, 31.5, 250 µM), or co-exposed to the NOAEL of Eth (1.7 mM) and to different concentrations of FLUCO or were co-exposed to the NOAEL of FLUCO (7.8 µM) and to different concentrations of Eth.

Approximately 100 embryos were used for each treatment and each experimental group. Each experiment was replicated at least three times (total n per groups ≈ 300). When controls reached swimming larva stage (22 hpf), all specimens were evaluated and the percentage of dead larvae was recorded. After fixation in 4% paraformaldehyde in PBS larvae were morphologically

examined in detail under a dissecting microscope. The number of larvae showing abnormalities at tail, trunk and pigmented sensory organs as well as plurimalformed larvae were recorded.

Statistical analysis

To evaluate any morphological abnormality in the different groups, larvae were examined under a dissecting microscope and any abnormality recorded. The percentage of abnormal larvae was determined. Data were statistically analysed using χ^2 test. The level of significance was set at $p < 0.05$.

Results

Morphological analysis of induced abnormalities

Ciona intestinalis larvae of each experimental group were morphologically examined under a dissecting microscope in order to evaluate the presence of abnormalities as well as plurimalformed larvae.

Nearly 80% of unexposed larvae (**Tab. 3.1; Tab. 3.2**) developed normally, displaying an elongated trunk with three elongated adhesive papillae, the sensory vesicle clearly visible and the two pigmented organs (otolith and ocellus) differentiated. The ocellus, the dorsally located photoreceptor, and the otolith, the gravity-sensing organ, were located inside the sensory vesicle. The tail was straight and elongated (**Fig. 3.1 A-B**).

Larval abnormalities were classified in four malformed phenotypes:

- trunk abnormalities, in which trunk appeared round in shape and the anterior side was flat, due to impairment of adhesive papillae development (**Fig. 3.1 B-C**);
- pigmented organ abnormalities, in which the pigmented organs (otolith and ocellus) appeared fused in a single spot and/or they were displaced on the dorsal portion of the sensory vesicle (**Fig. 3.1 D-F**). In the samples displaying sensory vesicle protrusion on the trunk dorsal side, the pigmented organs were exposed to the surface;
- tail abnormalities, in which the larval tail appeared coiled, flexed or reduced in length (**Fig. 3.1 G**);
- severe malformations, in which plurimalformed larvae were characterized by absence of sensory vesicle cavity, presence of a short, bent tail, round trunk with not elongated papillae. This group includes also larvae that failed the hatching event (**Fig. 3.1 H**).

RA

All the concentrations tested resulted effective (**Tab. 3.1**) confirming what was already described by other authors in *C. intestinalis* and in other ascidian species (De Bernardi et al., 1994; Katsuyama et al., 1995; Hinman and Degnan, 1998; Nagatomo et al., 2003). RA-treated larvae showed malformations of the anterior trunk portion, with shortened trunk and head, and severe anomalies at the pigmented organs compared to controls. Larvae exposed to RA 1 µM showed also a shortened tail and a higher incidence of plurimalformed larvae.

Eth

During the development of *C. intestinalis* embryos, exposure to Eth increased the total number of malformed larvae. The percentage of malformed larvae increased in a concentration-related manner (**Tab. 3.2**). The lower effective concentration was 8.5 mM (**Fig. 3.2**). The Eth lower tested concentration (1.7 mM) did not cause a significant increase of malformations at any district compared to the controls. The main target for Eth were specifically the pigmented sensory organs: otolith and ocellus appeared fused or protruded at any effective concentration. Eth determined also a significant increase on trunk malformations, but this effect was evident only from concentration 1.7 mM (**Fig. 3.2**). The incidence of tail abnormalities was not significantly affected by Eth. The percentage of total malformations increased significantly with Eth concentration from the concentration of 1.7 mM on (**Tab. 3.2**). Overall, Eth 1.7 mM resulted the NOAEL for *C. intestinalis* development, as did not cause a significant increase of any abnormalities.

FLUCO

The incidence of total number of malformations induced by FLUCO during the development of *C. intestinalis* embryos was dose-dependent. FLUCO specifically affected the pigmented organs and the trunk. FLUCO concentrations ≥ 15.75 μM significantly increased the total number of malformations, compared to controls, while FLUCO 7.8 μM resulted effective only as concern the pigmented organs abnormalities (**Tab. 3.3**). Larvae showed significantly more malformations than controls if FLUCO dose was ≥ 15.75 μM. The severity of FLUCO induced malformations was dose dependent, and the phenotype induced closely resembled that caused by RA treatment. Tail abnormalities were not significantly affected by FLUCO at any tested concentration, as well as the number of severe malformations.

Overall, FLUCO 7.8 μM could not be considered the NOAEL for C. intestinalis, as it causes a significant increase of abnormalities at the pigmented organs compared to control groups (**Tab. 3.3**).

ETH + FLUCO fixed

Comparing the larvae developed from embryos exposed to Eth alone and from embryos exposed to the Eth + FLUCO 7.8 μM mixture, we found that the co-exposure increased in a significant and dose-dependent manner the number of larvae with trunk abnormalities and the total number of observed malformations. Pigmented organs and tail abnormalities were not significantly affected by co-exposure with FLUCO (**Tab. 3.2**, **Fig. 3.2**). Overall, in co-exposure with FLUCO,

Eth 1.7 mM caused a significant increase of total malformations and of the trunk abnormalities (**Tab. 3.2**). There is a clear and specific mixture effect of FLUCO in increasing the total number of trunk abnormalities.

FLUCO + Eth fixed

Comparing the larvae developed from embryos exposed to FLUCO alone and from embryos exposed to the FLUCO + 1.7 mM ethanol mixture, we found that the co-exposure increased in a significant and dose-dependent manner the total number of malformed larvae.
(**Tab. 3.3**, **Fig. 3.3**). Overall, there is a general effect of Eth in increasing the FLUCO effects.

Discussion

The main aim of the present work was to evaluate the suitability of the ascidian developmental model (AET) to test mixture effects. In particular, AET was used as new alternative invertebrate model to test the developmental effects of the co-exposure to Eth and FLUCO.

The teratogenic potential of Eth had never been previously evaluated in ascidians, while teratogenic effects of FLUCO were observed in the ascidian *Phallusia mammillata* at concentrations similar to those used in the present work (Groppelli et al., 2007). Data obtained in both ascidian species after FLUCO exposure and those obtained after the exposure of *C. intestinalis* to the azole Imazalil (Zega et al., 2009) showed that the elicited phenotype after azole exposure is striking similar to that induced by RA. According to literature, exposure to RA during development causes stereotypical malformations in ascidian larvae, which develop with a rounded trunk and malformed sensory vesicle and pigmented organs (De Bernardi et al., 1994; Katsuyama et al., 1995; Hinman and Degnan, 1998; Nagatomo and Fujiwara, 2003).

Results from the present study showed that Eth is teratogenic in the ascidian *C. intestinalis* at concentrations equal or higher than 8.5 mM.

Remarkably, the co-exposure to the sub-teratogenic concentration of Eth (1.7 mM) significantly increased the general teratogenicity of the effective concentrations of FLUCO alone, suggesting the presence of a mixture effect. In addition, co-exposure to increasing concentrations of Eth and FLUCO 7.8 µM significantly increases the incidence of number of trunk-malformed larvae, suggesting the presence of a specific effect exert by FLUCO at the level of the anterior structures with a consequent synergistic effect.

These data support the hypothesis that both Eth and FLUCO could act affecting the same pathway. In vertebrate embryos the MOA proposed is the inhibition of cytochrome P-450 (CYP26) enzymes, involved in RA catabolism, with the consequent increase in local RA levels in vertebrate embryos (Menegola et al., 2004; E. Menegola et al., 2006). The similarity between FLUCO- and RA-induced phenotypes suggests that a similar pathway could be suggested also in tunicates. In ascidians, the role of RA cascade and the expression of CYP26 has been described and compared to the expression of CYP26 in vertebrate embryos. Considering that both the expression pattern of ascidian *CYP26* and of *Hox-1* (a key gene in RA controlled cascade) were considered corresponding to those described in vertebrate hindbrain (Nagatomo and Fujiwara, 2003), it could be hypothesized that FLUCO alters the RA morphogenetic activity in specific responsive ascidian embryonic tissues, with a consequent significant alterations at the anterior structures.

Evidence obtained by the phenotypes of Eth-exposed larvae by mixture data suggests that Eth can alter ascidian morphogenesis, probably by interfering with the same pathway. Eth involvement in this process represents an intriguing but still highly speculative hypothesis and further analyses to confirm Eth interferences in RA pathways are needed.

In conclusion, this work shows that AET assay offers several advantages as a model system for the study of mixture effects. First, the adults are widespread in coastal area, easily handled as aquarium animals, and by *in vitro* fertilization it is possible to produce thousands of synchronously dividing embryos. Moreover, since the ascidian embryos develop quickly into swimming tadpole larvae (18 hours at 18 °C; Hotta et al., 2007), it is possible to observe the effects of treatment within a day. Finally, considering that ascidians are basal chordates recognized as belonging to the sister group of vertebrates (Delsuc et al., 2006), results obtained in these species could be considered indicative for deep toxicological investigation in mammal embryos. Concerning the issue of exposure to mixtures, our data support the need of a cumulative risk assessment not only for chemicals grouped on the base of similarities in chemical structure or derived from mechanistic considerations but also for any chemical acting on the same biological pathway.

Tables and Figures

Figure 3.1. Morphological analysis of *Ciona intestinalis* larvae.

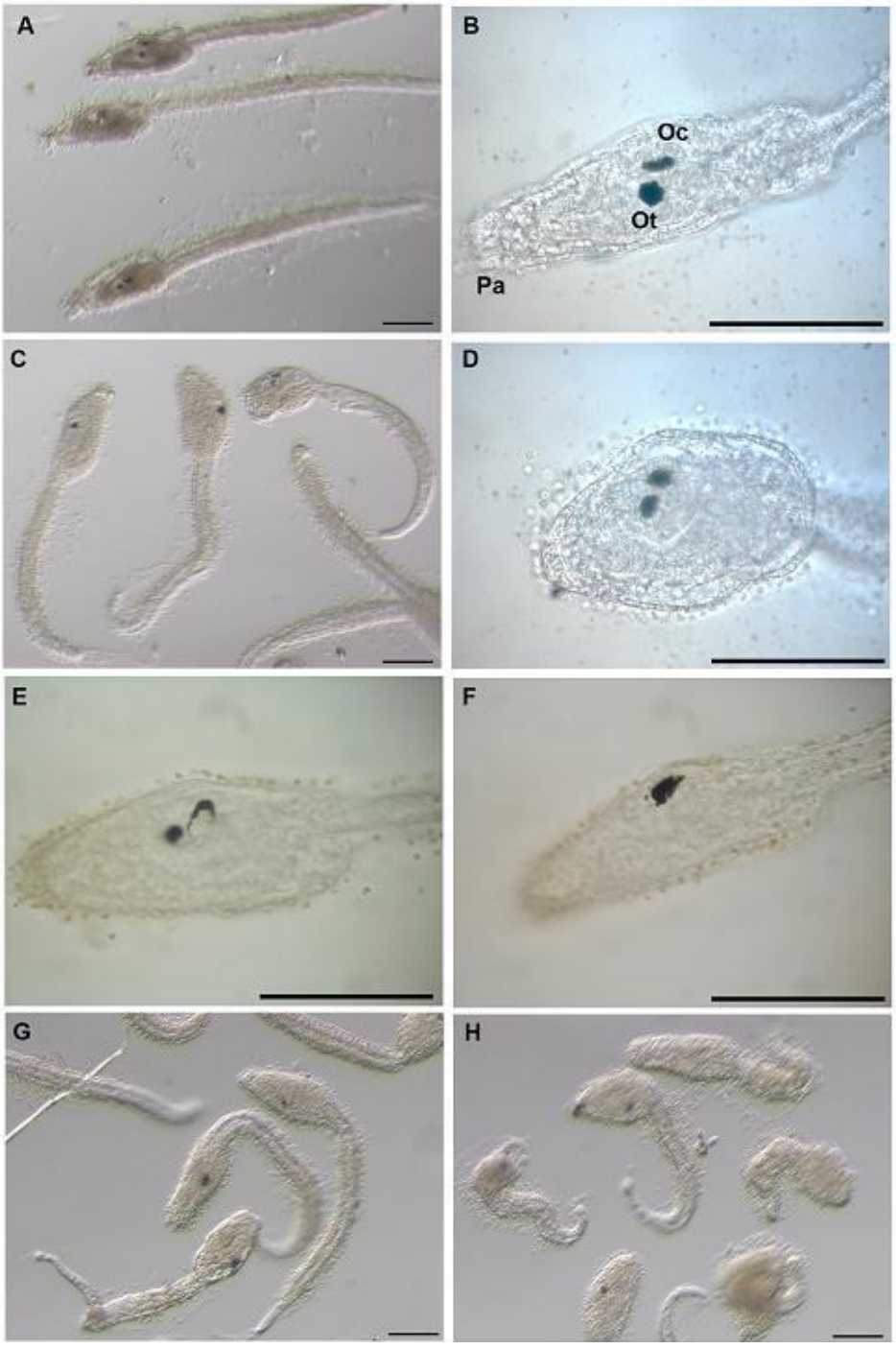

Figure 3.1: (A and B) Normally developed larvae. The lateral view of the trunk (B) allows to distinguish the otolith (Ot) and the ocellus (Oc), separated and well-differentiated. Adhesive papillae (Pa) are also visible at the anterior end. (C and D) Larvae displaying trunk abnormalities. The trunk appears round in shape with impairment of adhesive papillae development. (D and F) Larvae displaying malformed pigmented organs, abnormal in shape (D – E) or fused (F). (G) Larvae with coiled or flexed tail. (H) Plurimalformed larvae displaying severe malformations to almost all organs. Magnifications: 60X (A, C, G, H), 120X (B, D, E, F). Scale bar: 100 µm.

Figure 3.2. Histograms showing the effect of the co-exposure to increasing Eth concentration with FLUCO 62.5 µM on different categories of malformation.

* = Effect of FLUCO compared to Eth alone.

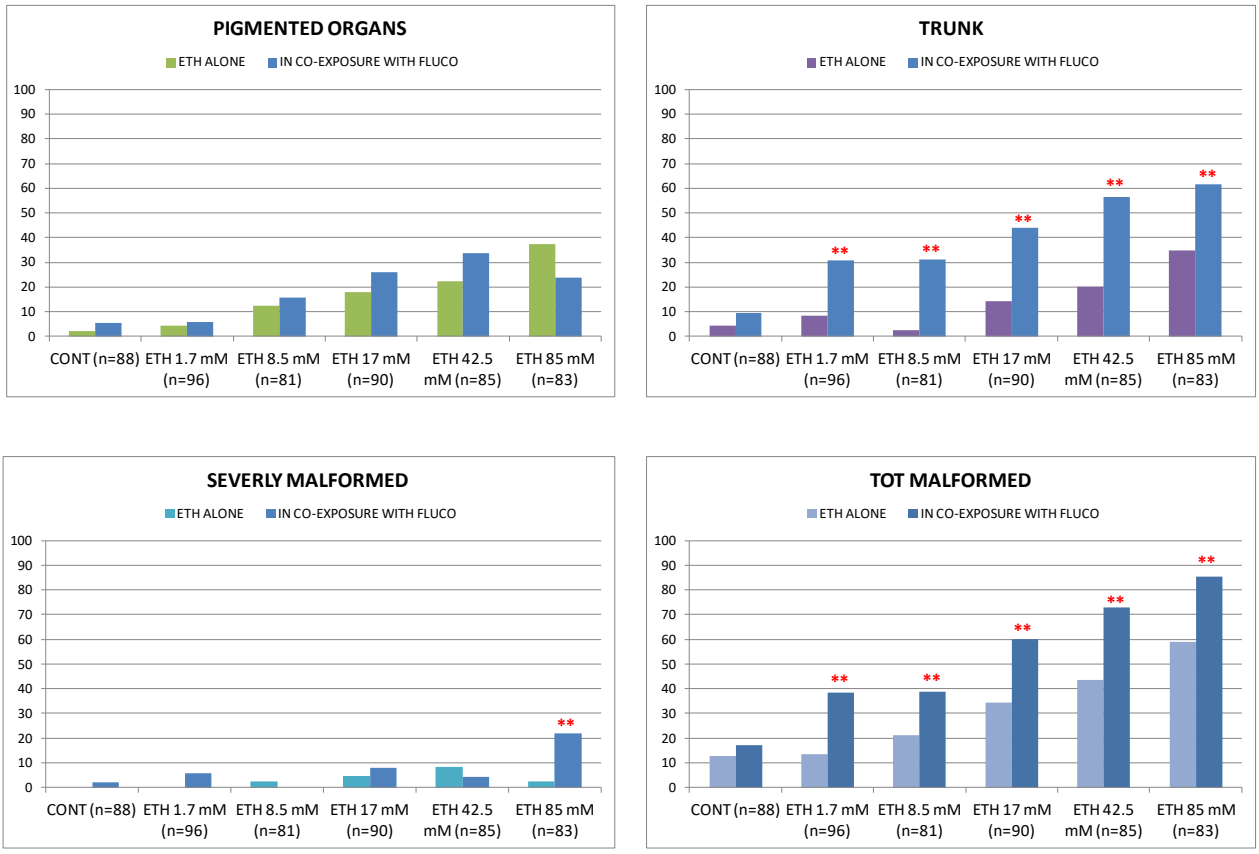

Figure 3.3. Histograms showing the effect of the co-exposure to increasing FLUCO concentration with Eth 0.01% on different categories of malformation.

* = Effect of Eth compared to FLUCO alone.

Table 3.1. Abnormalities (%) of larvae exposed to increasing RA concentrations (µM).

	CONT (n=300)	CONT+DMSO (n=283)	RA 0.1 µM (n=266)		RA 0.2 µM (n=233)		RA 0.5 µM (n=207)		RA 1 µM (n=145)	
NORMAL	82.33	80.86	0.00	AB	0.44	AB	0.00	AB	0.00	AB
TAIL	5.26	2.34	5.16		4.42		6.63	ABCd	32.09	ABCDE
PIGMENTED ORGANS	1.88	1.17	5.95	AB	13.27	AB	25.51	AB	29.10	ABCDE
TRUNK	6.77	8.98	82.94	α	80.97	Ab	81.63	Ab	59.70	ABCDE
SEVERELY MALFORMED	5.26	7.42	17.06	AB	18.14	AB	18.37	AB	40.30	ABCDE
TOT ABNORMALITIES	12.41	11.72	82.94	AB	81.42	AB	81.63	AB	59.70	ABCDE
TOT MALFORMED	17.67	19.14	100.00	AB	99.56	AB	100.00	AB	100.00	AB

α p<0.05 vs. CONT
A p<0.01 vs. CONT
b p<0.05 vs. CONT+DMSO
B p<0.01 vs. CONT+DMSO
C p<0.01 vs. RA 0.1 µM
d p<0.05 vs. RA 0.2 µM
D p<0.01 vs. RA 0.2 µM
E p<0.01 vs. RA 0.5 µM

Table 3.2. Abnormalities (%) of larvae exposed to increasing Eth concentrations (mM) and to the mixture Eth + FLUCO fixed.

	CONT (n=88)	ETH 1.7 mM (n=96)	ETH 8.5 mM (n=81)	ETH 17 mM (n=90)	ETH 42.5 mM (n=85)	ETH 85 mM (n=83)
NORMAL	87.50	86.46	79.01	65.56 AB	56.47 ABC	40.96 ABCD
TAIL	5.68	1.04	4.94	1.11	1.18	8.43 bde
PIGMENTED ORGANS	2.27	4.17	12.35 a	17.78 AB	22.35 AB	37.35 ABCDe
TRUNK	4.55	8.33	2.47	14.44 c	20.00 AbC	34.94 ABCDe
SEVERELY MALFORMED	0.00	0.00	2.47	4.44	8.24 ab	2.41
TOT ABNORMALITIES	12.50	13.54	18.52	30.00 Ab	35.29 ABC	56.63 ABCDE
TOT MALFORMED	12.50	13.54	20.99	34.44 ABc	43.53 ABC	59.04 ABCDe

a p<0.05 vs. ETH 0
A p<0.01 vs. ETH 0
b p<0.05 vs. ETH 1.7 mM
B p<0.01 vs. ETH 1.7 mM
c p<0.05 vs. ETH 8.5 mM
d p<0.05 vs. ETH 17 mM
D p<0.01 vs. ETH 17 mM
e p<0.05 vs. ETH 42.5 mM
E p<0.01 vs. ETH 42.5 mM

	FLUCO 7.8 (n=94)	ETH 1.7 + FLUCO (n=52)	ETH 8.5 + FLUCO (n=90)	ETH 17 + FLUCO (n=50)	ETH 42.5 + FLUCO (n=92)	ETH 85 + FLUCO (n=96)
NORMAL	82.98	61.54 A	61.11 A	40.00 ABC	27.17 ABC	14.58 ABCD
TAIL	0.00	0.00	1.11	2.00	5.43	4.17
PIGMENTED ORGANS	5.32	5.77	15.56 ab	26.00 AB	33.70 ABC	23.96 AB
TRUNK	9.57	30.77 A	31.11 A	44.00 ABC	56.52 ABC	61.46 ABCd
SEVERELY MALFORMED	2.13	5.77	0.00 b	8.00 c	4.35	21.88 ABCdE
TOT ABNORMALITIES	14.89	32.69 A	38.89 A	52.00 Ab	68.48 ABCd	63.54 ABC
TOT MALFORMED	17.02	38.46 A	38.89 A	60.00 ABC	72.83 ABC	85.42 ABCD

a p<0.05 vs. FLUCO 7.8
A p<0.01 vs. FLUCO 7.8
b p<0.05 vs. ETH 1.7 + FLUCO 7.8
B p<0.01 vs. ETH 1.7 + FLUCO 7.8
c p<0.05 vs. ETH 8.5 + FLUCO 7.8
C p<0.01 vs. ETH 8.5 + FLUCO 7.8
d p<0.05 vs. ETH 17 + FLUCO 7.8
D p<0.01 vs. ETH 17 + FLUCO 7.8
E p<0.01 vs. ETH 42.5 + FLUCO 7.8

Table 3.3. Abnormalities (%) of larvae exposed to increasing FLUCO concentrations (µM) and to the mixture FLUCO + Eth fixed.

	CONT (n=234)	FLUCO 7.8 µM (n=176)	FLUCO 15.75 µM (n=250)	FLUCO 31.5 µM (n=239)	FLUCO 250 µM (n=199)
NORMAL	68.80	59.66	50.00 A	30.96 ABC	16.08 ABCd
TAIL	10.68	9.09	4.00	17.99 Ab	10.05 ABc
PIGMENTED ORGANS	4.27	13.07 a	19.60 A	27.20 ABc	35.68 ABC
TRUNK	8.97	18.18	26.00 A	41.00	54.27 Bc
SEVERELY MALFORMED	7.69	1.70	3.60	5.44 ABc	12.56 ABC
TOT ABNORMALITIES	23.50	38.64 a	46.40 A	63.60 ABC	71.36 ABCd
TOT MALFORMED	31.20	40.34	50.00 A	69.04	83.92

a p<0.05 vs. FLUCO 0 µM
A p<0.01 vs. FLUCO 0 µM
b p<0.05 vs. FLUCO 7.8 µM
B p<0.01 vs. FLUCO 7.8 µM
c p<0.05 vs. FLUCO 15.75 µM
C p<0.01 vs. FLUCO 15.75 µM
d p<0.05 vs. FLUCO 31.5 µM

	CONT + ETH (n=218)	FLUCO 7.8+ETH (n=273)	FLUCO 15.75+ETH (n=248)	FLUCO 31.5+ETH (n=249)	FLUCO 250+ETH (n=234)
NORMAL	70.18	42.86 A	22.58 AB	15.26 AB	4.27 ABCd
TAIL	7.34	10.26	12.10	11.65	7.69
PIGMENTED ORGANS	11.01	23.81 a	33.06 A	32.53 A	63.68 ABCD
TRUNK	10.09	26.37 A	44.76 AB	43.78 AB	49.57 AB
SEVERELY MALFORMED	4.13	8.42	14.92 a	22.89 AB	17.95 A
TOT ABNORMALITIES	25.69	48.72 A	62.50 A	61.85 A	77.78 ABcd
TOT MALFORMED	29.82	57.14 A	77.42 AB	84.74 AB	95.73 ABCd

a p<0.05 vs. FLUCO 0 + ETH 1.7 mM
A p<0.01 vs. FLUCO 0 + ETH 1.7 mM
B p<0.01 vs. FLUCO 7.8 + ETH 1.7 mM
c p<0.05 vs. FLUCO 17.75 + ETH 1.7 mM
C p<0.01 vs. FLUCO 17.75 + ETH 1.7 mM
d p<0.05 vs. FLUCO 31.5 + ETH 1.7 mM
D p<0.01 vs. FLUCO 31.5 + ETH 1.7 mM

GENERAL DISCUSSION

Congenital anomalies are a major cause of infant mortality and childhood morbidity, affecting 2-3% of newborns. Exposure of the embryo to environmental chemicals (pesticides, air and water pollutants) can result in congenital malformations or developmental defects such as oro-facial cleftings (cleft lip and/or palate alone or associated with other cranio-facial deformities), which are one of the most frequent (1:700 live births) (Mossey et al., 2009). Usually, the human embryo is not usually exposed to a single substance, but to many substances simultaneously. Despite the efforts in elucidating mechanism of action of substances that perturb the normal embryonic development, only a small part of involved pathways have been understood to date (Giavini and Menegola, 2004). This is why, evaluating the toxicity of mixtures of multiple chemicals is one of the major objectives of today's toxicology despite the effect of exposure to a mixture is still difficult to understand.

The EPA Guidelines of 2002 suggest investigating a few mixtures considered "high priority" and recommend the use of the models of dose additivity in the absence of adequate information on the presence of chemical interactions. However, recent studies suggest that the similarity of molecular initiating events (MIEs) is not an essential requirement to induce additive effects, because mixtures composed of chemicals with different MIE can exhibit mixture effects too, probably acting on the same biological pathway and contributing to the same adverse outcome (P. on P. P. P. and their R. (PPR) EFSA, 2013). In addition, it has been argued that grouping criteria based solely on chemical similarity or similar mechanisms may lead to unrealistically narrow groupings, with the exclusion of chemicals that also might contribute to combination effects (Boobis et al., 2011). This is in recognition of emerging evidence that biological effects can be similar, although the molecular details of toxicological mechanisms may profoundly differ in many respects (Kortenkamp, 2007). It appears evident that a clear and efficient test strategy for risk assessment of mixtures is still lacking. Furthermore, there is an increasing societal need to reduce animal testing.

In the case of a possible, multiple aetiology of an adverse outcome (AO), the risk of a multiple exposure to different risk factors showing additive effect should be taken into account.

One concept that has been proposed to aid in addressing these challenges and the resulting regulatory needs is the Adverse Outcome Pathway (AOP). An AOP (**Fig. 10**) describes a framework of information about the progression of toxicity events starting from one or more molecular initiating events (MIEs). Alterations along a sequence of more and more complex biological organizations are described as key events (KEs) and lead, at the end, to the AO (Villeneuve et al., 2014).

Detailed mechanistic knowledge is necessary in order to develop alternative testing methods on chemicals potentially acting on the same AOP. The elucidation of the different potential chemical actors switching on the same or different MIEs/ KEs but contributing to the same AO (for our purposes cranio-facial defects) is fundamental in order to plan researches on the contribution of multiple exposures for facial cleftings.

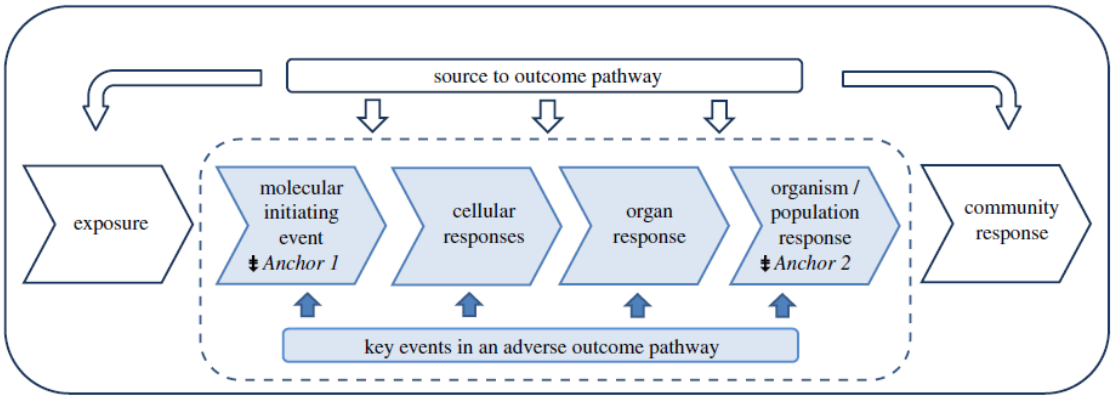

Fig. 10. Representation of a generic Adverse Outcome Pathway (AOP) (Figure from Madden et al., 2014)

Respect to the MoA framework developed for analysing the relevance of toxicological effects observed in animals to human risk assessment, the AOP framework is substance independent (knowing the specific molecules trigging the MIE is not relevant). Fundamentally, AOPs are not intended to be a complete representation of complex biological processes but rather provide a structured and simplified way to organizing toxicological knowledge in a manner that enhances its utility in decision support and chemical risk assessment. In fact, each AOP need to be clear, transparent, easy to understand and apply and must provide a large degree of flexibility and accommodate varying levels of detail (Meek et al., 2014). Generally, an individual AOP, defined as a single chain of KEs connecting a specific type of MIE to an AO, is the simplest functional unit of prediction. In real world, the exposure scenarios involve exposure to complex mixture, not individual chemicals. Therefore, a more realistic representation of the complex biological interactions that would occur in response to mixtures are systems of multiple interacting AOPs (AOP networks) sharing one or more common KEs or KERs (Villeneuve et al., 2014). One advantage of the AOPs is that they are "living documents" that have the potential to develop and evolve over time as additional knowledge became available. The other advantage is their ability to incorporate data from a wide range of sources (*in silico*, *in vitro*, *in vivo*, etc.) and use this information to provide the linkages between the MIE and the adverse outcome (Madden et al., 2014).

In fact, to arrive in the future to the creation of a realistic overall picture of human exposure to mixtures, the development of integrated approaches between *in vitro* and *in silico* techniques and computational systems biology able to predict the effects of mixtures starting from the concentrations of their individual components will be essential. In this context, the AOP framework provides an ideal opportunity for the integrated use of data from *in silico*, *in vitro* and *in vivo* approaches, essential to address the scientific challenge that mixtures pose us.

Mechanistic studies of some teratogenic agents such as retinoids, ethanol and some pesticides of the class of the azoles fungicides suggested that they could exert their teratogenic action by interfering with the same pathway.

Azoles are synthetic antifungal compounds, derived from triazole or imidazole, selected to test possible methodologies to assess cumulative effects on human health (EFSA, 2009).

The postulated mechanism of action is the inhibition of CYP26 enzymes (involved in retinoic acid (RA) degradation during early embryonic development), with the consequent increase in RA local content. Excess of RA at the critical window of sensitivity has been shown to be responsible for the specific branchial arch malformations and the subsequent craniofacial malformations described after experimental azole exposure (Menegola et al., 2006a; Marotta and Tiboni, 2010) (**Fig. 11**).

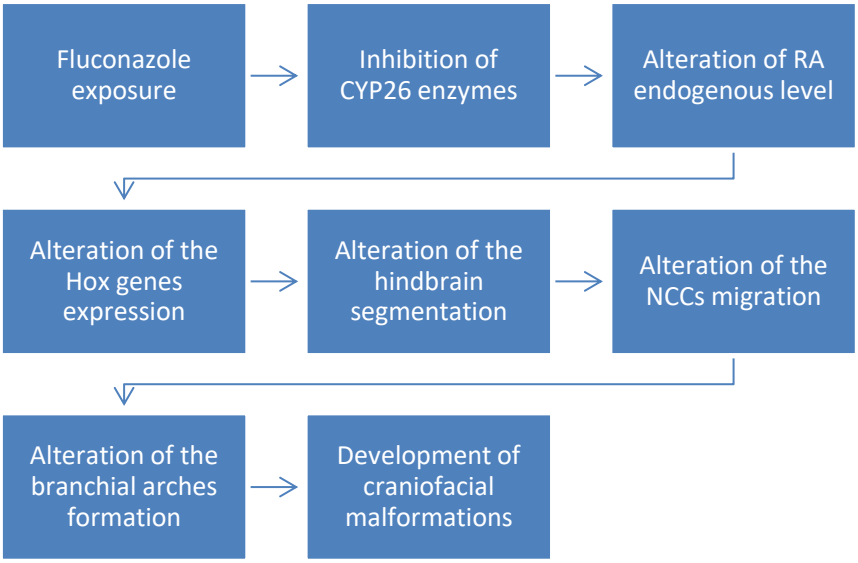

Fig. 11. Postulated MoA of fluconazole.

Craniofacial morphogenesis is affected also by ethanol (Eth). Eth in fact is a commonly consumed in alcoholic beverages also during pregnancy even if it is known to be a teratogen. The teratogenic effects of Eth have been deeply investigated, but the specific molecular initiating events (MIEs) have not been completely clarify until now. One of the potential mechanism by which Eth could act as teratogen, is the possible interference with ADH7, a key enzyme in retinoic acid (RA) pathway, responsible of its production (**Fig. 12**).

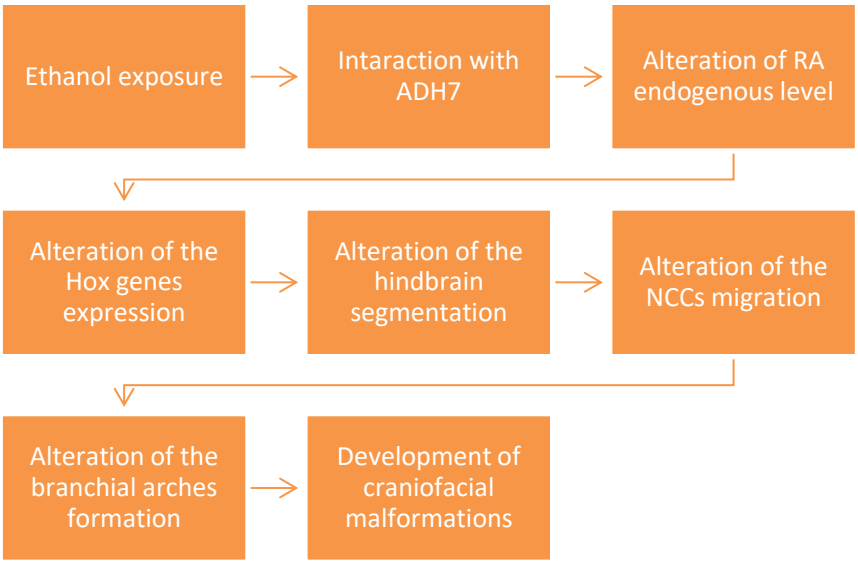

Fig. 12. Postulated MoA of ethanol.

From literature data, it is clear that ethanol (Eth) and azoles can lead to the same adverse outcome (craniofacial abnormalities after embryonic exposure) acting with different MIEs both potentially converging on RA metabolic pathway, altering the RA production (Eth) and the RA catabolism (azoles) (Menegola et al., 2000, 2001, 2003, 2005a, 2005b; E. Menegola et al., 2006; Menegola et al., 2006b; Di Renzo et al., 2007, 2011a, 2011b; Deltour et al., 1996; Dunty Jr. et al., 2002; Kot-Leibovich and Fainsod, 2009; Kane et al., 2010). Whereby, considering these data, the co-exposure to FLUCO and Eth, limited to the branchial pathogenesis, could produce additive effect affecting the same pathway but with different MoA.

This PhD project was conducted with the specific aim to investigate the mechanisms of action which we assume at the basis of the observed effects through the development of an *in silico* tool, validated by *in vitro* experiments, useful to simulate and predict the effects on embryo development after co-exposure to substances with independent MoA but acting on the same pathway and potentially contributing to the same adverse outcome (cranio-facial malformations). For this purpose, the project was divided into three parts.

In the first part, we verified the teratogenic mechanism exert by RA, FLUCO and Eth in post-implantation rat embryos exposed *in vitro* to increasing concentration of RA (0.025-0.0375-0.05-0.125-0.25 µM), to increasing concentrations of Eth (17-42.5-85-127 mM), to increasing concentrations of FLUCO (62.5-125-250-500 µM), or co-exposed to binary mixtures of FLUCO and Eth, in order to draw its toxicity dose-response curve. Concentration related effects were observed after the exposure to Eth (42.5-127mM) or FLUCO (125-500µM) comparable to those elicited by RA. The observed abnormalities were specifically at the level of the branchial apparatus (reductions or fusions), confirming the branchial apparatus as the main target of the teratogenic effects induced by FLUCO as previously observed (Menegola et al., 2000, 2001, 2003, 2004, 2006b). The co exposure to Eth and FLUCO at their NOAELs resulted effective, inducing almost 40% of branchial arch abnormalities. A significant enhancement of teratogenic effects were also observed in the other groups co-exposed to FLUCO and Eth in comparison to the single exposure. It seems that the co-exposure to FLUCO and Eth is able to induce mixture effects. In particular, the presence of sub-teratogenic concentrations of one chemical in the culture medium can influence the other one's embryotoxicity *in vitro*. The results confirm those from BMD approach, which suggest that there are no significant deviations from concentration additivity. In addition, the performed *whole mount* immunostainings allowed to correlate the defects at the branchial arches induced by both Eth and FLUCO with severe alterations in the migration and specification pattern of the neural crest cells (NCCs). From these results, it is clear that both molecules could affect the craniofacial morphogenesis acting with different MIEs both converging on the same biological pathway, altering the RA production (Eth) and the RA catabolism (azoles). This study moreover promotes the use of *in vitro* whole embryo culture approach as a good method to assess the toxicological outcome of combined exposures to azole fungicides and ethanol on embryo development. This work represents an example that alternative *in vitro* tools can provide suitable means for reducing and refining the use of animal procedures.

In the second part, we decided to investigate the mechanism of action which we assume at the basis of the observed effects, by obtaining an *in silico* tool, validated by our previous *in vitro* experiments, useful to simulate and predict the effects on embryo development after co-exposure to substances with independent MoA but acting on the same pathway and potentially contributing to the same adverse outcome (cranio-facial malformations). Using an integrated approach combining mathematical modelling, molecular docking and *in vitro* experiments, we have developed an integrated system biology model, which is reasonably predictive for the mixture's effects and for the estimations of the RA levels in rat hindbrain after FLUCO and Eth co-exposure starting from the concentrations of the individual substances. The model seems to confirm the accuracy of the hypothesized pathogenic pathway: in fact, experimental data and model predictions have a promising agreement. Anyway, this model, in spite of its limitations, has many potential mechanistic or predictive applications for the study of risk assessment of both exposure to mixtures of azoles acting with the same MoA and exposure to mixtures of Eth and azoles, which probably act on the same pathway but with different MoA

The aim of the third part of this work was to evaluate the Ascidian Embryo Teratogenicity assay (AET) as an alternative invertebrate model to test the developmental effects of the co-exposure to Eth and FLUCO. *C. intestinalis* embryos at early neurula stage (7 hpf) were exposed for 15 h to Eth alone (1.7-8.5-17-42.5-85 mM), to FLUCO alone (7.8-15.75-31.5-250 µM), or co-exposed to binary mixtures of FLUCO and Eth. At the end of the exposure period, larvae were morphologically analysed. Both compounds were teratogenic in a concentration-related manner. Moreover, the co-exposure to the sub-teratogenic concentration of Eth (17 mM) significantly increased the general teratogenicity of the effective concentrations of FLUCO, suggesting the presence of a mixture effect. The co-exposure to increasing concentrations of Eth and FLUCO 7.8 µM significantly increases the incidence of number of trunk-malformed larvae, suggesting the presence of a specific effect exert by FLUCO at the level of the anterior structures with a consequent synergistic effect. These data, similar to those induced in vertebrates, support the hypothesis that both Eth and FLUCO could affect *C. intestinalis* morphogenesis affecting the same pathway also in tunicates with subsequent alteration of their anterior structures. Finally, considering that ascidians are basal chordates recognized as belonging to the sister group of vertebrates (Delsuc et al., 2006), the results obtained with the Ascidian Embryo Teratogenicity assay could be considered indicative for deep toxicological investigation in mammal embryos. The results encourage the use AET as a complementary alternative method for embryotoxicity studies. The possibility to apply mathematical models on AET is to evaluate.

In conclusion, our overall results demonstrate that embryonic exposure to FLUCO and Eth could lead to the same adverse outcome by acting with different MIEs converging on the same AOP, altering the RA production (Eth) and the RA catabolism (azoles). The KEs subsequent to the alteration of the RA endogenous level (alteration of the *Hox* genes expression, alteration of the hindbrain segmentation, alteration of the NCCs migration and incorrect branchial arches formation) shared by both MoA of FLUCO and Eth, could lead to the same adverse outcome: craniofacial abnormalities in the foetus and in the adult (**Fig. 13**).

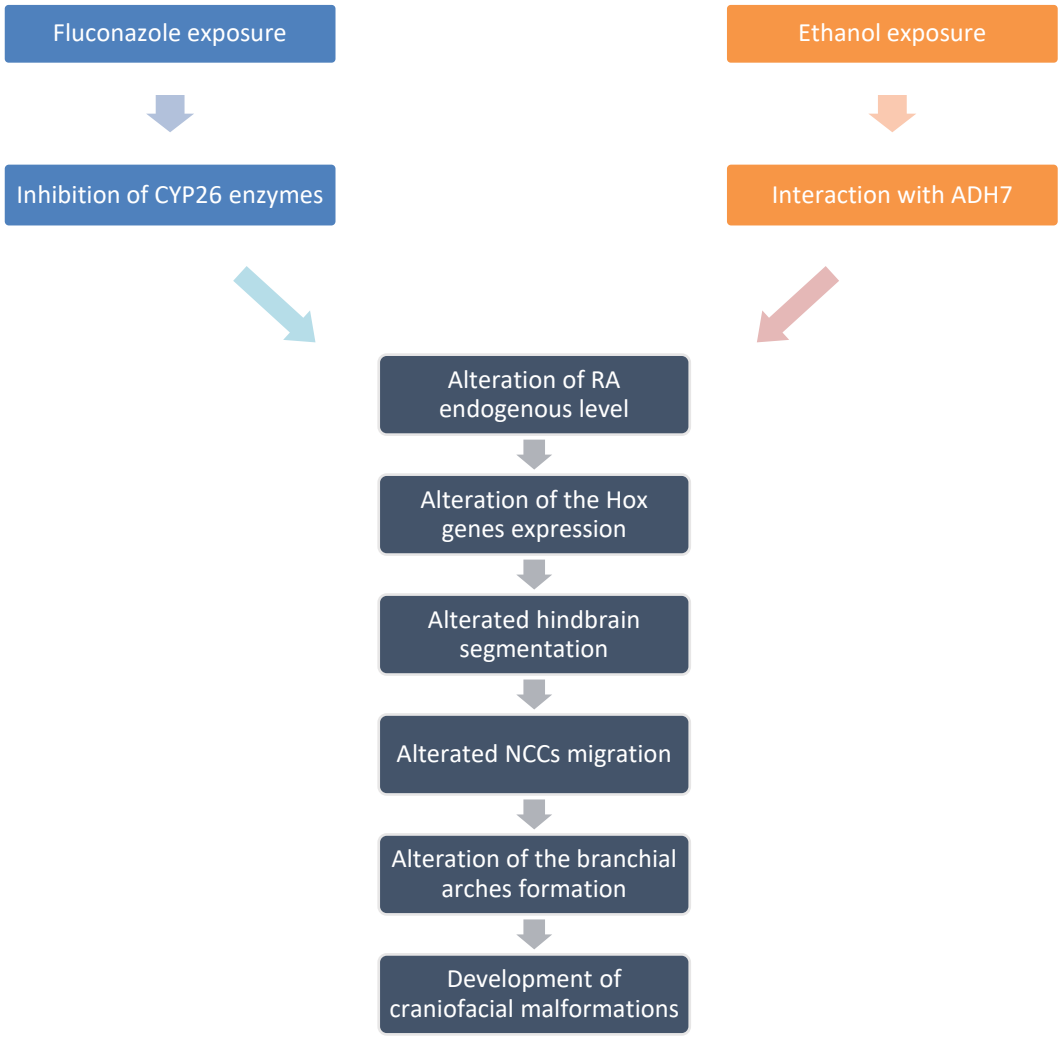

Fig. 13. Postulated interaction between the MoA of fluconazole and ethanol leading to craniofacial abnormalities

The integrated use of data from *in vitro* and *in silico* approaches in the AOP framework used in this study allows us to demonstrate that substances with different MoA but acting on the same pathway could produce an additive effect also at concentrations considered not effective. This is particularly relevant considering the molecules under examination.

Eth, in fact, as alcoholic beverages, is often consumed also during pregnancy. A blood alcohol percentage equal to our experimental NOAEL (17 mM) can be reached by a woman with a normal body weight with just three alcoholic doses (**Fig. 14**).

Male Female	Approximate blood alcohol percentage (by vol.)[4] One drink has 0.5 US fl oz (15 ml) alcohol by volume								
Drinks	Body weight								
	40 kg	45 kg	55 kg	64 kg	73 kg	82 kg	91 kg	100 kg	109 kg
	90 lb	100 lb	120 lb	140 lb	160 lb	180 lb	200 lb	220 lb	240 lb
1	– 0.05	0.04 0.05	0.03 0.04	0.03 0.03	0.02 0.03	0.02 0.03	0.02 0.02	0.02 0.02	0.02 0.02
2	– 0.10	0.08 0.09	0.06 0.08	0.05 0.07	0.05 0.06	0.04 0.05	0.04 0.05	0.03 0.04	0.03 0.04
3	– 0.15	0.11 0.14	0.09 0.11	0.08 0.10	0.07 0.09	0.06 0.08	0.06 0.07	0.05 0.06	0.05 0.06
4	– 0.20	0.15 0.18	0.12 0.15	0.11 0.13	0.09 0.11	0.08 0.10	0.08 0.09	0.07 0.08	0.06 0.08
5	– 0.25	0.19 0.23	0.16 0.19	0.13 0.16	0.12 0.14	0.11 0.13	0.09 0.11	0.09 0.10	0.08 0.09
6	– 0.30	0.23 0.27	0.19 0.23	0.16 0.19	0.14 0.17	0.13 0.15	0.11 0.14	0.10 0.12	0.09 0.11
7	– 0.35	0.26 0.32	0.22 0.27	0.19 0.23	0.16 0.20	0.15 0.18	0.13 0.16	0.12 0.14	0.11 0.13
8	– 0.40	0.30 0.36	0.25 0.30	0.21 0.26	0.19 0.23	0.17 0.20	0.15 0.18	0.14 0.17	0.13 0.15
9	– 0.45	0.34 0.41	0.28 0.34	0.24 0.29	0.21 0.26	0.19 0.23	0.17 0.20	0.15 0.19	0.14 0.17
10	– 0.51	0.38 0.45	0.31 0.38	0.27 0.32	0.23 0.28	0.21 0.25	0.19 0.23	0.17 0.21	0.16 0.19
Subtract approximately 0.01 every 40 minutes after drinking.									

Fig. 14. Approximate blood alcohol percentage in relationship with body weight and alcohol doses in women. 17 mM is equal to 0. 1 %.

The use of FLUCO for prophylaxis and treatment of mycotic infections is also widespread among pregnant women and our experimental NOAEL (62 µM) could be reached with the lower therapeutic dose. In fact, vaginal candidiasis is usually treated with a 150-mg single dose; oropharyngeal and oesophageal candidiasis are generally treated for weeks or months with 50–150 mg FLUCO daily. Higher doses (200–400 mg daily) for long periods are used to treat deep mycoses (meningitis, ophthalmitis, pneumonia, hepatosplenic mycosis, endocarditis), whereas systemic mycoses are treated for several months with 400 mg FLUCO daily, respecting the total maximum daily recommended dose of 1,600 mg (Menegola et al., 2003). The FLUCO linear

pharmacokinetic has been demonstrated at doses of 200-400-800 mg/day (corresponding to a maximum plasma concentration of 33-163-229 μM) (Santos et al., 2010).

The results highlight the potential additive effect that could occur after exposure to azoles and ethanol, suggesting a precautionary position in alcohol consumption during azoles exposure in pregnancy. In addition, our data support the need of a cumulative risk assessment not only for chemicals grouped on the base of similarities in chemical structure or derived from mechanistic considerations but also for chemicals differently acting on the same biological pathway as FLUCO and Eth. This aspect may contribute to the development of a methodology to ensure that the missing aspects in the risk assessment of mixtures can be addressed in future risk management.

Finally, as seen in this study, the *in vitro* tests as WEC are particularly suitable to reinforce the relevance of key events in Adverse Outcome Pathway (AOP) constructs in providing a better understanding of mechanism of toxicity and the role of these data in risk assessment (Madden et al., 2014). The impact of WEC on the field of teratology is evident and, thanks to its flexibility, its rapidity and its sensitivity and with increasing pressure to reduce the use of animals in toxicity testing, it is expected that WEC will remain an ideal mechanistic research model for many years to come. In addition, it is more and more evident the emerging contributions of systems biology in shaping new directions for physiologically-based pharmacokinetic models (PBPK), and dose - response modelling in quantitative human health risk assessment and reproductive toxicology. Data obtained in this study could be, for example, the starting point for the development of PBPK which could make more accurate predictions for different exposure situations.

ACKNOWLEDGEMENT

I would like to thank the EuroMix project, of the Horizon 2020 framework program of the European Union, which financed part of this research.

I would also sincerely thank the EuroMix team of Università degli Studi di Milano (the Biochemistry and Computational Biophysics Unit directed by Dr. Ivano Eberini, and the International Centre for Pesticides and Health Risk Prevention directed by Prof. Angelo Moretto) and the Models for Ecotoxicology and Toxicology Unit of INERIS (Verneuil-en-Halatte, France) directed by Prof. Frederic Yves Bois for their skilful technical assistance and the constant support.

REFERENCES

Abel, E.L., Hannigan, J.H., 1995. Maternal risk factors in fetal alcohol syndrome: Provocative and permissive influences. Neurotoxicol. Teratol. 17, 445–462. doi:10.1016/0892-0362(95)98055-6

Abrams, J.M., White, K., Fessler, L.I., Steller, H., 1993. Programmed cell death during Drosophila embryogenesis. Dev. Camb. Engl. 117, 29–43.

Abu-Abed, S., MacLean, G., Fraulob, V., Chambon, P., Petkovich, M., Dollé, P., 2002. Differential expression of the retinoic acid-metabolizing enzymes CYP26A1 and CYP26B1 during murine organogenesis. Mech. Dev. 110, 173–177. doi:10.1016/S0925-4773(01)00572-X

Alberghina, L., Westerhoff, H., 2005. Systems biology: definitions and perspectives.

Alsaad, A.M.S., Kaplan, Y.C., Koren, G., 2015. Exposure to fluconazole and risk of congenital malformations in the offspring: A systematic review and meta-analysis. Reprod. Toxicol. 52, 78–82. doi:10.1016/j.reprotox.2015.02.009

Andersen, M.E., 1995. Development of physiologically based pharmacokinetic and physiologically based pharmacodymamic models for applications in toxicology and risk assessment. Toxicol. Lett. 79, 35–44. doi:10.1016/0378-4274(95)03355-O

Andersen, M.E., Thomas, R.S., Gaido, K.W., Conolly, R.B., 2005. Dose–response modeling in reproductive toxicology in the systems biology era. Reprod. Toxicol. 19, 327–337. doi:10.1016/j.reprotox.2004.12.004

Andrews, J.E., Ebron-McCoy, M., Schmid, J.E., Svendsgaard, D., 1998. Effects of combinations of methanol and formic acid on rat embryos in culture. Teratology 58, 54–61. doi:10.1002/(SICI)1096-9926(199808)58:2<54::AID-TERA6>3.0.CO;2-0

Anon, 2002. INVITTOX protocol no. 68. Embryotoxicity testing using a whole embryo culture WEC procedure, List of INVITTOX protocols.

Bakker, B.M., Mensonides, F.I.C., Teusink, B., van Hoek, P., Michels, P.A.M., Westerhoff, H.V., 2000. Compartmentation protects trypanosomes from the dangerous design of glycolysis. Proc. Natl. Acad. Sci. 97, 2087–2092. doi:10.1073/pnas.030539197

Blaauboer, B.J., Barratt, M.D., Houston, J.B., 1999. The Integrated Use of Alternative Methods in Toxicological Risk Evaluation - ECVAM Integrated Testing Strategies Task Force Report 1. Altern. Lab. Anim. ATLA 27, 229–237.

Blum, R.A., Wilton, J.H., Hilligoss, D.M., Gardner, M.J., Henry, E.B., Harrison, N.J., Schentag, J.J., 1991. Effect of fluconazole on the disposition of phenytoin. Clin. Pharmacol. Ther. 49, 420–425. doi:10.1038/clpt.1991.49

Bois, F.Y., 2009. GNU MCSim: Bayesian statistical inference for SBML-coded systems biology models. Bioinformatics 25, 1453–1454. doi:10.1093/bioinformatics/btp162

Boobis, A., Budinsky, R., Collie, S., Crofton, K., Embry, M., Felter, S., Hertzberg, R., Kopp, D., Mihlan, G., Mumtaz, M., Price, P., Solomon, K., Teuschler, L., Yang, R., Zaleski, R., 2011. Critical analysis of literature on low-dose synergy for use in screening chemical mixtures for risk assessment. Crit. Rev. Toxicol. 41, 369–383. doi:10.3109/10408444.2010.543655

Bossche, H.V., Lauwers, W., Willemsens, G., Marichal, P., Cornelissen, F., Cools, W., 1984. Molecular basis for the antimycotic and antibacterial activity of *N* -substituted imidazoles and triazoles: The inhibition of isoprenoid biosynthesis. Pestic. Sci. 15, 188–198. doi:10.1002/ps.2780150210

Brown, N.A., Fabro, S., 1981. Quantitation of rat embryonic development in vitro: A morphological scoring system. Teratology 24, 65–78. doi:10.1002/tera.1420240108

Campo-Paysaa, F., Marlétaz, F., Laudet, V., Schubert, M., 2008. Retinoic acid signaling in development: Tissue-specific functions and evolutionary origins. genesis 46, 640–656. doi:10.1002/dvg.20444

Carney, E.W., Liberacki, A.B., Bartels, M.J., Breslin, W.J., 1996. Identification of proximate toxicant for ethylene glycol developmental toxicity using rat whole embryo culture. Teratology 53, 38–46. doi:10.1002/(SICI)1096-9926(199601)53:1<38::AID-TERA5>3.0.CO;2-5

Carstens, M., Ewings, E., 2009. Neuroembryology and functional anatomy of craniofacial clefts. Indian J. Plast. Surg. 42, 19. doi:10.4103/0970-0358.57184

CEC, C. of the E.C., 2007. Monitoring of pesticides reisdues in products of plant origin in the European Union, Norway, Iceland and Liechtenstein.

Chase, J.R., Poolman, M.G., Fell, D.A., 2009. Contribution of NADH Increases to Ethanol's Inhibition of Retinol Oxidation by Human ADH Isoforms. Alcohol. Clin. Exp. Res. 33, 571–580. doi:10.1111/j.1530-0277.2008.00871.x

Choudhary, D., Jansson, I., Schenkman, J.B., Sarfarazi, M., Stoilov, I., 2003. Comparative expression profiling of 40 mouse cytochrome P450 genes in embryonic and adult tissues. Arch. Biochem. Biophys. 414, 91–100. doi:10.1016/S0003-9861(03)00174-7

Cima, F., Ballarin, L., Bressa, G., Martinucci, G., Burighel, P., 1996. Toxicity of Organotin Compounds on Embryos of a Marine Invertebrate (Styela plicata;Tunicata). Ecotoxicol. Environ. Saf. 35, 174–182. doi:10.1006/eesa.1996.0097

Clagett-Dame, M., Knutson, D., 2011. Vitamin A in Reproduction and Development. Nutrients 3, 385–428. doi:10.3390/nu3040385

Clarke, D.O., Mebus, C.A., Miller, F.J., Welsch, F., 1991. Protection against 2-methoxyethanol-induced teratogenesis by serine enantiomers: Studies of potential alteration of 2-methoxyethanol pharmacokinetics. Toxicol. Appl. Pharmacol. 110, 514–526. doi:10.1016/0041-008X(91)90051-F

Climent, E., Pascual, M., Renau-Piqueras, J., Guerri, C., 2002. Ethanol exposure enhances cell death in the developing cerebral cortex: Role of brain-derived neurotrophic factor and its signaling pathways. J. Neurosci. Res. 68, 213–225. doi:10.1002/jnr.10208

Cockroft, D.L., New, D.A.T., 1978. Abnormalities induced in cultured rat embryos by hyperthermia. Teratology 17, 277–283. doi:10.1002/tera.1420170306

Cohlan, S.Q., 1953. Excessive intake of vitamin A as a cause of congenital anomalies in the rat. Science 117, 535–536.

Cornish-Bowden, A., 1979. Fundamentals of enzyme kinetics. Butterworths, London ; Boston.

Couly, G.F., Coltey, P.M., Le Douarin, N.M., 1993. The triple origin of skull in higher vertebrates: a study in quail-chick chimeras. Dev. Camb. Engl. 117, 409–429.

Czarnobaj, J., Bagnall, K.M., Bamforth, J.S., Milos, N.C., 2014. The different effects on cranial and trunk neural crest cell behaviour following exposure to a low concentration of alcohol in vitro. Arch. Oral Biol. 59, 500–512. doi:10.1016/j.archoralbio.2014.02.005

De Bernardi, F., Sotgia, C., Ortoloani, G., 1994. Retinoic acid treatment of ascidian embryos: effects on larvae and metamorphosis. Anim Biol 3, 75–81.

Dehal, P., 2002. The Draft Genome of Ciona intestinalis: Insights into Chordate and Vertebrate Origins. Science 298, 2157–2167. doi:10.1126/science.1080049

del Corral, R.D., Storey, K.G., 2004. Opposing FGF and retinoid pathways: a signalling switch that controls differentiation and patterning onset in the extending vertebrate body axis. BioEssays 26, 857–869. doi:10.1002/bies.20080

Delsuc, F., Brinkmann, H., Chourrout, D., Philippe, H., 2006. Tunicates and not cephalochordates are the closest living relatives of vertebrates. Nature 439, 965–968. doi:10.1038/nature04336

Deltour, L., Ang, H.L., Duester, G., 1996. Ethanol inhibition of retinoic acid synthesis as a potential mechanism for fetal alcohol syndrome. FASEB J. Off. Publ. Fed. Am. Soc. Exp. Biol. 10, 1050–1057.

De Rosa, C.T., El-Masri, H.A., Pohl, H., Cibulas, W., Mumtaz, M.M., 2004. IMPLICATIONS OF CHEMICAL MIXTURES IN PUBLIC HEALTH PRACTICE. J. Toxicol. Environ. Health Part B 7, 339–350. doi:10.1080/10937400490498075

de Sanctis, L., Memo, L., Pichini, S., Tarani, L., Vagnarelli, F., 2011. Fetal alcohol syndrome: new perspectives for an ancient and underestimated problem. J. Matern. Fetal Neonatal Med. 24, 34–37. doi:10.3109/14767058.2011.607576

Di Renzo, Broccia, M., Giavini, E., Menegola, E., 2007. Citral, an inhibitor of retinoic acid synthesis, attenuates the frequency and severity of branchial arch abnormalities induced by triazole-derivative fluconazole in rat embryos cultured in vitro. Reprod. Toxicol. 24, 326–332. doi:10.1016/j.reprotox.2007.07.012

Di Renzo, F., Corsini, E., Broccia, M.L., Marinovich, M., Galli, C.L., Giavini, E., Menegola, E., 2009. Molecular mechanism of teratogenic effects induced by the fungicide triadimefon: Study of the expression of TGF-β mRNA and TGF-β and CRABPI proteins during rat in vitro development. Toxicol. Appl. Pharmacol. 234, 107–116. doi:10.1016/j.taap.2008.09.025

Di Renzo, Broccia, M.L., Giavini, E., Menegola, E., 2011a. Stage-dependent abnormalities induced by the fungicide triadimefon in the mouse☆. Reprod. Toxicol. 31, 194–199. doi:10.1016/j.reprotox.2010.10.011

Di Renzo, Rossi, F., Prati, M., Giavini, E., Menegola, E., 2011b. Early genetic control of craniofacial development is affected by the in vitro exposure of rat embryos to the fungicide triadimefon. Birth Defects Res. B. Dev. Reprod. Toxicol. 92, 77–81. doi:10.1002/bdrb.20284

Dorman, D.C., Bolon, B., Struve, M.F., LaPerle, K.M.D., Wong, B.A., Elswick, B., Welsch, F., 1995. Role of formate in methanol-induced exencephaly in CD-1 mice. Teratology 52, 30–40. doi:10.1002/tera.1420520105

Dubrulle, J., McGrew, M.J., Pourquié, O., 2001. FGF Signaling Controls Somite Boundary Position and Regulates Segmentation Clock Control of Spatiotemporal Hox Gene Activation. Cell 106, 219–232. doi:10.1016/S0092-8674(01)00437-8

Duester, G., 1998. Alcohol dehydrogenase as a critical mediator of retinoic acid synthesis from vitamin A in the mouse embryo. J. Nutr. 128, 459S–462S.

Duester, G., 2008. Retinoic acid synthesis and signaling during early organogenesis. Cell 134, 921–931. doi:10.1016/j.cell.2008.09.002

Dunty Jr., W.C., Zucker, R.M., Sulik, K.K., 2002. Hindbrain and Cranial Nerve Dysmorphogenesis Result from Acute Maternal Ethanol Administration. Dev. Neurosci. 24, 328–342. doi:10.1159/000066748

Edelsbrunner, H., Facello, M., Ping Fu, Jie Liang, 1995. Measuring proteins and voids in proteins. IEEE Comput. Soc. Press, pp. 256–264. doi:10.1109/HICSS.1995.375331

EFSA, 2009. Scientific Opinion on risk assessment for a selected group of pesticides from the triazole group to test possible methodologies to assess cumulative effects from exposure through food from these pesticides to human health.

EFSA, 2013. Human Risk Assessment of Combined Exposure to Mutliple Chemicals.

EFSA, P. on P.P.P. and their R. (PPR), 2013. Scientific Opinion on the relevance of dissimilar mode of action and its appropriate application for cumulative risk assessment of pesticides residues in food: Relevance of dissimilar mode of action. EFSA J. 11, 3472. doi:10.2903/j.efsa.2013.3472

Ellis-Hutchings, R.G., Carney, E.W., 2010. Whole embryo culture: a "New" technique that enabled decades of mechanistic discoveries. Birth Defects Res. B. Dev. Reprod. Toxicol. 89, 304–312. doi:10.1002/bdrb.20263

EPA, 1986. Guidelines for the Health Risk Assessment of Chemical Mixtures.

EPA, 2002. Guidance on cumulative risk assessment of pesticide chemicals that have a common mechanism of toxicity.

European Commission, D.E., 2009. State of the art report on mixture toxicity.

Ewald, S.J., Shao, H., 1993. Ethanol Increases Apoptotic Cell Death of Thymocytes in Vitro. Alcohol. Clin. Exp. Res. 17, 359–365. doi:10.1111/j.1530-0277.1993.tb00776.x

Feron, V.J., Cassee, F.R., Groten, J.P., 1998. Toxicology of chemical mixtures: international perspective. Environ. Health Perspect. 106, 1281–1289. doi:10.1289/ehp.98106s61281

Feron, V.J., Groten, J.P., 2002. Toxicological evaluation of chemical mixtures. Food Chem. Toxicol. 40, 825–839. doi:10.1016/S0278-6915(02)00021-2

Fujii, H., 1997. Metabolic inactivation of retinoic acid by a novel P450 differentially expressed in developing mouse embryos. EMBO J. 16, 4163–4173. doi:10.1093/emboj/16.14.4163

Fujinaga, M., Baden, J.M., Shepard, T.H., Mazze, R.I., 1990. Nitrous oxide alters body laterality in rats. Teratology 41, 131–135. doi:10.1002/tera.1420410202

Geenen, S., Taylor, P.N., Snoep, J.L., Wilson, I.D., Kenna, J.G., Westerhoff, H.V., 2012. Systems biology tools for toxicology. Arch. Toxicol. 86, 1251–1271. doi:10.1007/s00204-012-0857-8

Gianazza, E., Parravicini, C., Primi, R., Miller, I., Eberini, I., 2016. In silico prediction and characterization of protein post-translational modifications. J. Proteomics 134, 65–75. doi:10.1016/j.jprot.2015.09.026

Giavini, E., Broccia, M.L., Prati, M., Bellomo, D., Menegola, E., 1992. Effects of ethanol and acetaldehyde on rat embryos developing in vitro. Vitro Cell. Dev. Biol. - Anim. 28, 205–210. doi:10.1007/BF02631093

Giavini, E., Menegola, E., 2004. Gene-Teratogen Interactions in Chemically Induced Congenital Malformations. Neonatology 85, 73–81. doi:10.1159/000074962

Giavini, E., Menegola, E., 2010. Are azole fungicides a teratogenic risk for human conceptus? Toxicol. Lett. 198, 106–111. doi:10.1016/j.toxlet.2010.07.005

Goldbeter, A., Gonze, D., Pourquié, O., 2007. Sharp developmental thresholds defined through bistability by antagonistic gradients of retinoic acid and FGF signaling. Dev. Dyn. 236, 1495–1508. doi:10.1002/dvdy.21193

Graham, A., Heyman, I., Lumsden, A., 1993. Even-numbered rhombomeres control the apoptotic elimination of neural crest cells from odd-numbered rhombomeres in the chick hindbrain. Dev. Camb. Engl. 119, 233–245.

Graham, A., 2003. Development of the pharyngeal arches. Am. J. Med. Genet. 119A, 251–256. doi:10.1002/ajmg.a.10980

Groppelli, S., Pennati, R., De Bernardi, F., Menegola, E., Giavini, E., Sotgia, C., 2005. Teratogenic effects of two antifungal triazoles, triadimefon and triadimenol, on Xenopus laevis development: Craniofacial defects. Aquat. Toxicol. 73, 370–381. doi:10.1016/j.aquatox.2005.04.004

Groppelli, S., Zega, G., Biggiogero, M., De Bernardi, F., Sotgia, C., Pennati, R., 2007. Fluconazole induces teratogenic effects in the tunicate Phallusia mammillata. Environ. Toxicol. Pharmacol. 23, 265–271. doi:10.1016/j.etap.2006.11.005

Groten, J.., 2000. Mixtures and interactions. Food Chem. Toxicol. 38, S65–S71. doi:10.1016/S0278-6915(99)00135-0

Groten, J.P., Feron, V.J., Sühnel, J., 2001. Toxicology of simple and complex mixtures. Trends Pharmacol. Sci. 22, 316–322. doi:10.1016/S0165-6147(00)01720-X

Hackshaw, A., Rodeck, C., Boniface, S., 2011. Maternal smoking in pregnancy and birth defects: a systematic review based on 173 687 malformed cases and 11.7 million controls. Hum. Reprod. Update 17, 589–604. doi:10.1093/humupd/dmr022

Hamon, J., Renner, M., Jamei, M., Lukas, A., Kopp-Schneider, A., Bois, F.Y., 2015. Quantitative in vitro to in vivo extrapolation of tissues toxicity. Toxicol. In Vitro 30, 203–216. doi:10.1016/j.tiv.2015.01.011

Hansen, J.M., Carney, E.W., Harris, C., 1999. Differential alteration by thalidomide of the glutathione content of rat vs. rabbit conceptuses in vitro. Reprod. Toxicol. 13, 547–554. doi:10.1016/S0890-6238(99)00053-2

Hernandez, R.E., Putzke, A.P., Myers, J.P., Margaretha, L., Moens, C.B., 2007. Cyp26 enzymes generate the retinoic acid response pattern necessary for hindbrain development. Development 134, 177–187. doi:10.1242/dev.02706

Hinman, V.F., Degnan, B.M., 1998. Retinoic acid disrupts anterior ectodermal and endodermal development in ascidian larvae and postlarvae. Dev. Genes Evol. 208, 336–345.

Hof, H., 2001. Critical Annotations to the Use of Azole Antifungals for Plant Protection. Antimicrob. Agents Chemother. 45, 2987–2990. doi:10.1128/AAC.45.11.2987-2990.2001

Holownia, A., Ledig, M., Ménez, J.-F., 1997. Ethanol-induced cell death in cultured rat astroglia. Neurotoxicol. Teratol. 19, 141–146. doi:10.1016/S0892-0362(96)00226-7

Horton, V.L., Sleet, R.B., John-Greene, J.A., Welsch, F., 1985. Developmental phase-specific and dose-related teratogenic effects of ethylene glycol monomethyl ether in CD-1 mice. Toxicol. Appl. Pharmacol. 80, 108–118. doi:10.1016/0041-008X(85)90105-X

Horton, C., Maden, M., 1995. Endogenous distribution of retinoids during normal development and teratogenesis in the mouse embryo. Dev. Dyn. 202, 312–323. doi:10.1002/aja.1002020310

Hotta, K., Mitsuhara, K., Takahashi, H., Inaba, K., Oka, K., Gojobori, T., Ikeo, K., 2007. A web-based interactive developmental table for the ascidian *Ciona intestinalis* , including 3D real-image embryo reconstructions: I. From fertilized egg to hatching larva. Dev. Dyn. 236, 1790–1805. doi:10.1002/dvdy.21188

Ian Mason, J., Murry, B.A., Olcott, M., Sheets, J.J., 1985. Imidazole antimycotics: Inhibitors of steroid aromatase. Biochem. Pharmacol. 34, 1087–1092. doi:10.1016/0006-2952(85)90613-6

Ikonomidou, C., 2000. Ethanol-Induced Apoptotic Neurodegeneration and Fetal Alcohol Syndrome. Science 287, 1056–1060. doi:10.1126/science.287.5455.1056

Jeffery, W.R., Strickler, A.G., Yamamoto, Y., 2004. Migratory neural crest-like cells form body pigmentation in a urochordate embryo. Nature 431, 696–699. doi:10.1038/nature02975

Jeffery, W.R., 2006. Ascidian neural crest-like cells: phylogenetic distribution, relationship to larval complexity, and pigment cell fate. J. Exp. Zoolog. B Mol. Dev. Evol. 306B, 470–480. doi:10.1002/jez.b.21109

Jeffery, W.R., 2007. Chordate ancestry of the neural crest: New insights from ascidians. Semin. Cell Dev. Biol. 18, 481–491. doi:10.1016/j.semcdb.2007.04.005

Jeffery, W.R., Chiba, T., Krajka, F.R., Deyts, C., Satoh, N., Joly, J.-S., 2008. Trunk lateral cells are neural crest-like cells in the ascidian Ciona intestinalis: Insights into the ancestry and evolution of the neural crest. Dev. Biol. 324, 152–160. doi:10.1016/j.ydbio.2008.08.022

Jonker, D., Woutersen, R.A., Feron, V.J., 1996. Toxicity of mixtures of nephrotoxicants with similar or dissimilar mode of action. Food Chem. Toxicol. 34, 1075–1082. doi:10.1016/S0278-6915(97)00077-X

Joya, X., Friguls, B., Ortigosa, S., Papaseit, E., Martínez, S.E., Manich, A., Garcia-Algar, O., Pacifici, R., Vall, O., Pichini, S., 2012. Determination of maternal-fetal biomarkers of prenatal exposure to ethanol: A review. J. Pharm. Biomed. Anal. 69, 209–222. doi:10.1016/j.jpba.2012.01.006

Kale, P., Johnson, L.B., 2005. Second-generation azole antifungal agents. Drugs Today 41, 91. doi:10.1358/dot.2005.41.2.882661

Kanda, M., Wada, H., Fujiwara, S., 2009. Epidermal expression of Hox1 is directly activated by retinoic acid in the Ciona intestinalis embryo. Dev. Biol. 335, 454–463. doi:10.1016/j.ydbio.2009.09.027

Kane, M.A., Folias, A.E., Wang, C., Napoli, J.L., 2010. Ethanol elevates physiological all-trans-retinoic acid levels in select loci through altering retinoid metabolism in multiple loci: a potential mechanism of ethanol toxicity. FASEB J. 24, 823–832. doi:10.1096/fj.09-141572

Kantola, T., Backman, J.T., Niemi, M., Kivistö, K.T., Neuvonen, P.J., 2000. Effect of fluconazole on plasma fluvastatin and pravastatin concentrations. Eur. J. Clin. Pharmacol. 56, 225–229. doi:10.1007/s002280000127

Katsuyama, Y., Wada, S., Yasugi, S., Saiga, H., 1995. Expression of the labial group Hox gene HrHox-1 and its alteration induced by retinoic acid in development of the ascidian Halocynthia roretzi. Dev. Camb. Engl. 121, 3197–3205.

Kiecker, C., 2016. The chick embryo as a model for the effects of prenatal exposure to alcohol on craniofacial development. Dev. Biol. 415, 314–325. doi:10.1016/j.ydbio.2016.01.007

Kilburn, B.A., Chiang, P.J., Wang, J., Flentke, G.R., Smith, S.M., Armant, D.R., 2006. Rapid Induction of Apoptosis in Gastrulating Mouse Embryos by Ethanol and Its Prevention by HB-EGF. Alcohol. Clin. Exp. Res. 30, 127–134. doi:10.1111/j.1530-0277.2006.00008.x

King, C.T., Rogers, P.D., Cleary, J.D., Chapman, S.W., 1998. Antifungal Therapy During Pregnancy. Clin. Infect. Dis. 27, 1151–1160. doi:10.1086/514977

Kitano, H., 2002. Systems Biology: A Brief Overview. Science 295, 1662–1664. doi:10.1126/science.1069492

Klug, S., Lewandowski, C., Wildi, L., Neubert, D., 1989. All-trans retinoic acid and 13-cis-retinoic acid in the rat whole-embryo culture: abnormal development due to the all-trans isomer. Arch. Toxicol. 63, 440–444. doi:10.1007/BF00316445

Klug, S., Merker, H.-J., Jäckh, R., 2001. Effects of ethylene glycol and metabolites on in vitro development of rat embryos during organogenesis. Toxicol. In Vitro 15, 635–642. doi:10.1016/S0887-2333(01)00083-2

Kochhar, D.M., 2009. TERATOGENIC ACTIVITY OF RETINOIC ACID. Acta Pathol. Microbiol. Scand. 70, 398–404. doi:10.1111/j.1699-0463.1967.tb01308.x

Kortenkamp, A., 2007. Ten Years of Mixing Cocktails: A Review of Combination Effects of Endocrine-Disrupting Chemicals. Environ. Health Perspect. 115, 98–105. doi:10.1289/ehp.9357

Kotch, L.E., Sulik, K.K., 1992. Experimental fetal alcohol syndrome: Proposed pathogenic basis for a variety of associated facial and brain anomalies. Am. J. Med. Genet. 44, 168–176. doi:10.1002/ajmg.1320440210

Kotch, L.E., Chen, S.-Y., Sulik, K.K., 1995. Ethanol-induced teratogenesis: Free radical damage as a possible mechanism. Teratology 52, 128–136. doi:10.1002/tera.1420520304

Kot-Leibovich, H., Fainsod, A., 2009. Ethanol induces embryonic malformations by competing for retinaldehyde dehydrogenase activity during vertebrate gastrulation. Dis. Model. Mech. 2, 295–305. doi:10.1242/dmm.001420

Krumlauf, R., 1993. Hox genes and pattern formation in the branchial region of the vertebrate head. Trends Genet. 9, 106–112. doi:10.1016/0168-9525(93)90203-T

Kudoh, T., Wilson, S.W., Dawid, I.B., 2002. Distinct roles for Fgf, Wnt and retinoic acid in posteriorizing the neural ectoderm. Dev. Camb. Engl. 129, 4335–4346.

Landesmann, B., Mennecozzi, M., Berggren, E., Whelan, M., 2013. Adverse outcome pathway-based screening strategies for an animal-free safety assessment of chemicals. Altern. Lab. Anim. ATLA 41, 461–471.

Laverda, A.M., Ruga, E., Pagliaro, A., Pinello, M.L., Giaquinto, C., 1996. Intracranial hypertension and cryptococcal meningitis in a girl with AIDS. Brain Dev. 18, 330–331. doi:10.1016/0387-7604(96)00022-8

Le Douarin, N.M., Kalcheim, C., 1999. The Neural Crest. Cambridge University Press.

Lee, Q.P., Juchau, M.R., 1994. Dysmorphogenic effects of nitric oxide (NO) and NO-synthase inhibition: Studies with intra-amniotic injections of sodium nitroprusside and NG-monomethyl-L-arginine. Teratology 49, 452–464. doi:10.1002/tera.1420490605

Lee, Y.M., Osumi-Yamashita, N., Ninomiya, Y., Moon, C.K., Eriksson, U., Eto, K., 1995. Retinoic acid stage-dependently alters the migration pattern and identity of hindbrain neural crest cells. Dev. Camb. Engl. 121, 825–837.

Light, K.., Belcher, S.., Pierce, D.., 2002. Time course and manner of Purkinje neuron death following a single ethanol exposure on postnatal day 4 in the developing rat. Neuroscience 114, 327–337. doi:10.1016/S0306-4522(02)00344-5

Loose, D.S., Kan, P.B., Hirst, M.A., Marcus, R.A., Feldman, D., 1983. Ketoconazole blocks adrenal steroidogenesis by inhibiting cytochrome P450-dependent enzymes. J. Clin. Invest. 71, 1495–1499. doi:10.1172/JCI110903

Lumsden, A., Sprawson, N., Graham, A., 1991. Segmental origin and migration of neural crest cells in the hindbrain region of the chick embryo. Dev. Camb. Engl. 113, 1281–1291.

MacLean, G., Abu-Abed, S., Dollé, P., Tahayato, A., Chambon, P., Petkovich, M., 2001. Cloning of a novel retinoic-acid metabolizing cytochrome P450, Cyp26B1, and comparative expression analysis with Cyp26A1 during early murine development. Mech. Dev. 107, 195–201. doi:10.1016/S0925-4773(01)00463-4

MacLean, G., Li, H., Metzger, D., Chambon, P., Petkovich, M., 2007. Apoptotic Extinction of Germ Cells in Testes of *Cyp26b1* Knockout Mice. Endocrinology 148, 4560–4567. doi:10.1210/en.2007-0492

MacLean, G., Dollé, P., Petkovich, M., 2009. Genetic disruption of CYP26B1 severely affects development of neural crest derived head structures, but does not compromise hindbrain patterning. Dev. Dyn. 238, 732–745. doi:10.1002/dvdy.21878

Madden, J.C., Rogiers, V., Vinken, M., 2014. Application of in silico and in vitro methods in the development of adverse outcome pathway constructs in wildlife. Philos. Trans. R. Soc. B Biol. Sci. 369, 20130584–20130584. doi:10.1098/rstb.2013.0584

Maden, M., Holder, N., 1992. Retinoic acid and development of the central nervous system. BioEssays 14, 431–438. doi:10.1002/bies.950140702

Manda, K., Ueno, M., Moritake, T., Anzai, K., 2007. α-Lipoic acid attenuates x-irradiation-induced oxidative stress in mice. Cell Biol. Toxicol. 23, 129–137. doi:10.1007/s10565-006-0137-6

Mark, M., Lohnes, D., Mendelsohn, C., Dupé, V., Vonesch, J.L., Kastner, P., Rijli, F., Bloch-Zupan, A., Chambon, P., 1995. Roles of retinoic acid receptors and of Hox genes in the patterning of the teeth and of the jaw skeleton. Int. J. Dev. Biol. 39, 111–121.

Marotta, F., Tiboni, G.M., 2010. Molecular aspects of azoles-induced teratogenesis. Expert Opin. Drug Metab. Toxicol. 6, 461–482. doi:10.1517/17425251003592111

Massa, V., Gaudenzi, G., Sangiorgio, L., Cotelli, F., Giavini, E., 2007. Krox20 is down-regulated following triazole in vitro embryonic exposure: A polycompetitor-based assay. Toxicol. Lett. 169, 196–204. doi:10.1016/j.toxlet.2007.01.007

Mastroiacovo, P., Mazzone, T., Botto, L.D., Serafini, M.A., Finardi, A., Caramelli, L., Fusco, D., 1996. Prospective assessment of pregnancy outcomes after first-trimester exposure to fluconazole. Am. J. Obstet. Gynecol. 175, 1645–1650. doi:10.1016/S0002-9378(96)70119-9

Matsushima, A., Ryan, K., Shimohigashi, Y., Meinertzhagen, I.A., 2013. An endocrine disruptor, bisphenol A, affects development in the protochordate Ciona intestinalis: Hatching rates and swimming behavior alter in a dose-dependent manner. Environ. Pollut. 173, 257–263. doi:10.1016/j.envpol.2012.10.015

Meek, M.E., Boobis, A., Cote, I., Dellarco, V., Fotakis, G., Munn, S., Seed, J., Vickers, C., 2014. New developments in the evolution and application of the WHO/IPCS framework on mode of action/species concordance analysis: WHO/IPCS framework on mode of action/species concordance analysis. J. Appl. Toxicol. 34, 1–18. doi:10.1002/jat.2949

Memo, L., Gnoato, E., Caminiti, S., Pichini, S., Tarani, L., 2013. Fetal alcohol spectrum disorders and fetal alcohol syndrome: the state of the art and new diagnostic tools. Early Hum. Dev. 89, S40–S43. doi:10.1016/S0378-3782(13)70013-6

Menegola, Broccia, M.L., Renzo, F.D., Prati, M., Giavini, E., 2000. IN VITRO TERATOGENIC POTENTIAL OF TWO ANTIFUNGAL TRIAZOLES: TRIADIMEFON AND TRIADIMENOL. Vitro Cell. Dev. Biol. - Anim. 36, 88. doi:10.1290/1071-2690(2000)036<0088:IVTPOT>2.0.CO;2

Menegola, Broccia, M.L., Di Renzo, F., Giavini, E., 2001. Antifungal triazoles induce malformations in vitro. Reprod. Toxicol. 15, 421–427. doi:10.1016/S0890-6238(01)00143-5

Menegola, E., Broccia, M.L., Di Renzo, F., Giavini, E., 2001. Acetaldehyde in vitro exposure and apoptosis: a possible mechanism of teratogenesis. Alcohol 23, 35–39. doi:10.1016/S0741-8329(00)00132-4

Menegola, Broccia, M.L., Di Renzo, F., Giavini, E., 2003. Pathogenic pathways in fluconazole-induced branchial arch malformations. Birt. Defects Res. A. Clin. Mol. Teratol. 67, 116–124. doi:10.1002/bdra.10022

Menegola, Broccia, M.L., Di Renzo, F., Massa, V., Giavini, E., 2004. Relationship between hindbrain segmentation, neural crest cell migration and branchial arch abnormalities in rat embryos exposed to fluconazole and retinoic acid in vitro. Reprod. Toxicol. 18, 121–130. doi:10.1016/j.reprotox.2003.09.004

Menegola, Broccia, M.L., Di Renzo, F., Massa, V., Giavini, E., 2005a. Study on the common teratogenic pathway elicited by the fungicides triazole-derivatives. Toxicol. In Vitro 19, 737–748. doi:10.1016/j.tiv.2005.04.005

Menegola, Broccia, M.L., Di Renzo, F., Massa, V., Giavini, E., 2005b. Craniofacial and axial skeletal defects induced by the fungicide triadimefon in the mouse. Birth Defects Res. B. Dev. Reprod. Toxicol. 74, 185–195. doi:10.1002/bdrb.20035

Menegola, Broccia, M.L., Di Renzo, F., Giavini, E., 2006a. Postulated pathogenic pathway in triazole fungicide induced dysmorphogenic effects. Reprod. Toxicol. 22, 186–195. doi:10.1016/j.reprotox.2006.04.008

Menegola, Broccia, M.L., Renzo, F.D., Giavini, E., 2006b. Dysmorphogenic effects of some fungicides derived from the imidazole on rat embryos cultured in vitro. Reprod. Toxicol. 21, 74–82. doi:10.1016/j.reprotox.2005.07.008

Menegola, E., Di Renzo, F., Metruccio, F., Moretto, A., Giavini, E., 2013. Effects of mixtures of azole fungicides in postimplantation rat whole-embryo cultures. Arch. Toxicol. 87, 1989–1997. doi:10.1007/s00204-013-1048-y

Miller, M.W., Kuhn, P.E., 1995. Cell Cycle Kinetics in Fetal Rat Cerebral Cortex: Effects of Prenatal Treatment with Ethanol Assessed by a Cumulative Labeling Technique with Flow Cytometry. Alcohol. Clin. Exp. Res. 19, 233–237. doi:10.1111/j.1530-0277.1995.tb01497.x

Moretto, A., 2008. Exposure to multiple chemicals: when and how to assess the risk from pesticide residues in food. Trends Food Sci. Technol. 19, S56–S63. doi:10.1016/j.tifs.2008.06.004

Moretto, A., Di Renzo, F., Giavini, E., Metruccio, F., Menegola, E., 2015. The use of in vitro testing to refine cumulative assessment groups of pesticides: The example of teratogenic conazoles. Food Chem. Toxicol. 79, 65–69. doi:10.1016/j.fct.2014.07.006

Morriss, G.M., Steele, C.E., 1974. The effect of excess vitamin A on the development of rat embryos in culture. J. Embryol. Exp. Morphol. 32, 505–514.

Morriss, G.M., Steele, C.E., 1977. Comparison of the effects of retinol and retinoic acid on postimplantation rat embryos in vitro. Teratology 15, 109–119. doi:10.1002/tera.1420150115

Morriss-Kay, G., 1992. Retinoic Acid and Development. Pathobiology 60, 264–270. doi:10.1159/000163733

Mossey, P., Little, J., 2002. Epidemiology of oral clefts: An international perspective In: Wyszynski DF, editor Cleft lip and palate: From origin to treatment.

Mossey, P.A., Little, J., Munger, R.G., Dixon, M.J., Shaw, W.C., 2009. Cleft lip and palate. The Lancet 374, 1773–1785. doi:10.1016/S0140-6736(09)60695-4

Nagano, K., Nakayama, E., Oobayashi, H., Yamada, T., Adachi, H., Nishizawa, T., Ozawa, H., Nakaichi, M., Okuda, H., Minami, K., Yamazaki, K., 1981. Embryotoxic effects of ethylene glycol monomethyl ether in mice. Toxicology 20, 335–343. doi:10.1016/0300-483X(81)90040-8

Nagatomo, K., Fujiwara, S., 2003. Expression of Raldh2, Cyp26 and Hox-1 in normal and retinoic acid-treated Ciona intestinalis embryos. Gene Expr. Patterns 3, 273–277. doi:10.1016/S1567-133X(03)00051-6

Nagatomo, K., Ishibashi, T., Satou, Y., Satoh, N., Fujiwara, S., 2003. Retinoic acid affects gene expression and morphogenesis without upregulating the retinoic acid receptor in the ascidian Ciona intestinalis. Mech. Dev. 120, 363–372. doi:10.1016/S0925-4773(02)00441-0

New, D.A.T., 1978. WHOLE-EMBRYO CULTURE AND THE STUDY OF MAMMALIAN EMBRYOS DURING ORGANOGENESIS. Biol. Rev. 53, 81–122. doi:10.1111/j.1469-185X.1978.tb00993.x

Nguyen, H.T.T., Sharma, V., McIntyre, R.S., 2009. Teratogenesis associated with antibipolar agents. Adv. Ther. 26, 281–294. doi:10.1007/s12325-009-0011-z

Niederreither, K., Subbarayan, V., Dollé, P., Chambon, P., 1999. Embryonic retinoic acid synthesis is essential for early mouse post-implantation development. Nat. Genet. 21, 444–448. doi:10.1038/7788

Noden, D.M., 1983. The role of the neural crest in patterning of avian cranial skeletal, connective, and muscle tissues. Dev. Biol. 96, 144–165. doi:10.1016/0012-1606(83)90318-4

Ornoy, A., Ergaz, Z., 2010. Alcohol Abuse in Pregnant Women: Effects on the Fetus and Newborn, Mode of Action and Maternal Treatment. Int. J. Environ. Res. Public. Health 7, 364–379. doi:10.3390/ijerph7020364

Osumi-Yamashita, N., Ninomiya, Y., Eto, K., Doi, H., 1994. The contribution of both forebrain and midbrain crest cells to the mesenchyme in the frontonasal mass of mouse embryos. Dev. Biol. 164, 409–419. doi:10.1006/dbio.1994.1211

Parman, T., Wiley, M.J., Wells, P.G., 1999. Free radical-mediated oxidative DNA damage in the mechanism of thalidomide teratogenicity. Nat. Med. 5, 582–585. doi:10.1038/8466

Passamaneck, Y.J., Di Gregorio, A., 2005. Ciona intestinalis: Chordate development made simple. Dev. Dyn. 233, 1–19. doi:10.1002/dvdy.20300

Pennati, R., Groppelli, S., Zega, G., Biggiogero, M., De Bernardi, F., Sotgia, C., 2006. Toxic effects of two pesticides, Imazalil and Triadimefon, on the early development of the ascidian Phallusia mammillata (Chordata, Ascidiacea). Aquat. Toxicol. 79, 205–212. doi:10.1016/j.aquatox.2006.05.012

Pennimpede, T., Cameron, D.A., MacLean, G.A., Li, H., Abu-Abed, S., Petkovich, M., 2010. The role of CYP26 enzymes in defining appropriate retinoic acid exposure during embryogenesis: CYP26 Enzymes in Mouse Embryonic Development. Birt. Defects Res. A. Clin. Mol. Teratol. 88, 883–894. doi:10.1002/bdra.20709

Quadro, L., 2004. Transplacental delivery of retinoid: the role of retinol-binding protein and lipoprotein retinyl ester. AJP Endocrinol. Metab. 286, E844–E851. doi:10.1152/ajpendo.00556.2003

Quignot, N., Hamon, J., Bois, F.Y., 2014. Extrapolating In Vitro Results to Predict Human Toxicity, in: Bal-Price, A., Jennings, P. (Eds.), In Vitro Toxicology Systems. Springer New York, New York, NY, pp. 531–550.

Reijntjes, S., Blentic, A., Gale, E., Maden, M., 2005. The control of morphogen signalling: Regulation of the synthesis and catabolism of retinoic acid in the developing embryo. Dev. Biol. 285, 224–237. doi:10.1016/j.ydbio.2005.06.019

Rogers, K.W., Schier, A.F., 2011. Morphogen Gradients: From Generation to Interpretation. Annu. Rev. Cell Dev. Biol. 27, 377–407. doi:10.1146/annurev-cellbio-092910-154148

Ross, S.A., McCaffery, P.J., Drager, U.C., De Luca, L.M., 2000. Retinoids in embryonal development. Physiol. Rev. 80, 1021–1054.

Sabbagh, H.J., Hassan, M.H.A., Innes, N.P.T., Elkodary, H.M., Little, J., Mossey, P.A., 2015. Passive Smoking in the Etiology of Non-Syndromic Orofacial Clefts: A Systematic Review and Meta-Analysis. PLOS ONE 10, e0116963. doi:10.1371/journal.pone.0116963

Sakai, Y., 2001. The retinoic acid-inactivating enzyme CYP26 is essential for establishing an uneven distribution of retinoic acid along the anterio-posterior axis within the mouse embryo. Genes Dev. 15, 213–225. doi:10.1101/gad.851501

Sannerstedt, R., Lundborg, P., Danielsson, B.R., Kihlström, I., Alván, G., Prame, B., Ridley, E., 1996. Drugs During Pregnancy An Issue of Risk Classification and Information to Prescribers: Drug Saf. 14, 69–77. doi:10.2165/00002018-199614020-00001

Santos, S.R.C.J., Campos, E.V., Sanches, C., Gomez, D.S., Ferreira, M.C., 2010. Fluconazole plasma concentration measurement by liquid chromatography for drug monitoring of burn patients. Clinics 65, 237–243. doi:10.1590/S1807-59322010000200017

Sasakura, Y., Mita, K., Ogura, Y., Horie, T., 2012. Ascidians as excellent chordate models for studying the development of the nervous system during embryogenesis and metamorphosis. Dev. Growth Differ. 54, 420–437. doi:10.1111/j.1440-169X.2012.01343.x

Satoh, 1994. Developmental Biology of Ascidians. Camb. Univ Press N. Y.

Satoh, N., 2003. The ascidian tadpole larva: comparative molecular development and genomics. Nat. Rev. Genet. 4, 285–295. doi:10.1038/nrg1042

Schilling, T.F., Kimmel, C.B., 1994. Segment and cell type lineage restrictions during pharyngeal arch development in the zebrafish embryo. Dev. Camb. Engl. 120, 483–494.

Schilling, T.F., Nie, Q., Lander, A.D., 2012. Dynamics and precision in retinoic acid morphogen gradients. Curr. Opin. Genet. Dev. 22, 562–569. doi:10.1016/j.gde.2012.11.012

Schneider, R.A., Hu, D., Rubenstein, J.L., Maden, M., Helms, J.A., 2001. Local retinoid signaling coordinates forebrain and facial morphogenesis by maintaining FGF8 and SHH. Dev. Camb. Engl. 128, 2755–2767.

Schuh, T.J., Hall, B.L., Kraft, J.C., Privalsky, M.L., Kimelman, D., 1993. v-erbA and citral reduce the teratogenic effects of all-trans retinoic acid and retinol, respectively, in Xenopus embryogenesis. Dev. Camb. Engl. 119, 785–798.

Schwartz, E.L., Hallam, S., Gallagher, R.E., Wiernik, P.H., 1995. Inhibition of all-trans-retinoic acid metabolism by fluconazole in vitro and in patients with acute promyelocytic leukemia. Biochem. Pharmacol. 50, 923–928. doi:10.1016/0006-2952(95)00213-J

Sheets, J.J., Mason, J.I., 1984. Ketoconazole: a potent inhibitor of cytochrome P-450-dependent drug metabolism in rat liver. Drug Metab. Dispos. Biol. Fate Chem. 12, 603–606.

Shi, Y., Li, J., Chen, C., Gong, M., Chen, Y., Liu, Y., Chen, J., Li, T., Song, W., 2014. 5-mehtyltetrahydrofolate rescues alcohol-induced neural crest cell migration abnormalities. Mol. Brain 7. doi:10.1186/s13041-014-0067-9

Simões-costa, M.S., Azambuja, A.P., Xavier-Neto, J., 2008. The search for non-chordate retinoic acid signaling: lessons from chordates. J. Exp. Zoolog. B Mol. Dev. Evol. 310B, 54–72. doi:10.1002/jez.b.21139

Sirbu, I.O., 2005. Shifting boundaries of retinoic acid activity control hindbrain segmental gene expression. Development 132, 2611–2622. doi:10.1242/dev.01845

Smith, T.L., 1997. Regulation of glutamate uptake in astrocytes continuously exposed to ethanol. Life Sci. 61, 2499–2505. doi:10.1016/S0024-3205(97)00985-5

Spilson, S.V., Kim, H.J., Chung, K.C., 2001. Association between maternal diabetes mellitus and newborn oral cleft. Ann. Plast. Surg. 47, 477–481.

Steele, C.E., Marlow, R., Turton, J., Hicks, R.M., 1987. In-vitro teratogenicity of retinoids. Br. J. Exp. Pathol. 68, 215–223.

Stoilov, I., Jansson, I., Sarfarazi, M., Schenkman, J.B., 2001. Roles of Cytochrome P450 in Development. Drug Metabol. Drug Interact. 18. doi:10.1515/DMDI.2001.18.1.33

Strate, I., Min, T.H., Iliev, D., Pera, E.M., 2009. Retinol dehydrogenase 10 is a feedback regulator of retinoic acid signalling during axis formation and patterning of the central nervous system. Development 136, 461–472. doi:10.1242/dev.024901

Sulik, K.K., 2005. Genesis of alcohol-induced craniofacial dysmorphism. Exp. Biol. Med. Maywood NJ 230, 366–375.

Suzuki, T., Oohara, I., Kurokawa, T., 1999. Retinoic acid given at late embryonic stage depresses sonic hedgehog and Hoxd-4 expression in the pharyngeal area and induces skeletal malformation in flounder (Paralichthys olivaceus) embryos. Dev. Growth Differ. 41, 143–152. doi:10.1046/j.1440-169x.1999.00420.x

Tahayato, A., Dollé, P., Petkovich, M., 2003. Cyp26C1 encodes a novel retinoic acid-metabolizing enzyme expressed in the hindbrain, inner ear, first branchial arch and tooth buds during murine development. Gene Expr. Patterns 3, 449–454. doi:10.1016/S1567-133X(03)00066-8

Tiboni, G.M., 1993. Second branchial arch anomalies induced by fluconazole, a bis-triazole antifungal agent, in cultured mouse embryos. Res. Commun. Chem. Pathol. Pharmacol. 79, 381–384.

Tiboni, G.M., Marotta, F., Carletti, E., 2009. Fluconazole alters CYP26 gene expression in mouse embryos. Reprod. Toxicol. 27, 199–202. doi:10.1016/j.reprotox.2009.01.001

Trainor, P.A., Tam, P.P., 1995. Cranial paraxial mesoderm and neural crest cells of the mouse embryo: co-distribution in the craniofacial mesenchyme but distinct segregation in branchial arches. Dev. Camb. Engl. 121, 2569–2582.

Trainor, P.A., Krumlauf, R., 2000. Patterning the cranial neural crest: hindbrain segmentation and Hox gene plasticity. Nat. Rev. Neurosci. 1, 116–124. doi:10.1038/35039056

Trainor, P.A., Sobieszczuk, D., Wilkinson, D., Krumlauf, R., 2002. Signalling between the hindbrain and paraxial tissues dictates neural crest migration pathways. Dev. Camb. Engl. 129, 433–442.

Uehara, M., Yashiro, K., Mamiya, S., Nishino, J., Chambon, P., Dolle, P., Sakai, Y., 2007. CYP26A1 and CYP26C1 cooperatively regulate anterior–posterior patterning of the developing brain and the production of migratory cranial neural crest cells in the mouse. Dev. Biol. 302, 399–411. doi:10.1016/j.ydbio.2006.09.045

Vanier, K.L., Mattiussi, A.J., Johnston, D.L., 2003. Interaction of all-trans-retinoic acid with fluconazole in acute promyelocytic leukemia. J. Pediatr. Hematol. Oncol. 25, 403–404.

Van Wauwe, J.P., Coene, M.C., Goossens, J., Cools, W., Monbaliu, J., 1990. Effects of cytochrome P-450 inhibitors on the in vivo metabolism of all-trans-retinoic acid in rats. J. Pharmacol. Exp. Ther. 252, 365–369.

Villeneuve, D.L., Crump, D., Garcia-Reyero, N., Hecker, M., Hutchinson, T.H., LaLone, C.A., Landesmann, B., Lettieri, T., Munn, S., Nepelska, M., Ottinger, M.A., Vergauwen, L., Whelan, M., 2014. Adverse Outcome Pathway (AOP) Development I: Strategies and Principles. Toxicol. Sci. 142, 312–320. doi:10.1093/toxsci/kfu199

Waltman, R., Iniquez, E.S., 1972. Placental transfer of ethanol and its elimination at term. Obstet. Gynecol. 40, 180–185.

Wei, X., Makori, N., Peterson, P.E., Hummler, H., Hendrickx, A.G., 1999. Pathogenesis of retinoic acid-induced ear malformations in primate model. Teratology 60, 83–92. doi:10.1002/(SICI)1096-9926(199908)60:2<83::AID-TERA12>3.0.CO;2-O

Wentzel, P., Eriksson, U.J., 2009. Altered gene expression in neural crest cells exposed to ethanol in vitro. Brain Res. 1305, S50–S60. doi:10.1016/j.brainres.2009.08.057

White, R.J., Nie, Q., Lander, A.D., Schilling, T.F., 2007. Complex Regulation of cyp26a1 Creates a Robust Retinoic Acid Gradient in the Zebrafish Embryo. PLoS Biol. 5, e304. doi:10.1371/journal.pbio.0050304

White, R.J., Schilling, T.F., 2008. How degrading: CYP26S in hindbrain development. Dev. Dyn. 237, 2775–2790. doi:10.1002/dvdy.21695

Whiting, J., 1997. Craniofacial abnormalities induced by the ectopic expression of homeobox genes. Mutat. Res. Mol. Mech. Mutagen. 396, 97–112. doi:10.1016/S0027-5107(97)00177-2

Wilkinson, D.G., 1993. Molecular mechanisms of segmental patterning in the vertebrate hindbrain and neural crest. BioEssays 15, 499–505. doi:10.1002/bies.950150802

Wilkinson, C.F., Christoph, G.R., Julien, E., Kelley, J.M., Kronenberg, J., McCarthy, J., Reiss, R., 2000. Assessing the Risks of Exposures to Multiple Chemicals with a Common Mechanism of Toxicity: How to Cumulate? Regul. Toxicol. Pharmacol. 31, 30–43. doi:10.1006/rtph.1999.1361

Yelin, R., Ben-Haroush Schyr, R., Kot, H., Zins, S., Frumkin, A., Pillemer, G., Fainsod, A., 2005. Ethanol exposure affects gene expression in the embryonic organizer and reduces retinoic acid levels. Dev. Biol. 279, 193–204. doi:10.1016/j.ydbio.2004.12.014

Yonemoto, J., Brown, N.A., Webb, M., 1984. Effects of dimethoxyethyl phthalate, monomethoxyethyl phthalate, 2-methoxyethanol and methoxyacetic acid on post implantation rat embryos in culture. Toxicol. Lett. 21, 97–102. doi:10.1016/0378-4274(84)90229-7

Zarn, J.A., Brüschweiler, B.J., Schlatter, J.R., 2002. Azole Fungicides Affect Mammalian Steroidogenesis by Inhibiting Sterol 14α-Demethylase and Aromatase. Environ. Health Perspect. 111, 255–261. doi:10.1289/ehp.5785

Zega, G., De Bernardi, F., Groppelli, S., Pennati, R., 2009. Effects of the azole fungicide Imazalil on the development of the ascidian Ciona intestinalis (Chordata, Tunicata): Morphological and molecular characterization of the induced phenotype. Aquat. Toxicol. 91, 255–261. doi:10.1016/j.aquatox.2008.11.015

Zhou, F.C., Zhao, Q., Liu, Y., Goodlett, C.R., Liang, T., McClintick, J.N., Edenberg, H.J., Li, L., 2011. Alteration of gene expression by alcohol exposure at early neurulation. BMC Genomics 12, 124. doi:10.1186/1471-2164-12-124

APPENDIX: Papers under review

Manuscript Details

Manuscript number	RTX_2016_58
Title	The mixture effect of co-exposure to ethanol and fluconazole: a study in an alternative developmental model, the ascidian Ciona intestinalis
Article type	Full Length Article

Abstract

The aim of the present work was to evaluate the suitability of the Ascidian Embryo Teratogenicity assay (AET) to test mixture effects. In particular, AET was used as new alternative invertebrate model to test the developmental effects of the co-exposure to ethanol and fluconazole. Ciona.intestinalis embryos were exposed to the azolic fungicide fluconazole, (FLUCO, 7.8-250 μM), to ethanol (Eth, 0.01-0.5%) and to their mixtures (0.01% Eth + FLUCO 7.8-250 μM) from neurula to larval stage. At the end of the exposure period, larvae were morphologically evaluated. Both compounds were teratogenic in a concentration-related manner, particularly affecting the pigmented sensory organs. FLUCO exposure was also correlated to trunk abnormalities, while Eth determined a significant increase of trunk malformations only at the highest tested concentration. The co-exposure to the sub-teratogenic concentration of Eth enhanced the effects of FLUCO. These results suggest that both Eth and FLUCO could affect the same developmental pathway.

Keywords	Alternative test; Ascidian; Fluconazole; Ethanol; Mixture; Teratogenesis
Taxonomy	Invertebrate Model, Developmental System Toxicology
Manuscript region of origin	Europe
Corresponding Author	elena menegola
Order of Authors	Maria Battistoni, Silvia Mercurio, Gentile Francesco Ficetola, elena menegola, Roberta Pennati
Suggested reviewers	Leo Van der Ven, Lucia Manni, Anita Colombo

Submission Files Included in this PDF

File Name [File Type]

_Cover letter Battistoni et al.doc [Cover Letter]

Battistoni et al 12_SM.doc [Manuscript File]

Tavola malformazioni versione 7.tif [Figure]

grafici.tif [Figure]

tables.docx [Table]

Abstract.docx [Abstract]

Hightlights Battistoni et al.doc [Highlights]

To view all the submission files, including those not included in the PDF, click on the manuscript title on your EVISE Homepage, then click 'Download zip file'.

The mixture effect of co-exposure to ethanol and fluconazole: a study in an alternative developmental model, the ascidian *Ciona intestinalis*

Maria Battistoni, Silvia Mercurio, Gentile Francesco Ficetola, Elena Menegola and Roberta Pennati

Dipartimento di Bioscienze, Università degli Studi di Milano, via Celoria 26, 20133 Milan, Italy

Corresponding author: Prof. Elena Menegola
via Celoria, 26
20133 Milan, Italy
mail: elena.menegola@unimi.it
phone: +39-02-50314804 fax:
+39-02-50314802

Abstract:

The aim of the present work was to evaluate the suitability of the Ascidian Embryo Teratogenicity assay (AET) to test mixture effects. In particular, AET was used as new alternative invertebrate model to test the developmental effects of the co-exposure to ethanol and fluconazole.

*Ciona.intestinali*s embryos were exposed to the azolic fungicide fluconazole, (FLUCO, 7.8-250 μM), to ethanol (Eth, 0.01-0.5%) and to their mixtures (0.01% Eth + FLUCO 7.8-250 μM) from neurula to larval stage. At the end of the exposure period, larvae were morphologically evaluated. Both compounds were teratogenic in a concentration-related manner, particularly affecting the pigmented sensory organs. FLUCO exposure was also correlated to trunk abnormalities, while Eth determined a significant increase of trunk malformations only at the highest tested concentration. The co-exposure to the sub-teratogenic concentration of Eth enhanced the effects of FLUCO. These results suggest that both Eth and FLUCO could affect the same developmental pathway.

Keywords: Alternative test, Ascidian, Fluconazole, Ethanol, Mixture, Teratogenesis

1. Introduction

Everyday humans are exposed to multi-component chemical mixtures present in the surrounding environmental media (water, air, soil), in food or in consumer products [1,2]. The risk that may result from this exposure depends on how the effects of the different chemicals can combine in the mixture and whether there is any kind of interaction between them. Thus, evaluating the toxicity of mixtures is one of the major objectives of today toxicology. The infinite number of different combinations of chemicals in a mixture, the lacking of an efficient test strategy for mixtures risk assessment and the increasing societal need to reduce animal testing, make the study of mixtures a very complex issue [3].

In order to investigate the basis of mixture toxicology, triazole group has been selected as studied molecules to assess cumulative effects on human health [4]. The use of alternative models in toxicology has been strictly recommended to evaluate the potential effects of the co-exposure of chemicals in a mixture [3]. Considering all these points, the aim of the present work is to evaluate the effects of the co-exposure to the triazole fungicide fluconazole (FLUCO) and to ethanol (Eth) by using the ascidian *Ciona intestinalis* embryo model as new alternative teratological screening test (AET, Ascidian Embryo Teratogenicity assay).

Ascidians are marine sessile, filter-feeding chordate organisms belonging to the Subphylum *Urochordata*, which has been recognized as the sister group of vertebrates [5]. Particularly, ascidian embryos display striking similarities to vertebrate ones as they develop through a swimming, tadpole like larva, which represents a simple prototype of the chordate body plan [6], comprising a hollow neural tube lying dorsal to a rod-like notochord [7]. Thanks to their cosmopolitan distribution, basic body plan [8] and key phylogenetic position [5], ascidian larvae have been proposed as an excellent alternative experimental system for investigating the mechanisms underlying the development of chordates [5,9], and therefore of vertebrates, for applying embryo-toxicity tests and to evaluate embryotoxicity related to xenobiotic exposure as well [10–14].

Previous studies reported that ascidian larvae exposed to different azole fungicides showed characteristic malformations resembling those elicited by retinoic acid (RA) [11,12]. In both the analysed species, *Phallusia mammillata* and *Ciona intestinalis,* azole-induced malformations were specifically at the anterior region of the trunk, in which the sensory vesicle appeared reduced and the pigmented organs were severely altered. Moreover, the development of the adhesive papillae, the anterior most larval organs, was impaired. The observation that the affected structure are in ascidians those controlled by RA [15] and the evidence that the same alterations are produced by

exogenous RA exposure [15-18] suggest that, similarly to what proposed in vertebrates [19–21], also in ascidians the teratogenic action of azoles could depend on perturbation of RA pathway [11–13].

Among azoles, FLUCO (a bis-triazole derivative) is a clinically used fungicides commonly dosed for treating a variety of mycoses and infections [22]. Dose and administration period depend on type and severity of the infection: vaginal candidiasis is usually treated with a 150-mg single dose, while systemic mycoses are daily treated for several months with 400 mg FLUCO, respecting the total maximum daily recommended dose of 1600 mg. FLUCO excellent bioavailability has been reported after oral dosing and a linear pharmacokinetic has been demonstrated at doses of 200-400-800 mg/day (corresponding to a maximum plasma concentration of 33-163-229 μM) [23]. As far as the use in pregnancy is concerned, the American Food and Drug Administration agency (FDA) recently changed the indications on the risk category in pregnancy for high dose fluconazole from category C (animal reproduction studies have shown an adverse effect on the foetus and there are no adequate and well-controlled studies in humans, but potential benefits may warrant use of the drug in pregnant women despite potential risks) to category D (there is positive evidence of human foetal risk based on adverse reaction data from investigational or marketing experience or studies in humans, but potential benefits may warrant use of the drug in pregnant women despite potential risks), while the pregnancy category for a single, low dose of fluconazole remains category C [24].

Considering that teratogenic effects observed after *in vitro* exposure to FLUCO of whole postimplantation rodent embryos [25,26]) and after exposure of amphibian embryos [27] strictly resemble the alterations induced by RA excess in mammals [19,28] and in frogs [27] and that the inhibitory activity of FLUCO on the P-450 enzyme that degrades RA (CYP26) accounts for the use of FLUCO in patients with acute promyelocytic leukaemia [29–31], the proposed teratogenic mechanism for FLUCO is the inhibition of CYP26 embryonic enzymes with the consequent increase in local RA levels.

The observation that the *in vitro* co-exposure to sub-teratogenic doses of both RA and FLUCO leads to the same phenotype as the teratogenic doses of RA and FLUCO alone, definitively supported the hypothesis of local increase of RA as key event in FLUCO teratogenicity [28,32].

RA-like malformations have been reported after the exposure of mammalian and frog embryos to Eth as well. Eth is a well-known teratogen agent and its consumption during pregnancy can produce a wide range of physical, cognitive, and behavioural disabilities in newborns classified in a recognised syndromic picture named as foetal alcohol spectrum disorder (FASD) [33]. The most severe form, that includes morphological abnormalities, is defined as foetal alcohol syndrome

(FAS), characterized by microcephaly, flat midface with short palpebral fissures, low nasal bridge with short nose and long smooth or flat phyltrum [34–36]. In studies on postimplantation rat embryos exposed *in vitro* to Eth, the reported malformations are mostly neural tube defects, rotation and cardiac abnormalities and hypoplasia of the first branchial arch [37–40]. FAS pathogenesis has been deeply investigated and several teratogenic mechanisms identified. They comprise metabolic stress (including oxidative stress) and impaired signalling by transcription factor or growth factor signalling [41–50]. RA content impairment has also been described [38,40,51].

The aim of the present work is to evaluate the effects on *C. intestinalis* development of FLUCO and Eth alone or in mixture, in order to evaluate the AET assay as a new, rapid, inexpensive invertebrate alternative animal model for studies on mixture effects.

2. Materials and methods

2.1 Animals and embryos maintenance

Adults of *C. intestinalis* were collected by the fishing service of the Roscoff Biological Station (France). Animals were maintained in aquaria filled with artificial seawater (Instant Ocean, salinity 32‰) at 16° C and provided with circulation system as well as mechanical, chemical and biological filters. Constant light condition was preferred to promote gamete production.

Gametes of at least three adults were collected from dissected gonoducts and *in vitro* cross fertilization was performed in Petri glass dishes containing artificial seawater with Hepes (ASWH; pH 8). Embryos were maintained at 16 °C until they reached the hatching larva stage (22 hours post fertilization (hpf), [52].

2.2 Embryo exposure

All chemicals were of reagent grade. FLUCO and Eth absolute were purchased from Sigma, Italy. FLUCO stock solution (250 µM) was prepared in ASWH to reach the final treatment concentrations. All solutions were freshly prepared.

C. intestinalis embryos at early neurula stage (7 hpf) were exposed for 15 h, until control embryos reached the larval stage, to increasing concentrations of Eth (0.01, 0.05, 0.1, 0.25, 0.5%), to increasing concentrations of FLUCO (0, 7.8, 15.75, 31.5, 250 µM) and to mixtures of 0.01% Eth + FLUCO (0, 7.8, 15.75, 31.5, 250 µM) dissolved in 10 mL of ASWH. FLUCO concentrations were

chosen based on previous works [12] focusing on lower doses to identify the NOAEL (*No Observed Adverse Effect Level*), plus a high dose as positive control.

Approximately 100 embryos were used for each treatment and each experimental group. Each experiment was replicated at least three times (total n per groups ≈ 300). When controls reached swimming larva stage (22 hpf), all specimens were evaluated and the percentage of dead larvae was recorded. After fixation in 4% paraformaldehyde in PBS, larvae were morphologically examined in detail under a dissecting microscope.

The number of larvae showing abnormalities at tail, trunk and pigmented sensory organs as well as plurimalformed larvae were recorded.

2.3 Statistical analysis

We used generalized linear models (GLM) to test the significance of differences in the incidence of malformations between each treatment group. The number of individuals with/without malformation per each batch was the dependent variable, while treatments were the considered as fixed factors. GLMs showed overdispersion, as residual deviance was larger than the residual degrees of freedom, therefore we used a quasi-binomial error structure, and we tested significance using a F-test [53]. If substance exposures were significant, we performed Tukey's *post-hoc* tests (significant at $P < 0.05$) using the multcomp package in R [54], in order to identify specific effects of each concentration on larvae development.

3. Results

3.1 Morphological analysis of induced abnormalities

C. intestinalis larvae of each experimental group were morphologically examined under a dissecting microscope in order to evaluate the presence of abnormalities as well as plurimalformed larvae.

Nearly 80% of unexposed larvae (Tab. 1; Tab. 2; Tab. 3) developed normally, displaying an elongated trunk with three elongated adhesive papillae, a clearly visible sensory vesicle and two pigmented organs (otolith and ocellus) well-differentiated. Particularly, the ocellus, the dorsally located photoreceptor, and the otolith, the gravity-sensing organ, were normally located inside the sensory vesicle. The tail was straight and elongated (Fig. 1 A and B).

Larval abnormalities were classified in four malformed phenotypes:

- trunk abnormalities, in which trunk appeared round in shape and the anterior side was flat, due to impairment of adhesive papillae development (Fig. 1 C and D);

- pigmented organ abnormalities, in which the pigmented organs (otolith and ocellus) appeared fused in a single spot and/or displaced on the dorsal portion of the sensory vesicle (Fig. 1 E and F). In the samples displaying sensory vesicle protrusion on the trunk dorsal side, the pigmented organs were exposed to the surface;
- tail abnormalities, in which the larval tail appeared coiled, flexed or reduced in length (Fig 1 G);
- severe malformations, in which plurimalformed larvae were characterized by absence of sensory vesicle cavity, presence of a short, bent tail, round trunk with not elongated papillae. This group includes also larvae that failed the hatching event (Fig. 1 H);

The percentage of the total number of larvae with abnormalities and of plurimalformed larvae in different groups is reported in Table 1, 2 and 3.

3.2 Eth

During the development of *C. intestinalis* embryos, exposure to Eth increased the total number of malformed larvae (GLM: $F_{5,12} = 4.67$, $P = 0.013$). The percentage of malformed larvae increased in a concentration-related manner (Tab. 1). The lower effective concentration was 0.05% (Tukey's *post-hoc*, all $P \leq 0.001$). The Eth lower tested concentration (0.01%) did not cause a significant increase of malformations at any district compared to the controls (*post-hoc*, $P = 0.632$) and was thus considered as the NOAEL. The percentage of total malformations increased significantly with Eth concentration from 0.05% on (Tukey's *post-hoc* test: all $P<0.05$). The main target for Eth were specifically the pigmented sensory organs ($F_{5,12} = 15.33$, $P < 0.0001$): otolith and ocellus appeared fused or protruded at any effective concentrations. A strict dose-relationship was observed and confirmed also by *post-hoc* tests. Eth determined also, but every times At the highest tested concentration (0.5%) in less than 10% of larvae, Eth also determined a significant increase on trunk malformations ($F_{5,12} = 6.42$, $P \leq 0.001$), but this effect was evident only at the highest tested concentration (0.5%). The incidence of tail abnormalities was not significantly affected by Eth at any concentration level ($F_{5,12} = 1.58$, $P = 0.239$). Overall, Eth 0.01% resulted the NOAEL for *C. intestinalis* development, as did not cause a significant increase of any abnormalities.

3.3 FLUCO

The incidence of total number of malformations induced by FLUCO during the development of *C. intestinalis* embryos was dose-dependent (GLM: $F_{4,20} = 12.003$, $P<0.00001$): FLUCO concentrations ≥ 15.75 μM significantly increased the total number of malformations, compared to controls (*post-hoc*: all $P < 0.002$), while we did not detect significant differences between the controls and FLUCO 7.8 μM groups ($P = 0.170$) (Tab. 2). FLUCO specifically affected the

pigmented organs and the trunk (respectively GLM: $F_{4,20} = 10.43$, P<0.00001, GLM: $F_{4,20} = 16.34$, P<0.00001). The lower FLUCO concentration (7.8 µM) did not cause a significant increase of these malformations compared to the controls (Tukey's *post-hoc*, pigmented organs: $P = 0.15$, trunk: $P = 0.05$), while larvae showed significantly more malformations than controls if FLUCO concentration was ≥ 15.75 µM (*post-hoc*, all $P \leq 0.001$). A clear dose-dependence is visible for these abnormalities. Tail abnormalities were not significantly affected by FLUCO ($F_{4,20} = 1.48$, $P = 0.245$) at any tested concentration. The total number of severe malformations was significantly affected by FLUCO ($F_{4,20} = 3.52$, $P = 0.025$), even though *post-hoc* tests did not detect significant differences between specific treatments (all $P > 0.2$). Overall, FLUCO 7.8 µM resulted the NOAEL for *C. intestinalis*, as it did not cause a significant increase of abnormalities in any of the body parts considered (Tab. 2).

3.4 FLUCO + Eth

Similarly to what described after FLUCO exposure, after co-exposure to FLUCO (7.8 – 250 µM) and Eth (0.01%), larvae exposed at embryotoxic concentrations of FLUCO (15.75 – 250 µM) showed abnormalities at the level of pigmented organs ($F_{4,10} = 4.48$, P = 0.02479), trunk ($F_{4,10} = 5.89$, P = 0.01058), and severely malformed larvae ($F_{4,10} = 3.25$, P = 0.05942)(Tab. 3). Comparing the larvae developed from embryos exposed to FLUCO alone and from embryos exposed to the FLUCO + 0.01% ethanol mixture a worsened picture was evident (Fig. 2) in the total number of malformed larvae (GLM: $F_{1,20} = 7.69$, P = 0.012) and the number of malformed the pigmented organs (GLM: $F_{1,20} = 11.89$, P = 0.0025). By contrast, Eth was unable to increase the percentage of FLUCO-related trunk malformation (GLM: $F_{1,20} = 2.25$, P = 0.15) and tail development was not significantly affected by the co-exposure of FLUCO and Eth ($F_{4,20} = 0.02$, $P = 0.883$, Tab. 3).

4. Discussion

The evaluation of effects of chemicals in mixtures is of particular interest since humans and all other organisms are exposed to multi-component chemical mixtures. The classical theories on mixture toxicity indicate that the similarity of modes of action (MoA) is the main criterion to assess the mixture effect: evidence that mixtures of compounds sharing the same MoA show dose-additivity at low doses has been, in fact, reported [55,56]. Nevertheless, recent studies suggest that the similarity of molecular initiating events (MIEs) is not an essential requirement to induce additive effects, because mixtures composed of chemicals with different MIE can exhibit mixture effects too, if acting on the same biological pathway [57]. Recently, it has been argued that

grouping criteria based solely on chemical similarity or similar MoA may lead to unrealistically narrow groupings, with the exclusion of chemicals that also might contribute to combination effects [58]. This is in recognition of emerging evidence that biological effects can be similar, although the molecular details of toxicological mechanisms may profoundly differ in many respects [59].

The main aim of the present work was to evaluate the suitability of the ascidian embryo teratogenicity model (AET) to test mixture effects. In particular, AET was used as new alternative invertebrate model to test the developmental effects of the co-exposure to Eth and FLUCO.

The teratogenic potential of Eth had never been previously evaluated in ascidians, while teratogenic effects of FLUCO were observed in the ascidian *Phallusia mammillata* at concentrations similar to those used in the present work [12]. Results from the present study showed that Eth is teratogenic in the ascidian *C. intestinalis* at concentrations equal or higher than 0.05 specifically affecting the pigmented organs. Considering otolith and ocellus as a common target for both FLUCO and Eth, the aim of the present work was to evaluate the effects of FLUCO and Eth in mixture. Remarkably, co-exposure to FLUCO and to the sub-teratogenic concentration of Eth (0.01%), significantly increased the incidence of malformed larvae at pigmented organs if compared to the single exposure to FLUCO alone, suggesting an additive effect, as both Eth and FLUCO could act affecting the same pathway. In vertebrate embryos the MoA proposed is the inhibition of cytochrome P-450 (CYP26) enzymes, involved in RA catabolism, with the consequent increase in local RA levels in vertebrate embryos [28], [32]. Data obtained in both ascidian species after FLUCO exposure and those obtained after the exposure of *C. intestinalis* to the azole Imazalil [13] showed that the elicited phenotype after azole exposure is striking similar to that induced by RA. According to literature, exposure to RA during development causes stereotypical malformations in ascidian larvae, which develop with a rounded trunk and malformed sensory vesicle and pigmented organs [16,17,60,61]. In ascidians, the role of RA cascade and the expression of CYP26 has been described and compared to the expression of CYP26 in vertebrate embryos. Considering that both the expression pattern of ascidian *CYP26* and of *Hox-1* (a key gene in RA controlled cascade) were detected in Tunicates [17], it could be hypothesized that FLUCO could affect the ascidian development altering the RA morphogenetic activity in specific responsive embryonic tissues.

Evidence obtained by both the phenotypes of Eth-exposed larvae and by mixture data suggests that Eth could alter ascidian morphogenesis, interfering with the same pathway. Eth involvement in this process represents an intriguing but still highly speculative hypothesis and further analyses to confirm Eth interferences in RA pathways are needed.

In conclusion, this work shows that AET assay offers several advantages as a model system for the study of mixture effects. First, the ascidian adults are widespread in coastal area, easily maintained in aquarium, and by *in vitro* fertilization it is possible to produce thousands of synchronously dividing embryos. Moreover, since the embryos develop quickly into swimming tadpole larvae (18 hours at 18 °C; [52], it is possible to observe the effects of treatment within a day. Finally, considering that ascidians are basal chordates recognized as belonging to the sister group of vertebrates [5], results obtained in these species could be considered indicative for a need for toxicological investigation in mammals. Concerning the issue of exposure to mixtures, our data support the need of a cumulative risk assessment not only for chemicals grouped on the base of similarities in chemical structure or derived from mechanistic considerations but also for any chemical acting on the same biological pathway.

The present work was performed using an invertebrate species not subjected to regulative guidelines.

Acknowledgements

This work was sustained by the Environmental Science PhD course founds.

Conflict of interest

The authors declare that they have no conflict of interest.

Figure captions

Fig. 1. Morphological analysis of *C. intestinalis* larvae. A and B) Normally developed larvae. The lateral view of the trunk (B) allows to distinguish the otolith (Ot) and the ocellus (Oc), separated and well differentiated. Adhesive papillae (Pa) are also visible at the anterior end. C and D) Larvae displaying trunk abnormalities. The trunk appears round in shape with impairment of adhesive papillae development. D - F) Larvae displaying malformed pigmented organs, abnormal in shape (D and E) or fused (F). G) Larvae with coiled or flexed tail. H) Plurimalformed larvae displaying severe malformations to almost all organs. Magnification: 60X (A, C, G, H), 120X (B, D, E, F). Scale bar: 100 μm.

Fig. 2. Histograms showing the effect of the co-exposure to increasing FLUCO concentration with Eth 0.01% on different categories of malformation: pigmented organs, trunk and total malformed larvae.

* = Effect of Eth compared to the FLUCO dose alone.

Tab. 1. Percentage averages of frequency and standard error of malformed larvae at increasing Eth concentrations.

Tab. 2. Percentage averages of frequency and standard error of malformed larvae at increasing FLUCO concentrations (μM).

Tab. 3. Percentage averages of frequency and standard error of malformed larvae after co-exposure to increasing FLUCO concentration (μM) with Eth 0.01%.

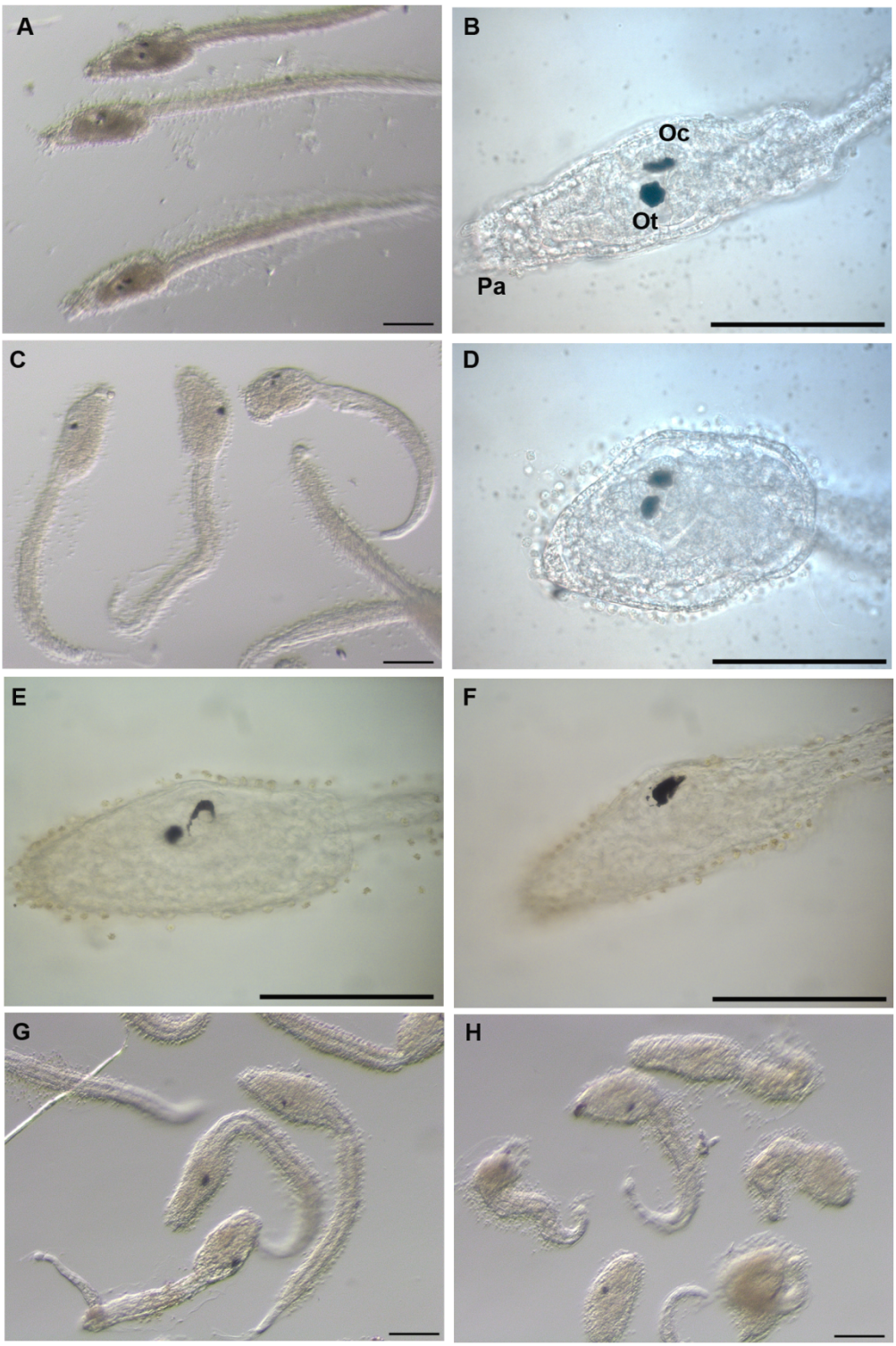

Figure 1

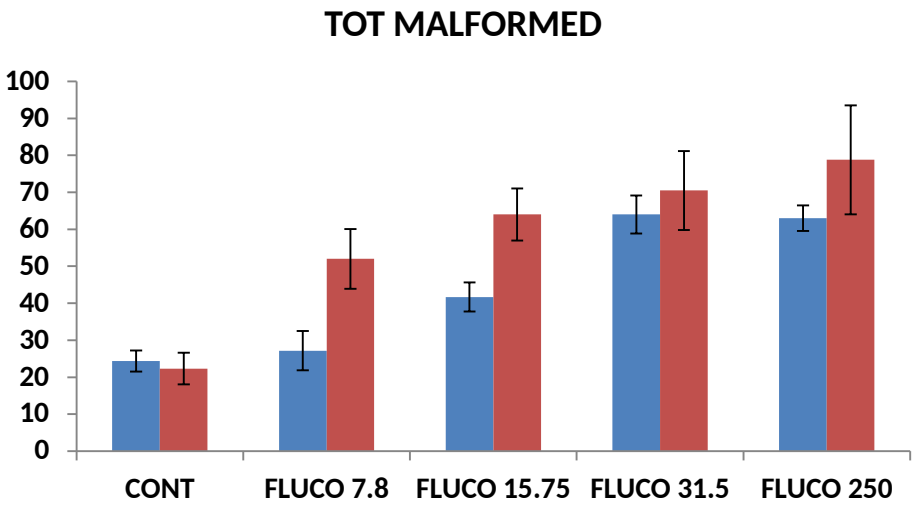
TOT MALFORMED
100
90
80
70
60
50
40
30
20
10
0
CONT
FLUCO 7.8
FLUCO 15.75
FLUCO 31.5
FLUCO 250

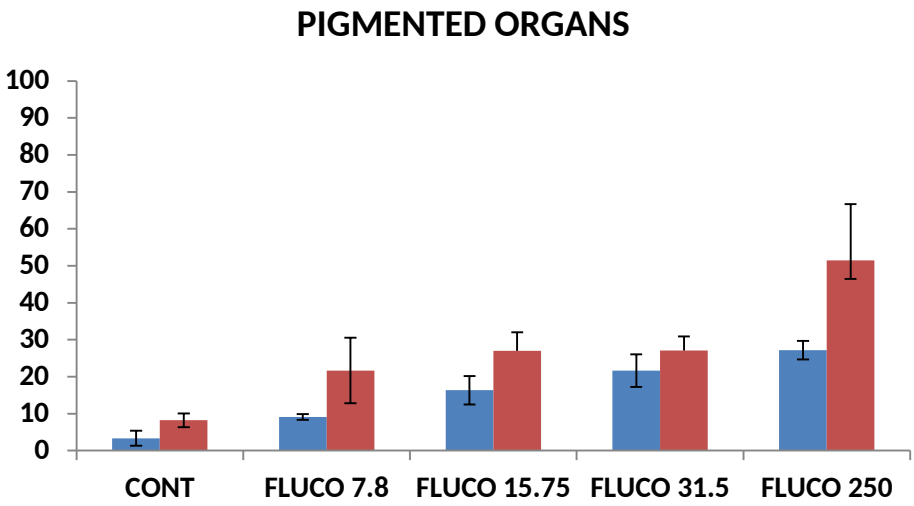
PIGMENTED ORGANS
100
90
80
70
60
50
40
30
20
10
0
CONT
FLUCO 7.8
FLUCO 15.75
FLUCO 31.5
FLUCO 250

Figure 2

TAB. 1

Percentage averages of frequency and standard error of malformed larvae at increasing Eth concentrations.

	0 (*N*=290)	0.01% (*N* = 300)	0.05% (*N* = 289)	0.1% (*N* = 290)	0.25% (*N* = 300)	0.5% (*N*= 300)
Tail	11.30 ± 1.48	15.00 ± 7.56	21.72 ± 5.91	29.11 ± 2.19	22 ± 3.52	20.67 ± 4.41
Pigmented organs	5.63 ± 1.63	10.00 ± 3.22	20.45 ± 4.70 **AB**	22.26 ± 2.26 **ABC**	31.00 ± 1.73 **ABCD**	35.33 ± 1.67 **ABCDE**
Trunk	0.00 ± 0.00	2.33 ± 1.45	4.83 ± 0.60	5.85 ± 0.60	3.33 ± 1.33	9.67 ± 3.39 **AB**
Severe malformations	4.59 ± 1.70	5.67 ± 3.48	5.47 ± 1.82	9.70 ± 1.87	7.33 ± 2.61	9.67 ± 3.18
Tot. Malformed	21.52 ± 2.04	31.33 ± 12.21	49.39 ± 5.71 **A**	56.96 ± 5.29 **AB**	53.00 ± 6.03 **A**	61.00 ± 2.89 **AB**

A p<0.01 vs. ETH 0
B p<0.01 vs. ETH 0.01%
C p<0.01 vs. ETH 0.05%
D p<0.01 vs. ETH 0.1%
E p<0.01 vs. ETH 0.25%

TAB. 2

Percentage averages of frequency and standard error of malformed larvae at increasing FLUCO concentrations (µM).

	0 (*N* = 300)	7.8 (*N* = 251)	15.75 (*N* = 300)	31.5 (*N* = 300)	250 (*N* = 264)
Tail	8.33 ± 1.86	6.26 ± 1.13	3.33 ± 1.20	14.33 ± 6.97	7.62 ± 1.79
Pigmented organs	3.33 ± 2.03	9.14 ± 0.78	16.33 ± 3.85 **A**	21.66 ± 4.41 **A**	27.18 ± 2.52 **ABC**
Trunk	7.00 ± 1.53	11.76 ± 3.45	21.66 ± 3.18 **A**	41.33 ± 7.70 **AB**	40.39 ± 3.87 **AB**
Severe malformations	6.00 ± 3.06	1.29 ± 0.66	3.00 ± 1.16	4.33 ± 1.86	9.72 ± 2.57
Tot. Malformed	24.33 ± 2.85	27.18 ± 5.30	41.67 ± 3.93 **A**	64.00 ± 5.14 **AB**	62.98 ± 3.46 **AB**

A p<0.01 vs. FLUCO 0 µM

B p<0.01 vs. FLUCO 7.8 µM

C p<0.01 vs. FLUCO 15.75 µM

TAB. 3

Percentage averages of frequency and standard error of malformed larvae after co-exposure to increasing FLUCO concentration (μM) with Eth 0.01%.

	0 + ETH 0.01% (*N* = 286)	7.8 + ETH 0.01% (*N* = 300)	15.75 + ETH 0.01% (*N* = 300)	31.5 + ETH 0.01% (*N* = 299)	250 + ETH 0.01% (*N* = 275)
Tail	5.60 ± 2.03	9.33 ± 0.88	10.00 ± 3.47	9.69 ± 1.31	6.56 ± 1.45
Pigmented organs	8.22 ± 1.88	21.66 ± 8.85	27.00 ± 5.01	27.09 ± 3.78	51.44 ± 15.21 [A]
Trunk	7.55 ± 1.45	24.00 ± 5.51	37.33 ± 6.07 [A]	36.42 ± 6.68 [A]	40.56 ± 9.71 [A]
Severe malformations	3.00 ± 2.08	7.66 ± 2.73	12.33 ± 3.93 [A]	19.05 ± 5.02	15.77 ± 3.62
Tot. Malformed	22.32 ± 4.28	52.00 ± 8.09	64.00 ± 7.01	70.50 ± 10.66 [AB]	78.80 ± 14.77 [AB]

A p<0.01 vs. FLUCO 0 + ETH 0.01%

B p<0.01 vs. FLUCO 7.8 + ETH 0.01%

C p<0.01 vs. FLUCO 17.75 + ETH 0.01%

References

[1] V. J. Feron, F. R. Cassee, and J. P. Groten, “Toxicology of chemical mixtures: international perspective,” *Environ. Health Perspect.*, vol. 106, no. Suppl 6, pp. 1281–1289, Dec. 1998.

[2] J. . Groten, “Mixtures and interactions,” *Food Chem. Toxicol.*, vol. 38, pp. S65–S71, Apr. 2000.

[3] EPA, “Guidance on cumulative risk assessment of pesticide chemicals that have a common mechanism of toxicity.” 2002.

[4] EFSA, “Scientific Opinion on risk assessment for a selected group of pesticides from the triazole group to test possible methodologies to assess cumulative effects from exposure through food from these pesticides to human health.” EFSA Journal, 7(9), 1167, 2009.

[5] F. Delsuc, H. Brinkmann, D. Chourrout, and H. Philippe, “Tunicates and not cephalochordates are the closest living relatives of vertebrates,” *Nature*, vol. 439, no. 7079, pp. 965–968, Feb. 2006.

[6] Y. J. Passamaneck and A. Di Gregorio, “Ciona intestinalis: Chordate development made simple,” *Dev. Dyn.*, vol. 233, no. 1, pp. 1–19, May 2005.

[7] Satoh, “Developmental Biology of Ascidians,” *Camb. Univ Press N. Y.*, 1994.

[8] N. Satoh, “The ascidian tadpole larva: comparative molecular development and genomics,” *Nat. Rev. Genet.*, vol. 4, no. 4, pp. 285–295, Apr. 2003.

[9] Y. Sasakura, K. Mita, Y. Ogura, and T. Horie, “Ascidians as excellent chordate models for studying the development of the nervous system during embryogenesis and metamorphosis,” *Dev. Growth Differ.*, vol. 54, no. 3, pp. 420–437, Apr. 2012.

[10] F. Cima, L. Ballarin, G. Bressa, G. Martinucci, and P. Burighel, “Toxicity of Organotin Compounds on Embryos of a Marine Invertebrate (Styela plicata;Tunicata),” *Ecotoxicol. Environ. Saf.*, vol. 35, no. 2, pp. 174–182, Nov. 1996.

[11] R. Pennati, S. Groppelli, G. Zega, M. Biggiogero, F. De Bernardi, and C. Sotgia, “Toxic effects of two pesticides, Imazalil and Triadimefon, on the early development of the ascidian Phallusia mammillata (Chordata, Ascidiacea),” *Aquat. Toxicol.*, vol. 79, no. 3, pp. 205–212, Sep. 2006.

[12] S. Groppelli, G. Zega, M. Biggiogero, F. De Bernardi, C. Sotgia, and R. Pennati, “Fluconazole induces teratogenic effects in the tunicate Phallusia mammillata,” *Environ. Toxicol. Pharmacol.*, vol. 23, no. 3, pp. 265–271, May 2007.

[13] G. Zega, F. De Bernardi, S. Groppelli, and R. Pennati, “Effects of the azole fungicide Imazalil on the development of the ascidian Ciona intestinalis (Chordata, Tunicata): Morphological and molecular characterization of the induced phenotype,” *Aquat. Toxicol.*, vol. 91, no. 3, pp. 255–261, Feb. 2009.

[14] A. Matsushima, K. Ryan, Y. Shimohigashi, and I. A. Meinertzhagen, “An endocrine disruptor, bisphenol A, affects development in the protochordate Ciona intestinalis: Hatching rates and swimming behavior alter in a dose-dependent manner,” *Environ. Pollut.*, vol. 173, pp. 257–263, Feb. 2013.

[15] K. Nagatomo, T. Ishibashi, Y. Satou, N. Satoh, and S. Fujiwara, “Retinoic acid affects gene expression and morphogenesis without upregulating the retinoic acid receptor in the ascidian Ciona intestinalis,” *Mech. Dev.*, vol. 120, no. 3, pp. 363–372, Mar. 2003.

[16] V. F. Hinman and B. M. Degnan, “Retinoic acid disrupts anterior ectodermal and endodermal development in ascidian larvae and postlarvae,” *Dev. Genes Evol.*, vol. 208, no. 6, pp. 336–345, Aug. 1998.

[17] K. Nagatomo and S. Fujiwara, “Expression of Raldh2, Cyp26 and Hox-1 in normal and retinoic acid-treated Ciona intestinalis embryos,” *Gene Expr. Patterns*, vol. 3, no. 3, pp. 273–277, Jun. 2003.

[18] M. Kanda, H. Wada, and S. Fujiwara, “Epidermal expression of Hox1 is directly activated by retinoic acid in the Ciona intestinalis embryo,” *Dev. Biol.*, vol. 335, no. 2, pp. 454–463, Nov. 2009.

[19] Menegola, M. L. Broccia, F. Di Renzo, and E. Giavini, “Pathogenic pathways in fluconazole-induced branchial arch malformations,” *Birt. Defects Res. A. Clin. Mol. Teratol.*, vol. 67, no. 2, pp. 116–124, Feb. 2003.

[20] F. Di Renzo *et al.*, “Molecular mechanism of teratogenic effects induced by the fungicide triadimefon: Study of the expression of TGF-β mRNA and TGF-β and CRABPI proteins during rat in vitro development,” *Toxicol. Appl. Pharmacol.*, vol. 234, no. 1, pp. 107–116, Jan. 2009.

[21] F. Marotta and G. M. Tiboni, “Molecular aspects of azoles-induced teratogenesis,” *Expert Opin. Drug Metab. Toxicol.*, vol. 6, no. 4, pp. 461–482, Apr. 2010.
[22] D. Debruyne, “Clinical Pharmacokinetics of Fluconazole in Superficial and Systemic Mycoses:,” *Clin. Pharmacokinet.*, vol. 33, no. 1, pp. 52–77, Jul. 1997.
[23] S. R. C. J. Santos, E. V. Campos, C. Sanches, D. S. Gomez, and M. C. Ferreira, “Fluconazole plasma concentration measurement by liquid chromatography for drug monitoring of burn patients,” *Clinics*, vol. 65, no. 2, pp. 237–243, 2010.
[24] FDA, “FDA Drug Safety Communication:Use of long-term, high-dose Diflucan (fluconazole) during pregnancy may be associated with birth defects in infants.” 2011.
[25] G. M. Tiboni, “Second branchial arch anomalies induced by fluconazole, a bis-triazole antifungal agent, in cultured mouse embryos,” *Res. Commun. Chem. Pathol. Pharmacol.*, vol. 79, no. 3, pp. 381–384, Mar. 1993.
[26] Menegola, M. L. Broccia, F. Di Renzo, and E. Giavini, “Antifungal triazoles induce malformations in vitro,” *Reprod. Toxicol.*, vol. 15, no. 4, pp. 421–427, Jul. 2001.
[27] S. Groppelli, R. Pennati, F. De Bernardi, E. Menegola, E. Giavini, and C. Sotgia, “Teratogenic effects of two antifungal triazoles, triadimefon and triadimenol, on Xenopus laevis development: Craniofacial defects,” *Aquat. Toxicol.*, vol. 73, no. 4, pp. 370–381, Jul. 2005.
[28] Menegola, M. L. Broccia, F. Di Renzo, V. Massa, and E. Giavini, “Relationship between hindbrain segmentation, neural crest cell migration and branchial arch abnormalities in rat embryos exposed to fluconazole and retinoic acid in vitro,” *Reprod. Toxicol.*, vol. 18, no. 1, pp. 121–130, Jan. 2004.
[29] J. P. Van Wauwe, M. C. Coene, J. Goossens, W. Cools, and J. Monbaliu, “Effects of cytochrome P-450 inhibitors on the in vivo metabolism of all-trans-retinoic acid in rats,” *J. Pharmacol. Exp. Ther.*, vol. 252, no. 1, pp. 365–369, Jan. 1990.
[30] K. L. Vanier, A. J. Mattiussi, and D. L. Johnston, “Interaction of all-trans-retinoic acid with fluconazole in acute promyelocytic leukemia,” *J. Pediatr. Hematol. Oncol.*, vol. 25, no. 5, pp. 403–404, May 2003.
[31] E. L. Schwartz, S. Hallam, R. E. Gallagher, and P. H. Wiernik, “Inhibition of all-trans-retinoic acid metabolism by fluconazole in vitro and in patients with acute promyelocytic leukemia,” *Biochem. Pharmacol.*, vol. 50, no. 7, pp. 923–928, Sep. 1995.
[32] E. Menegola, M. L. Broccia, F. Di Renzo, and E. Giavini, “Postulated pathogenic pathway in triazole fungicide induced dysmorphogenic effects,” *Reprod. Toxicol.*, vol. 22, no. 2, pp. 186–195, Aug. 2006.
[33] E. L. Abel and J. H. Hannigan, “Maternal risk factors in fetal alcohol syndrome: Provocative and permissive influences,” *Neurotoxicol. Teratol.*, vol. 17, no. 4, pp. 445–462, Jul. 1995.
[34] L. de Sanctis, L. Memo, S. Pichini, L. Tarani, and F. Vagnarelli, “Fetal alcohol syndrome: new perspectives for an ancient and underestimated problem,” *J. Matern. Fetal Neonatal Med.*, vol. 24, no. sup1, pp. 34–37, Oct. 2011.
[35] X. Joya *et al.*, “Determination of maternal-fetal biomarkers of prenatal exposure to ethanol: A review,” *J. Pharm. Biomed. Anal.*, vol. 69, pp. 209–222, Oct. 2012.
[36] L. Memo, E. Gnoato, S. Caminiti, S. Pichini, and L. Tarani, “Fetal alcohol spectrum disorders and fetal alcohol syndrome: the state of the art and new diagnostic tools,” *Early Hum. Dev.*, vol. 89, pp. S40–S43, Jun. 2013.
[37] E. Giavini, M. L. Broccia, M. Prati, D. Bellomo, and E. Menegola, “Effects of ethanol and acetaldehyde on rat embryos developing in vitro,” *Vitro Cell. Dev. Biol. - Anim.*, vol. 28, no. 3, pp. 205–210, Mar. 1992.
[38] L. Deltour, H. L. Ang, and G. Duester, “Ethanol inhibition of retinoic acid synthesis as a potential mechanism for fetal alcohol syndrome,” *FASEB J. Off. Publ. Fed. Am. Soc. Exp. Biol.*, vol. 10, no. 9, pp. 1050–1057, Jul. 1996.
[39] G. Duester, “Alcohol dehydrogenase as a critical mediator of retinoic acid synthesis from vitamin A in the mouse embryo,” *J. Nutr.*, vol. 128, no. 2 Suppl, p. 459S–462S, Feb. 1998.
[40] H. Kot-Leibovich and A. Fainsod, “Ethanol induces embryonic malformations by competing for retinaldehyde dehydrogenase activity during vertebrate gastrulation,” *Dis. Model. Mech.*, vol. 2, no. 5–6, pp. 295–305, May 2009.

[41] F. C. Zhou *et al.*, “Alteration of gene expression by alcohol exposure at early neurulation,” *BMC Genomics*, vol. 12, no. 1, p. 124, 2011.
[42] E. Climent, M. Pascual, J. Renau-Piqueras, and C. Guerri, “Ethanol exposure enhances cell death in the developing cerebral cortex: Role of brain-derived neurotrophic factor and its signaling pathways,” *J. Neurosci. Res.*, vol. 68, no. 2, pp. 213–225, Apr. 2002.
[43] M. W. Miller and P. E. Kuhn, “Cell Cycle Kinetics in Fetal Rat Cerebral Cortex: Effects of Prenatal Treatment with Ethanol Assessed by a Cumulative Labeling Technique with Flow Cytometry,” *Alcohol. Clin. Exp. Res.*, vol. 19, no. 1, pp. 233–237, Feb. 1995.
[44] C. Ikonomidou, “Ethanol-Induced Apoptotic Neurodegeneration and Fetal Alcohol Syndrome,” *Science*, vol. 287, no. 5455, pp. 1056–1060, Feb. 2000.
[45] K. . Light, S. . Belcher, and D. . Pierce, “Time course and manner of Purkinje neuron death following a single ethanol exposure on postnatal day 4 in the developing rat,” *Neuroscience*, vol. 114, no. 2, pp. 327–337, Oct. 2002.
[46] A. Holownia, M. Ledig, and J.-F. Ménez, “Ethanol-induced cell death in cultured rat astroglia,” *Neurotoxicol. Teratol.*, vol. 19, no. 2, pp. 141–146, Mar. 1997.
[47] L. E. Kotch and K. K. Sulik, “Experimental fetal alcohol syndrome: Proposed pathogenic basis for a variety of associated facial and brain anomalies,” *Am. J. Med. Genet.*, vol. 44, no. 2, pp. 168–176, Sep. 1992.
[48] K. K. Sulik, “Genesis of alcohol-induced craniofacial dysmorphism,” *Exp. Biol. Med. Maywood NJ*, vol. 230, no. 6, pp. 366–375, Jun. 2005.
[49] B. A. Kilburn, P. J. Chiang, J. Wang, G. R. Flentke, S. M. Smith, and D. R. Armant, “Rapid Induction of Apoptosis in Gastrulating Mouse Embryos by Ethanol and Its Prevention by HB-EGF,” *Alcohol. Clin. Exp. Res.*, vol. 30, no. 1, pp. 127–134, Jan. 2006.
[50] T. L. Smith, “Regulation of glutamate uptake in astrocytes continuously exposed to ethanol,” *Life Sci.*, vol. 61, no. 25, pp. 2499–2505, Nov. 1997.
[51] M. A. Kane, A. E. Folias, C. Wang, and J. L. Napoli, “Ethanol elevates physiological all-trans-retinoic acid levels in select loci through altering retinoid metabolism in multiple loci: a potential mechanism of ethanol toxicity,” *FASEB J.*, vol. 24, no. 3, pp. 823–832, Mar. 2010.
[52] K. Hotta *et al.*, “A web-based interactive developmental table for the ascidian *Ciona intestinalis* , including 3D real-image embryo reconstructions: I. From fertilized egg to hatching larva,” *Dev. Dyn.*, vol. 236, no. 7, pp. 1790–1805, Jul. 2007.
[53] M. J. Crawley, *The R Book*. Chichester, UK, 2007.
[54] T. Hothorn, F. Bretz, and P. Westfall, “Simultaneous Inference in General Parametric Models,” *Biom. J.*, vol. 50, no. 3, pp. 346–363, Jun. 2008.
[55] D. Jonker, R. A. Woutersen, and V. J. Feron, “Toxicity of mixtures of nephrotoxicants with similar or dissimilar mode of action,” *Food Chem. Toxicol.*, vol. 34, no. 11–12, pp. 1075–1082, Nov. 1996.
[56] A. Moretto, “Exposure to multiple chemicals: when and how to assess the risk from pesticide residues in food,” *Trends Food Sci. Technol.*, vol. 19, pp. S56–S63, Nov. 2008.
[57] P. on P. P. P. and their R. (PPR) EFSA, “Scientific Opinion on the relevance of dissimilar mode of action and its appropriate application for cumulative risk assessment of pesticides residues in food: Relevance of dissimilar mode of action,” *EFSA J.*, vol. 11, no. 12, p. 3472, Dec. 2013.
[58] A. Boobis *et al.*, “Critical analysis of literature on low-dose synergy for use in screening chemical mixtures for risk assessment,” *Crit. Rev. Toxicol.*, vol. 41, no. 5, pp. 369–383, May 2011.
[59] A. Kortenkamp, “Ten Years of Mixing Cocktails: A Review of Combination Effects of Endocrine-Disrupting Chemicals,” *Environ. Health Perspect.*, vol. 115, no. S-1, pp. 98–105, Jun. 2007.
[60] F. De Bernardi, C. Sotgia, and G. Ortoloani, “Retinoic acid treatment of ascidian embryos: effects on larvae and metamorphosis,” *Anim Biol*, vol. 3, pp. 75–81, 1994.
[61] Y. Katsuyama, S. Wada, S. Yasugi, and H. Saiga, “Expression of the labial group Hox gene HrHox-1 and its alteration induced by retinoic acid in development of the ascidian Halocynthia roretzi,” *Dev. Camb. Engl.*, vol. 121, no. 10, pp. 3197–3205, Oct. 1995.

Authors: Elena Menegola[1], Maria Battistoni[1], Francesca Di Renzo[1], Francesca Metruccio[2], Angelo Moretto[2,3].

Title:

Effects of fluconazole and ethanol in mixture on cranio-facial development: use of the post-implantation rat embryo model.

Affiliations: [1] Università degli Studi di Milano, Dipartimento di Bioscienze, via Celoria 26, 20133 Milan- Italy, [2] International Centre for Pesticides and Health Risks Prevention (ICPS), ASST Fatebenefratelli Sacco, Luigi Sacco Hospital; [3] Università degli Studi di Milano, Dipartimento di Scienze Biomediche e Cliniche, Milan, Italy.

Email addresses: elena.menegola@unimi.it, maria.battistoni@unimi.it, francesca.direnzo@unimi.it, francesca.metruccio@icps.it, angelo.moretto@unimi.it.

Corresponding Author: Prof. Elena Menegola,

Università degli Studi di Milano, Dipartimento di Bioscienze,

via Celoria 26, 20133 Milan- Italy.

Tel.: +39-02-50314802

Fax: +39-02-50314804

e-mail: elena.menegola@unimi.it

Abstract

Ethanol (Eth) and Fluconazole (FLUCO) are chemicals related to facial defects (including oral clefts), affecting the facial development also in *in vitro* models.FLUCO teratogenic Mode of Action (MoA) is probably due to the inhibition of retinoic acid (RA) catabolism. Eth is a teratogen with multifactorial not completely understood MoA. The aim is to evaluate the effects of Eth and FLUCO co-exposure in postimplantation rat whole embryo cultures (WEC). E9.5 embryos were exposed to Eth (17-85 mM), FLUCO (62.5-500 µM) or, according to the fix-and-moving model, co-exposed to Eth (17 mM, NOAEL) and FLUCO (62.5-500 µM) or, vice versa, to FLUCO NOAEL (62.5µM) and Eth (17-85 mM). Based on bench mark dose (BMD) and relative potency factor (RPF) approaches, the outcome of mixtures was modeled and the predicted effects, derived under the dose-additivity hypothesis, compared with the experimental results. Concentration-related effects were observed after the Eth or FLUCO exposure. The common targets for teratogenicity were the facial primordia (branchial arches). A significant enhancement of teratogenic effects was observed in the groups co-exposed to FLUCO and Eth in comparison to the single exposures. Results from BMD approach show that there are no significant deviations from concentration–additivity, suggesting a common MoA for both molecules. In order to test the hypothesis of an Eth-mediated imbalance on RA-related pathway, a mixture of Eth and RA at their NOAELs (17mM + 0.025) µM has been performed and results compared to a positive control (RA 0.25 µM), showing results in line with the hypothesis.

Key words: Mixture, facial defects, BMD, retinoic acid, embryo.

Acknowledgments: This research has been supported by the grant of the European Project ACROPOLIS (project N 245163)+ H2020 Framework EUROMIX (project N 633172).

Introduction

Among congenital anomalies, oral clefts (cleft lip and/or palate alone or associated with other cranio-facial deformities) are one of the most frequent (1:700 live births) both as isolated anomalies and in syndromic conditions (Mossey et al. 2009). The main environmental factors which have been reported as possibly increasing the risk of oro-facial clefts are tobacco smoking (Kallen 1997), alcohol consumption (Werler et al. 1991; Munger et al. 1996), solvents (Holmberg et al. 1982), agricultural chemicals (Gordon and Shy 1981; Thomas et al. 1992; Nurminen et al. 1995); and several classes of drugs (Jentink et al. 2010; Howley et al. 2016). Among antifungals, the specific teratogenic effect of some agrochemical and clinically-used azole fungicides, including fluconazole (FLUCO), has been documented in the past by other research groups and us, using postimplantation rodent whole embryo culture (Tiboni 1993; Menegola et al. 2001; 2003; 2004; 2005). FLUCO is a bis-triazole derivative used by oral, topic or intravenous administration for treating vaginal, oral, and esophageal mycoses, urinary tract infections, peritonitis, pneumonia and disseminated infections caused by *Candida*. FLUCO is also used for treating cryptococcal meningitis, and prevention of *Candida* infections in patients undergoing chemotherapy or radiation therapy. Excellent bioavailability has been reported after oral dosing, and a linear pharmacokinetics has been demonstrated at doses of 200-400-800 mg daily (corresponding to a maximum plasma concentration of 33-163-229μM) (Santos et al. 2010). A larger dosage (1200 mg/die) is suggested for deep mycoses. Similar to the other azole-derivative fungicides, FLUCO inhibits the fungal wall formation exerting a high fungistatic activity. The FDA pregnancy category for high dose FLUCO indications has been recently changed from category C (animal reproduction studies have shown an adverse effect on the fetus and there are no adequate and well-controlled studies in humans, but potential benefits may warrant use of the drug in pregnant women despite potential risks) to category D (there is positive evidence of human fetal risk based on adverse reaction data from investigational or marketing experience or studies in humans, but potential benefits may warrant use of the drug in pregnant women despite potential risks), while the pregnancy category for a single, low dose of FLUCO is category C. Animal *in vivo* studies, case reports and a recent birth defect prevention study reported cleft lip/palate after *in utero* exposure to FLUCO (Tachibana et al. 1987; Lee et al. 1992; Aleck and Bartley 1997; Sanchez and Moya 1998; Lopez-Rangel and Van Allen 2005; Pursley et al. 1996; Howley et al. 2016). Concentration-related teratogenic effects have been also observed after *in vitro* exposure of whole rodent embryos to FLUCO concentrations in the range of therapeutical plasma levels (125-500μM): the abnormalities were specifically at the branchial arch apparatus (the embryonic precursor of facial elements) (Tiboni, 1993; Menegola et al. 2001). During the whole culture period, severe alterations in migration of hindbrain neural crest cells (NCCs, the precursors of facial skeletal elements) into the branchial arches were observed in FLUCO-exposed embryos, while physiological apoptosis,

cell proliferation, and mesenchymal cell induction were unaffected (Menegola et al. 2003). In accordance to the Mode of Action (MoA) accounting for FLUCO therapeutical properties against acute promyelocytic leukaemia (Schwartz et al. 1995; Vanier et al. 2003; Holmes et al. 2012), it has been hypothesized that the inhibition of the retinoic acid (RA) catabolic enzyme CYP26 (with the consequent tissutal RA increase) could be at the basis of azole side effects in pregnancy (Menegola et al., 2003). A strict relationship between hindbrain segmentation, neural crest cell migration and branchial arch abnormalities elicited in rat embryos by the exposure *in vitro* to teratogenic concentrations of FLUCO or RA or to the mixture of the sub-teratogenic concentrations of FLUCO and RA has been described, and accounts for the imbalance of RA-related pathway as the MoA for FLUCO teratogenicity (Menegola et al. 2004).

Ethanol (Eth) is a known teratogenic agent and its consumption during pregnancy has been related to a wide range of adverse effects in newborns. The severity of damage due to Eth exposure depends on several factors which include the timing, pattern, and dose of consumption (Abel and Hannigan, 1995). The collective evidence from human and animal studies strongly suggests that even light drinking during pregnancy can produce significant long-lasting alterations (Flak et al. 2014). Maternal Eth consumption can develop a spectrum of physical, cognitive, and behavioral disabilities in newborns, known as fetal alcohol spectrum disorder (FASD) (Sulik, 2005; Kotch and Sulik, 1992; Willford et al. 2006). The most severe form, that includes morphological abnormalities, is defined as fetal alcohol syndrome (FAS) (de Sanctis et al. 2011; Joya et al. 2012; Memo et al. 2013). FAS facial characteristics include microcephaly, flat midface with short palpebral fissures, low nasal bridge with short nose and long smooth or flat phyltrum (de Sanctis et al. 2011). As many as 50% of affected children also exhibit identifiable facial anomalies, such as maxillary hypoplasia, cleft palate, and micrognathia (American Academy of Pediatrics report, 2000). After *in vitro* or *in utero* exposure to Eth, postimplantation rodent embryos show developmental delays, neural tube defects and branchial arch abnormalities related to alteration in hindbrain NCC migration (Fadel and Persaud, 1992; Giavini et al. 1992; Van Maele-Fabry et al. 1995; Kotch et al. 1995; Chen and Sulik, 1996; Dunty et al. 2001). In rodent whole embryos cultured *in vitro*, the reported effective teratogenic concentrations are 44-88 mM (Zhou et al. 2011), while 17 mM is considered safe and suggested when Eth is used as a solvent (Kitchin and Ebron 1984). In spite of the fact that FAS pathogenesis has been deeply investigated (Wentzel and Eriksson, 2009; Yamada et al. 2005; Czarnobaj et al. 2014), for Eth a univocal teratogenic MoA has not yet been established. Potential mechanistically relevant events include impaired RA signaling cascade (Sulik 2005; Zhou et al. 2011).

Considering that literature describes cranio-facial and branchial abnormalities as a common outcome elicited by FLUCO and Eth, the aim of the present work is to evaluate the effects of co-exposure of Eth and FLUCO by using a fix-and-moving model (one molecule at its No Adverse Effect Level (NOAEL) + the other one at increasing

concentrations, including NOAEL). The goals were: 1. to deeply describe and compare the effects of FLUCO and Eth on postimplantation rat whole embryo culture; 2. to verify if the co-exposure influences the dose-response relationship of the single molecule; 3. to evaluate if the teratogenic pathway is common for the two molecules. Finally, we tested the hypothesis that one MoA contributing to Eth teratogenicity could be the imbalance of RA-related pathway. For this reason, similarly to what previously described for FLUCO (Menegola et al. 2004), some embryos were co-exposed to the Eth and RA at their NOAELs and data compared to those obtained in a group exposed to the 100% teratogenic concentration of RA.

Materials and Methods

Materials and compound preparation. FLUCO (Sigma), Eth (Fluka), RA (Sigma) were used as test substances. FLUCO was dissolved in distilled water, RA was diluted in DMSO, Eth was used undiluted. The medium used for the extraction of embryos from the uteri was sterilized Tyrode solution (Sigma); the medium used for the postimplantation whole embryo culture was undiluted heat inactivated rat serum added with antibiotics (penicillin 100 IU/mL culture medium and streptomycin 100µg/mL culture medium, Sigma).

Selection of compound concentrations. The concentrations of test molecules were selected from previous published experiments: FLUCO 62.5-125-250-500µM (Menegola et al. 2001), Eth 17-42.5-85-127.5 mM (Priscott, 1982; Wynter et al. 1983; Kitchin and Ebron, 1984; Clode et al. 1987; Giavini et al. 1992; Hunter et al. 1994, Van Maele-Fabry, 1995), RA 0.025-0.25µM (Menegola et al. 2004). Mixture groups were performed following the fix and moving criterion: Eth fix (17 mM) + FLUCO moving (62.5-125-250-500µM); FLUCO fix (62.5 µM) + Eth moving (17-42.5-85mM); Eth + RA at their NOAELs (respectively 17 mM and 0.025 µM). An unexposed control group and a group exposed to the solvent used for RA (DMSO, 1µL/mL), were also performed.

Embryo culture. Virgin female CD:Crl rats (Charles River, Calco, Italy), housed in a thermostatically maintained room (T = 22 ± 2 °C; relative humidity 55 ± 5%) with a 12 h light cycle (light from 6.00 a.m. to 6.00 p.m.), free access to food (Italiana Mangimi, Settimo Milanese, Italy) and tap water *ad libitum*, were caged overnight with males of proven fertility. All animal use protocols were approved by the Ministry of Health - Department for Veterinary Public Health, Nutrition and Food Safety committee. Animals were treated humanely and with regard for alleviation of suffering.

Embryos were explanted from pregnant rats at E9.5 (early neurula stage, 1–3 somites; day of positive vaginal smear = 0) and cultured according to the New's method (1978) in 20 ml glass bottles (5 embryos/bottle), containing 5 mL culture medium. At least a triplicate was performed for each group.

The bottles, inserted in a thermostatic (37.8°C) roller (30 rpm) apparatus, were periodically gas equilibrated according to Giavini et al. (1992). After 48 h of culture, embryos were morphologically examined and processed for whole mount immunohistochemistry.

Morphological examination. To evaluate the developmental degree and any morphological abnormality in the different groups, embryos were examined under a dissecting microscope. Yolk sac diameter, crown-rump and head length, somite number and the morphological score (determined according to Brown and Fabro, 1981) were collected as morphometrical parameters. Any branchial or extra-branchial abnormality was recorded. Data were statistically analyzed using ANOVA followed by Tukey's test and chi square test. The level of significance was set at $p < 0.05$. If the overall tests for association between response and treatment were significant, the follow-up analyses were performed.

Bench mark dose (BMD) approach and modeling of combined exposure. Based on bench mark dose (BMD) and relative potency factor (RPF) approaches, the outcome of mixture of FLUCO and Eth was modeled and the predicted effects, derived under the dose-additivity hypothesis, compared with the experimentally obtained results. FLUCO and Eth single dose response curves for branchial abnormalities were retrieved and modeled using EPA BMDS version 2.6 software, the best fitting model has been chosen according to BMDS criteria.

Starting from the selected model, the appropriate BMR was chosen that would have given a BMD (central) equal or very close to the dose used in the mixture for each compound. For each mixture two different dose levels were found using, alternatively, one compound in the mixture as Index Compound.

In the last modeling step, the appropriate BMR (that would have given a BMD (central) equal or very close to the two different doses of the mixture) was chosen.

Finally, the modeled effect for the mixture has been compared with the empirical study results to confirm the hypothesis of additivity.

Whole mount immunohistochemistry. Embryos were immunostained according to the method described by Wei et al. (1999) using a primary antibody against a specific NCC marker (anti-CRABP, ABR). After morphological examination, embryos were fixed in Dent's fixative (1:4 in volume DMSO: methanol) and processed according the previously described method (Menegola et al. 2003). At the end of the procedure, stained cells appeared dark brown through the dissecting microscope. Images obtained from embryos of different groups were compared.

Results

Effects of the single exposure to RA, FLUCO and Eth on rat embryo development. After 48 h in culture, normal embryos were dorsally convex and reached the phylotypic stage: tripartite encephalon (forebrain, midbrain, hindbrain) with enlarged ventricles, open posterior neuropore, 21-25 somites, three well separated branchial arches (the embryonic precursors of facial structures) (Fig 1 a). Branchial abnormalities (reductions, fusions between branchial arches) were detected in affected embryos exposed to effective concentration levels of Eth, RA or FLUCO (Fig 1 b-c).

Morphometric parameters were unaffected in any exposed group (data not shown), while dose-related teratogenic effects were detected in embryos exposed to Eth or FLUCO (Tables 1, 2) and in the positive control (RA 0.25 μM) (Tab 3). A syndromic picture was observed after Eth or RA exposure (Tables 1, 3): the affected districts were the branchial arches (reduced or fused), and, at the extrabranchial level, the encephalon (swollen romboencephalon, microcephalia) and the tail (hook-shaped tail). By contrast, at the tested concentration levels, only the branchial apparatus resulted affected by FLUCO (reduced or fused branchial arches) (Table 2). Limited to the branchial morphology, the NOAELs were Eth 17mM and FLUCO 62.5μM (Tables 1, 2). RA 0.025 μM resulted ineffective too (Table 3).

Effects of mixtures on development. In all mixture groups, morphometric parameters were unchanged (data not shown), while a concentration-related effect was observed in groups co-exposed to Eth and FLUCO (Tables 4, 5). The co-exposure increased the percentage of embryos with branchial arch abnormalities in respect to groups exposed to the single molecules; the mixture of NOAELs (Eth 17mM + FLUCO 62.5μM) resulted effective too (Figures 2, 3), suggesting that a common pathway is altered by the two molecules. Branchial and extra-branchial abnormalities were induced by co-exposure to Eth 17mM + RA 0.025μM (Table 3), suggesting a common pathway involved in Eth and RA teratogenicity.

Considering the branchial apparatus the common target for Eth and FLUCO, the BMD approach was applied on branchial outcomes. Results suggested no significant deviations from concentration-additivity (Table 6), supporting the hypothesis that a common MoA triggers the branchial effects induced by Eth and FLUCO exposure.

Immunostaining. The immunostaining allowed the evaluation of distribution of cranial NCCs in the whole embryos at the end of the culture period. The immuno-localization of this cell population showed, in normal embryos, three separated cell flows migrating from hindbrain to branchial arches. By contrast, in embryos showing branchial arch defects, an abnormal unique flow emerging from the hindbrain and reaching the branchial region was observed. This evidence supports the hypothesis that branchial defects are related to an abnormal NCC migration pathway (Figure 4).

Discussion

We compared the effects of Eth, FLUCO and RA on branchial arch morphogenesis using the *in vitro* postimplantation rat whole embryo culture. The three molecules were able to induce quite similar branchial arch defects at their teratogenic concentrations. The concentrations without teratogenic effects at the level of the branchial apparatus were Eth 17 mM, FLUCO 62.5 μM, RA 0.025 μM. The effect of co-exposure to Eth plus FLUCO did not deviate from additivity on branchial abnormalities, as estimated by the BMD approach. Since it is generally assumed that dose/concentration addition occurs if chemicals in a mixture act by the same MoA, even if they differ in their potencies, this evidence suggests that, at the branchial level, Eth and FLUCO share, at least partly, a common MoA. For molecules sharing a same MoA, dose additivity is assumed, in fact, in the dose range around or below the individual NOAELs of the mixture components, whereas at higher doses deviations are more likely to occur because of toxicokinetics or, less frequently, toxicodynamic interactions (Moretto, 2008; Boobis et al. 2011). The addition of doses implies that toxicity can be expected if the summed dose is high enough to exceed the threshold of toxicity of the mixture, even when the dose level of each individual chemical is below its own effect threshold. Due to this assumption, the dose-additivity approach is suggested in order to correctly group chemicals. As reviewed by Kortenkamp et al. (2009), in fact, there is evidence that dose/concentration addition can produce reliable estimates of combined effects, if the components share a strictly identical molecular mechanism of action. A dose-additive approach was, also, used by Wolansky et al. (2009) who showed that sub-threshold doses of chemicals with the same MoA, when combined in a mixture, produced measurable toxicity.

As far as FLUCO is concerned, branchial arch abnormalities have been indirectly related to a local increase of RA (Menegola et al. 2003; Tiboni et al. 2009). In order to evaluate the hypothesis of Eth MoA imbalancing RA pathway, we performed a group co-exposed to the NOAELs of Eth and RA. The effect of the mixture on branchial morphology suggests that an abnormal RA pathway could link Eth exposure and branchial defects.

The mixture effect of the co-exposure to azole fungicides and Eth has not been investigated so far, but it could be hypothesized that both the molecules concur to imbalance the RA pathway in specific responsive embryonic tissues. Further investigations are needed to explain the different specific molecular events leading to the RA pathway deregulation after Eth and FLUCO embryo exposure. Moreover, our data support the need of a cumulative risk assessment not only for chemicals grouped on the base of similarities in chemical structure but also for chemicals differently acting on the same biological pathway.

Considering that the lowest tested Eth concentrations are largely plausible (the legal limit of Eth blood concentrations for drivers is nearly equal to 10 mM in the majority of European Countries and in Australia, 18 mM in United States and United Kingdom) and that the tested FLUCO concentrations are at therapeutic effective plasma levels, our data strongly suggest a precautionary position in alcohol consumption during FLUCO exposure in pregnancy.

Compliance with ethical standards

The authors declare that they have no conflict of interest.

All applicable international, national, and/or institutional guidelines for the care and the use of animals were followed.

Animals were kept in pathogen-free/controlled conditions and all procedures were conformed to Italian law (D. Lgs n° 2014/26, implementation of the 2010/63/UE) and approved by the Animal Welfare Body of the University of Milan and by the Italian Minister of Health.

The manuscript does not contain any studies with participants.

References

Abel EL, Hannigan JH (1995) Maternal risk factors in fetal alcohol syndrome: provocative and permissive influences. Neurotoxicol Teratol 17(4):445-462. Erratum in: Neurotoxicol Teratol 17(6):689

Aleck KA, Bartley DL (1997) Multiple malformation syndrome following fluconazole use in preg- nancy: report of an additional patient. Am J Med Genet 72:253-256

American Academy of Pediatrics report (2000) Fetal Alcohol Syndrome and Alcohol-Related Neurodevelopmental Disorders. Pediatrics 106 (2): 358-361

Boobis A, Budinsky R, Collie S et al (2011) Critical analysis of literature on low-dose synergy for use in screening chemical mixtures for risk assessment. Crit Rev Toxicol 41(5): 369-383.

Brown N A, Fabro S (1981) Quantitation of rat embryonic development in vitro: a morphological scoring system. Teratology 24 : 65-78

Chen SY, Sulik KK (1996) Free radicals and ethanol-induced cytotoxicity in neural crest cells. Alcohol Clin Exp Res 20(6):1071-1076

Clode AM, Pratten MK, Beck F (1987) A stage-dependent effect of ethanol on 9.5-day rat embryos grown in culture and the role played by the concomitant rise in osmolality. Teratology 35(3):395-403

Czarnobaj J, Bagnall KM, Bamforth JS, Milos NC (2014) The different effects on cranial and trunk neural crest cell behaviour following exposure to a low concentration of alcohol in vitro. Arch Oral Biol 59(5):500-512

de Sanctis L, Memo L, Pichini S, Tarani L, Vagnarelli F (2011) Fetal alcohol syndrome: new perspectives for an ancient and underestimated problem. J Matern Fetal Neonatal Med 24 Suppl 1:34-37

Dunty WC Jr, Chen SY, Zucker RM, Dehart DB, Sulik KK (2001) Selective vulnerability of embryonic cell populations to ethanol-induced apoptosis: implications for alcohol-related birth defects and neurodevelopmental disorder. Alcohol Clin Exp Res 25(10):1523-1535

Fadel RA, Persaud TV (1992) Effects of alcohol and caffeine on cultured whole rat embryos. Acta Anat (Basel) 144(2):114-119

Flak AL, Su S, Bertrand J, Denny CH, Kesmodel US, Cogswell ME (2014) The association of mild, moderate, and binge prenatal alcohol exposure and child neuropsychological outcomes: a meta-analysis. Alcohol Clin Exp Res 38(1):214-226

Giavini E, Broccia ML, Prati M, Bellomo D, Menegola E (1992) Effects of ethanol and acetaldehyde on rat embryos developing in vitro. In vitro Cell Dev Biol 28A: 205–210

Gordon JE, Shy CM (1981) Agricultural chemical use and congenital cleft lip and/ or palate. Arch Environ Health 36:213–221

Holmberg PC, Hernberg S, Kurppa K, Rantala K, Riala R (1982) Orofacial clefts and organic solvent exposure during pregnancy. Int Arch Occup Environ Health 50:371–376

Holmes AR, Keniya MV, Ivnitski-Steele I, Monk BC, Lamping E, Sklar LA, Cannon RD (2012) The monoamine oxidase A inhibitor clorgyline is a broad-spectrum inhibitor of fungal ABC and MFS transporter efflux pump activities which reverses the azole resistance of Candida albicans and Candida glabrata clinical isolates. Antimicrob Agents Chemother 56(3):1508-1515

Howley MM, Carter TC, Browne ML, et al (2016) Fluconazole use and birth defects in the National Birth Defects Prevention Study. Am J Obstet Gynecol 214:657 e1-9

Hunter ES, Tugman JA, Sulik KK, Sadler TW (1994) Effects of short-term exposure to ethanol on mouse embryos in vitro. Toxicol In Vitro 8(3):413-421

Jentink J, Loane MA, Dolk H, Barisic I, Garne E, Morris JK, de Jong-van den Berg LT; EUROCAT Antiepileptic Study Working Group (2010) Valproic acid monotherapy in pregnancy and major congenital malformations. N Engl J Med 362(23):2185-2193

Joya X, Friguls B, Ortigosa S et al (2012) Determination of maternal-fetal biomarkers of prenatal exposure to ethanol: a review. Pharm Biomed Anal 69:209-222

Kallen K (1997) Maternal smoking and orofacial clefts. Cleft Palate-Craniofac J 34:11–16

Kitchin KT, Ebron MT (1984) Further development of rodent whole embryo culture: solvent toxicity and water insoluble compound delivery system. Toxicology 30(1):45-57

Kortenkamp A, Backhaus T, Faust M (2009) State of the Art Report on Mixture Toxicity, Final Report, 22 December Study Contract Number 070307/2007/485103/ETU/D.1 University of London (ULSOP)

Kotch LE, Chen SY, Sulik KK (1995) Ethanol-induced teratogenesis: free radical damage as a possible mechanism. Teratology 52(3):128-136

Kotch LE, Sulik KK (1992) Experimental fetal alcohol syndrome: proposed pathogenic basis for a variety of associated facial and brain anomalies. Am J Med Genet 44: 168-176

Lee BE, Feinberg M, Abraham JJ, Murthy AR (1992) Congenital malformations in an infant born to a woman treated with fluconazole. Pediatr Infect Dis J 11:1062-1064

Lopez-Rangel E, Van Allen MI (2005) Prenatal exposure to fluconazole: an identifiable dysmorphic phenotype. Birth Defects Res A Clin Mol Teratol 73:919-923

Memo L, Gnoato E, Caminiti S, Pichini S, Tarani L (2013) Fetal alcohol spectrum disorders and fetal alcohol syndrome: the state of the art and new diagnostic tools. Early Hum Dev 89 Suppl 1:S40-43

Menegola E, Broccia ML, Di Renzo F, Giavini E (2001) Antifungal triazoles induce malformations in vitro. Reprod Toxicol 15: 421-427

Menegola E, Broccia ML, Di Renzo F, Giavini E (2003) Pathogenic pathways in fluconazole-induced branchial arch malformations. Birth Defects Res A 67: 116-124

Menegola E, Broccia ML, Di Renzo F, Massa V, Giavini E (2004) Relationship between hindbrain segmentation, neural crest cell migration and branchial arch abnormalities in rat embryos exposed to fluconazole and retinoic acid in vitro. Reprod Toxicol 18: 121-130

Menegola E, Broccia ML, Di Renzo F, Massa V, Giavini E (2005) Study on the common teratogenic pathway elicited by the fungicides triazole-derivatives. Toxicol In Vitro 19: 737-748

Moretto A (2008) Exposure to multiple chemicals: when and how to assess the risk from pesticide residues in food. Trends in Food Science & Technology 19 S52 S59

Mossey PA, Little J, Munger RG, Dixon MJ, Shaw WC (2009) Cleft lip and palate. Lancet 374(9703):1773-1785

Munger RG, Romitti PA, Daack-Hirsch S, Burns TL, Murray JC, Hanson J (1996) Maternal alcohol use and risk of orofacial cleft birth defects. Teratology 54:27–33

New DAT (1978) Whole embryo culture and the study of mammalian embryos during organogenesis. Biol Rev 53: 81–122

Nurminen T, Rantala K, Kurppa K, Holmberg PC (1995) Agricultural work during pregnancy and selected structural malformations in Finland. Epidemiology 6:23–30

Priscott PK (1982) The effects of ethanol on rat embryos developing in vitro. Biochem Pharmacol 31(22):3641-3643

Pursley TJ, Blomquist IK, Abraham J, Andersen HF, Bartley JA (1996) Fluconazole-induced congenital anomalies in three infants. Clin Infect Dis 22(2):336-340

Sanchez JM, Moya G (1998) Fluconazole teratogenicity. Prenat Diagn 18:862-863

Santos SR, Campos EV, Sanches C, Gomez DS, Ferreira MC (2010) Fluconazole plasma concentration measurement by liquid chromatography for drug monitoring of burn patients. Clinics 65: 237-243

Schwartz EL, Hallam S, Gallagher RE, Wiernik PH (1995) Inhibition of all-trans retinoic acid metabolism by fluconazole in vitro and in patients with acute promyelocytic leukemia. Biochem Pharmacol 7:923–928

Sulik KK (2005) Genesis of alcohol-induced craniofacial dysmorphism. Exp Biol Med 230: 366-375

Tachibana M, Noguchi Y, Monro AM (1987) Toxicology of fluconazole in experimental animals. In: Fromtling RA, editor. Recent trends in the discovery, development, and evaluation of antifungal agents. Barcelona, Spain: J Proust Science Publishers. pp. 93–102

Thomas DC, Petitti DB, Goldhaber M, Swan SH, Rappaport EB, Hertz-Picciotto I (1992) Reproductive outcomes in relation to malathion spraying in the San Francisco Bay Area, 1981-1982. Epidemiology 3:32–39

Tiboni GM (1993) Second branchial arch anomalies induced by fluconazole, a bis-triazole antifungal agent, in cultured mouse embryos. Res Commun Chem Pathol Pharmacol 79: 381-384

Tiboni GM, Marotta F, Carletti E (2009) Fluconazole alters CYP26 gene expression in mouse embryos. Reprod Toxicol 27: 199-202

Van Maele-Fabry G, Gofflot F, Clotman F, Picard JJ (1995) Alterations of mouse embryonic branchial nerves and ganglia induced by ethanol. Neurotoxicol Teratol 17(4):497-506

Vanier KL, Mattiussi AJ, Johnston DL (2003) Interaction of all-trans-retinoic acid with fluconazole in acute promyelocytic leukemia. J Pediatr Hematol Oncol 25(5):403-404

Wei X, Makori N, Peterson PE, Hummler H, Hendrickx AG (1999) Pathogenesis of retinoic acid-induced ear malformations in a primate model. Teratology 60: 83–92

Wentzel P, Eriksson UJ (2009) Altered gene expression in neural crest cells exposed to ethanol in vitro. Brain Res 11, 1305 Suppl:S50-60

Werler MM, Lammer EJ, Rosenberg L, Mitchell AA (1991) Maternal alcohol use in relation to selected birth defects. Am J Epidemiol 134:691–698

Willford J, Leech S, Day N (2006) Moderate prenatal alcohol exposure and cognitive status of children at age 10. Alcohol Clin Exp Res 30: 1051-1059

Wolansky MJ, Gennings C, DeVito MJ, Crofton KM (2009) Evidence for dose-additive effects of pyrethroids on motor activity in rats. Environ Health Perspect 117(10):1563-1570

Wynter JM, Walsh DA, Webster WS, McEwen SE, Lipson AH (1983) Teratogenesis after acute alcohol exposure in cultured rat embryos. Teratog Carcinog Mutagen 3(5):421-428

Yamada Y, Nagase T, Nagase M, Koshima I (2005) Gene expression changes of sonic hedgehog signaling cascade in a mouse embryonic model of fetal alcohol syndrome. J Craniofac Surg 16(6):1055-1056

Zhou FC, Zhao Q, Liu Y, Goodlett CR, Liang T, McClintick JN, Edenberg HJ, Li L (2011) Alteration of gene expression by alcohol exposure at early neurulation. BMC Genomics 12: 124

Figure legends

Fig. 1 Rat embryos after 48h of culture. a) Normal morphology. Note the structure of the branchial apparatus with three separated branchial arches (I, II, III). The dotted line marks the limit of the cephalic region; b-c) Embryos showing specific branchial abnormalities, b) reduced second branchial arch (*); c) fusion among I-II-III branchial arches (#). Magnification 20x/40x.

Fig. 2 Percentage of embryos with branchial defects in groups exposed to FLUCO alone (62.5-500 μM) or to the ineffective level of Eth (17 mM) plus the increasing concentrations of FLUCO (62.5-500 μM).

Fig. 3 Percentage of embryos with branchial defects in groups exposed to Eth alone (17-85 mM) or to the ineffective level of FLUCO (62.5 μM) plus the increasing concentrations of Eth (17-85 mM).

Fig. 4 Head region of rat embryos after 48h of culture, immunostained in order to visualize NCCs. a) Normal morphology. Note the stained mass condensed at the level of the fronto-nasal region (°) and at the level of the branchial apparatus: the maxillary region of the first branchial arch (Ia), the mandibular region of the first branchial arch (Ib) and the stained region corresponding to the second (II) and posterior (III) branchial arches. Branchial arch immunostained tissues resulted well separated by not stained borders; b) Embryo showing unseparated stained tissues at the level of the branchial region (dotted square). Magnification: 40x.

Table 1. Evaluation of the teratogenic effects, as detected at term of the culture period, of the exposure to Eth at increasing concentrations. The observed teratogenic effects were at the level of both branchial and extrabranchial districts.

	CONTROL	Eth 17 mM	Eth 42.5 mM	Eth 85 mM	Eth 127.5 mM
TOTAL EXAMINED	36	30	11	15	11
EMBRYOS WITH BA ABNORMALITIES (FUSED AND/OR REDUCED BA), % **	0	0	aabb 72.72	aabb 80	aabbccdd 100
EMBRYOS WITH FUSED BA, %	0	0	0	6.67	0
EMBRYOS WITH REDUCED BA, % **	0	0	aabb 72.72	aabb 80	aabbccdd 100
EMBRYOS WITH EXTRABRANCHIAL ABNORMALITIES, % **	0	aa 10	aabb 27.27	aabbcc 53.33	aabbccdd 100

Post hoc analysis performed if overall test showed that there is a significant linear trend among the ordered categories
(** $p<0.01$, chi-square test)

aa $p<0.01$ vs. CONTROL; bb $p<0.01$ vs. Eth 17 mM; cc $p<0.01$ vs. Eth 42.5 mM; dd $p<0.01$ vs. Eth 85 mM

Table 2. Evaluation of the teratogenic effects of the exposure to FLUCO at increasing concentrations. The teratogenic effects observed at the end of the culture period were specifically at the level of the branchial apparatus.

	CONTROL	FLUCO 62.5 µM	FLUCO 125 µM	FLUCO 250 µM	FLUCO 500 µM
TOTAL EXAMINED	36	15	9	18	10
			aabb	aabbcc	aabbccdd
EMBRYOS WITH BA ABNORMALITIES (FUSED AND/OR REDUCED BA), % **	0	0	44.44	72.22	100
EMBRYOS WITH FUSED BA, % **	0	0	0	aabbcc 33.33	aabbccdd 100
EMBRYOS WITH REDUCED BA, % **	0	0	aabb 44.44	aabb 38.89	ccdd 0
EMBRYOS WITH EXTRABRANCHIAL ABNORMALITIES, %	0	0	0	0	0

Post hoc analysis performed if overall test showed that there is a significant linear trend among the ordered categories (** $p<0.01$, chi-square test)

aa $p<0.01$ vs. CONTROL; bb $p<0.01$ vs. FLUCO 62.5 µM; cc $p<0.01$ vs. FLUCO 125 µM; dd $p<0.01$ vs. FLUCO 250 µM

Table 3

Table 3. Evaluation of the effects of RA and of the co-exposure to Eth and RA (at concentrations ineffective for branchial development). The clear effect of the mixture supports the hypothesis of a contribution of Eth in RA pathway deregulation.

	SOLVENT CONTROL GROUP (DMSO 1µL/mL)		POSITIVE CONTROL (RA 0.25 µM)		Eth 17 mM	RA 0.025 µM	Eth 17 mM + RA 0.025 µM
TOTAL EXAMINED	10		10		30	8	12
							aaccdd
EMBRYOS WITH BA ABNORMALITIES (FUSED AND/OR REDUCED BA), %	0		100		0	0	100
EMBRYOS WITH FUSED BA, %	0		100		0	0	bb 0
EMBRYOS WITH REDUCED BA, %	0		0		0	0	aabbccdd 100
EMBRYOS WITH EXTRABRANCHIAL ABNORMALITIES, %	0		100		10	0	aaccdd 100

Statystical analysis was performed in order to compare data obtained in mixture group with controls (DMSO, RA 0.25) and with the single exposure to Eth or RA 0.025 µM.

aa $p<0.01$ vs. SOLVENT (DMSO); bb $p<0.01$ vs. POSITIVE CONTROL (RA 0.25 µM); cc $p<0.01$ vs. Eth 17 mM; dd $p<0.01$ vs. RA 0.025 µM.

Table 4. Evaluation of the effects of the co-exposure to Eth (at the fixed concentration level, 17 mM) and FLUCO (at moving concentrations). The observed teratogenic effect was specifically at the level of the branchial apparatus.

	CONTROL	Eth 17 mM	Eth 17 mM + FLUCO 62.5 µM	Eth 17 mM + FLUCO 125 µM	Eth 17 mM + FLUCO 250 µM	Eth 17 mM + FLUCO 500 µM
TOTAL EXAMINED	36	30	19	18	18	9
EMBRYOS WITH BA ABNORMALITIES (FUSED AND/OR REDUCED BA), % **	0	0	aabb 47.37	aabbcc 72.22	aabbccdd 94.44	aabbccddee 100
EMBRYOS WITH FUSED BA, % **	0	0	aabb 26.31	aabbcc 50	aabbccdd 72.22	aabbccddee 100
EMBRYOS WITH REDUCED BA, % **	0	0	aabb 47.37	aabbcc 22.22	aabbcc 22.22	ccddee 0
EMBRYOS WITH EXTRABRANCHIAL ABNORMALITIES, %	0	10	5.26	0	16.67	0

Post hoc analysis performed if overall test showed that there is a significant linear trend among the ordered categories
(** $p<0.01$, chi-square test)
aa $p<0.01$ vs. CONTROL
bb $p<0.01$ vs. Eth 17 mM
c $p<0.05$; cc $p<0.01$ vs. Eth 17 mM + FLUCO 62.5 µM
dd $p<0.01$ vs. Eth 17 mM+ FLUCO 125 µM
ee $p<0.01$ vs. Eth 17 mM + FLUCO 250 µM

Table 5. Evaluation of the effects of the co-exposure to FLUCO (at the fixed concentration level, 62.5 µM) and Eth (at moving concentrations). The observed teratogenic effects included branchial and extrabranchial districts.

	CONTROL	FLUCO 62.5 µM	FLUCO 62.5 µM + Eth 17 mM	FLUCO 62.5 µM + Eth 42.5 mM	FLUCO 62.5 µM + Eth 85 mM
TOTAL EXAMINED	36	15	19	8	10
EMBRYOS WITH BA ABNORMALITIES (FUSED AND/OR REDUCED BA), % **	0	0	aabb 47.37	aabbcc 87.5	aabbccdd 100
EMBRYOS WITH FUSED BA, % **	0	0	aabb 26.31	aabb 25	aabbccdd 100
EMBRYOS WITH REDUCED BA, % **	0	0	aabb 47.37	aabbc 62.5	ccdd 0
EMBRYOS WITH EXTRABRANCHIAL ABNORMALITIES, % **	0	0	5.26	aabb 12.5	aabbccdd 100

Post hoc analysis performed if overall test showed that there is a significant linear trend among the ordered categories
(** $p<0.01$, chi-square test)
aa $p<0.01$ vs. CONTROL; bb $p<0.01$ vs. FLUCO 62.5 µM; c $p<0.05$; cc $p<0.01$ vs. FLUCO 62.5 µM + Eth 17 mM; dd $p<0.01$ vs. FLUCO 62.5 µM + Eth 42.5 mM

Table 6

Table 6. Parameters used for BMD approach: starting from the selected model, compound specific BMRs have been chosen to find the equivalent BMDs (central equal or very close to the two different doses of the mixture) for the other compound in order to calculate the total dose in the mixture. Finally, the model extimate effects for the mixture has been compared with the empirical results to confirm (mixture effect <3) or reject the hypothesis of additivity. Concentrations are expressed as micromolar.

	BMR	DOSE (BMD)	DOSE (MIXTURE)	EXPECTED EFFECT (BMD modeling)	OBSERVED EFFECT (% abnormal embryos)	**MIXTURE EFFECT (ratio observed/expected)**
fluconazole	8.1	62.5	143.3	36.0	47.4	**1.3**
ethanol fluconazole equivalent	13.2	80.8				
fluconazole ethanol equivalent	8.1	12055	29055.0	28.2		**1.7**
ethanol	13.2	17000				
fluconazole	28.7	125	205.8	58.7	72.2	**1.2**
ethanol fluconazole equivalent	13.2	80.8				
fluconazole ethanol equivalent	28.7	29413	46413.0	52.2		**1.4**
ethanol	13.2	17000				
fluconazole	74.2	250	330.8	90.5	94.4	**1.0**
ethanol fluconazole equivalent	13.2	80.8				
fluconazole ethanol equivalent	74.2	65222	82222.0	87.4		**1.1**
ethanol	13.2	17000				
fluconazole	99.6	500	580.8	99.9	100	**1.0**
ethanol fluconazole equivalent	13.2	80.8				
fluconazole ethanol equivalent	99.6	138726	155726.0	99.9		**1.0**
ethanol	13.2	17000				

fluconazole	8.1	62.5	143.3	36.0	47.4	**1.3**
ethanol fluconazole equivalent	13.2	80.8				
fluconazole ethanol equivalent	8.1	12055	29055.0	28.2		**1.7**
ethanol	13.2	17000				

fluconazole	8.1	62.5	233.7	70.0	77.8	**1.1**
ethanol fluconazole equivalent	47	171.2				
fluconazole ethanol equivalent	8.1	12055	54555.0	62.0		**1.3**
ethanol	47	42500				

fluconazole	8.1	62.5	383.7	96.0	100	**1.0**
ethanol fluconazole equivalent	89.3	321.2				
fluconazole ethanol equivalent	8.1	12055	97055.0	94.0		**1.1**
ethanol	89.3	85000				

Figure 1

Click here to download Figure Fig 1.psd

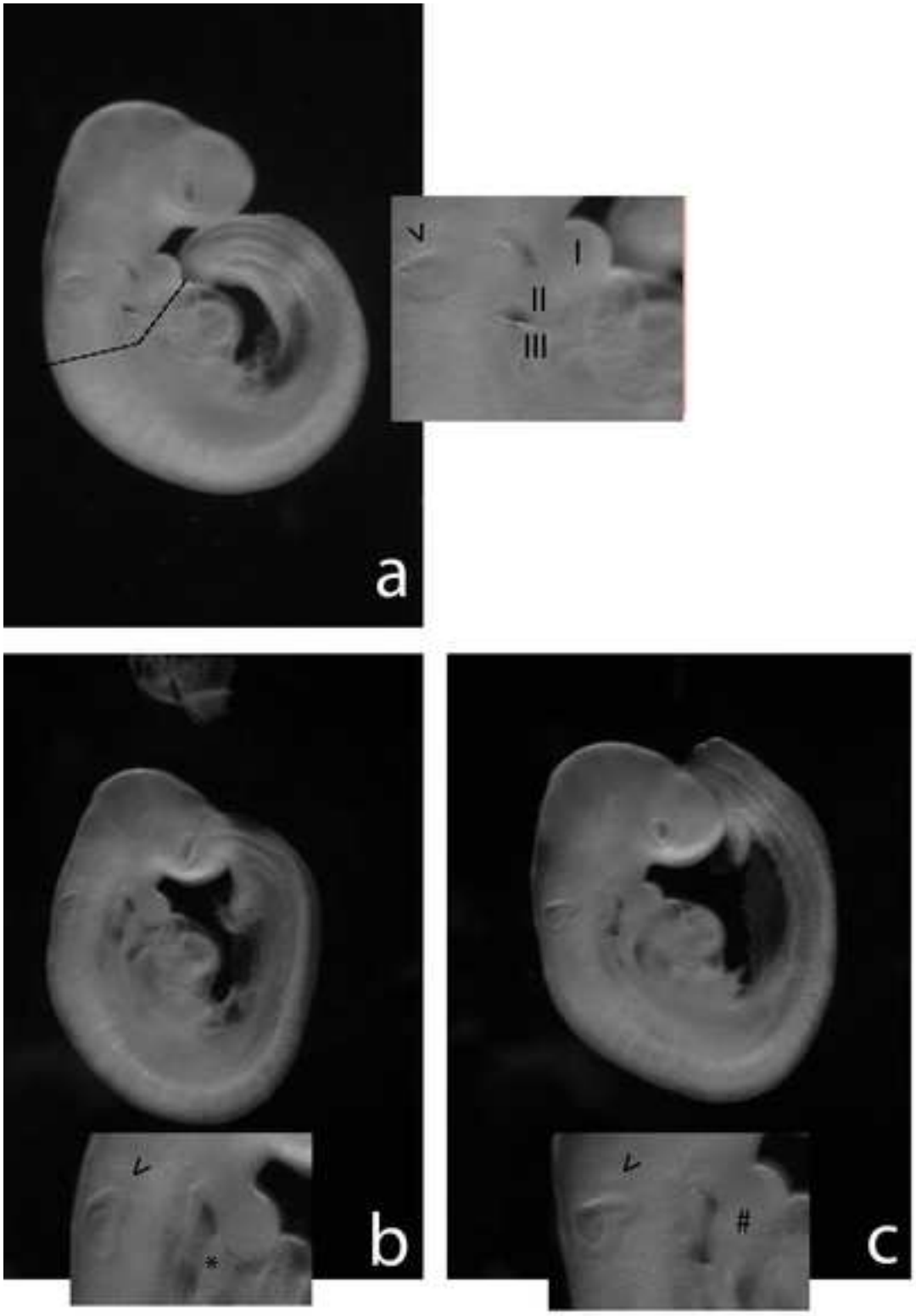

Figure 2

Click here to download Figure Figure 2.psd

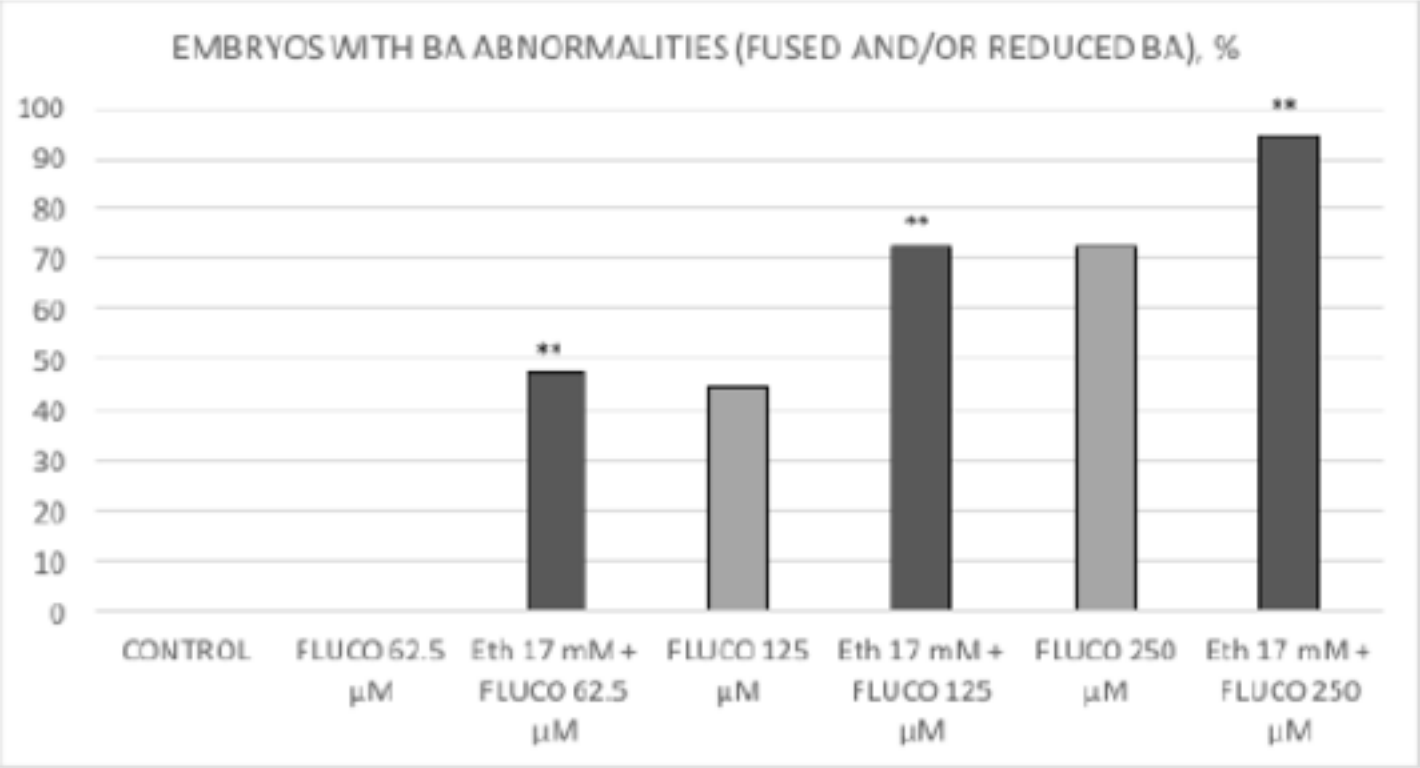

Figure 3

Click here to download Figure Figure 3.psd

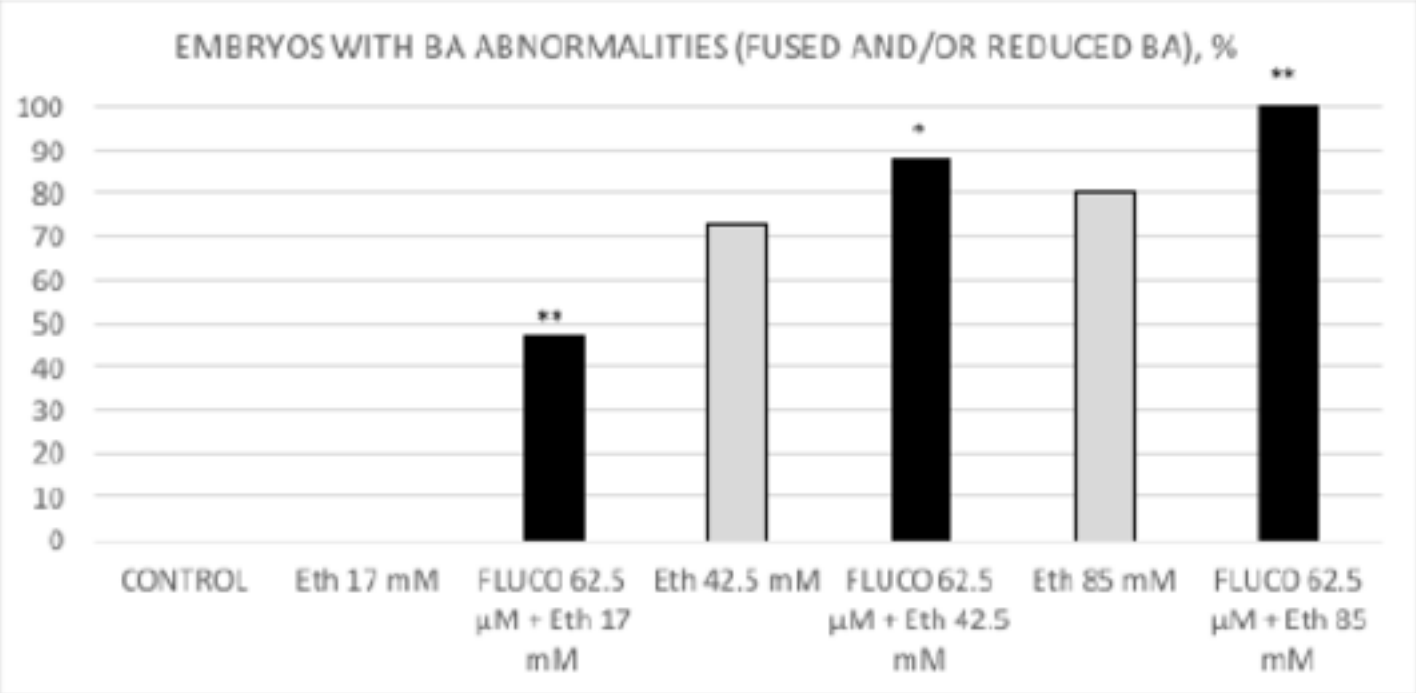

Figure 4

Click here to download Figure Fig 4 crabp .tif